

Inaugural dissertation
for
obtaining the doctoral degree
of the
Combined Faculty of Mathematics, Engineering and Natural Sciences
of the
Ruprecht - Karls - University
Heidelberg

presented by

M.Sc Pooja Joshi

Born in Belgaum, India

Oral examination: 08.12.2022

**Impact of a single nucleotide polymorphism in the
CD40 gene and diabetes-associated stress factors on
endothelial dysfunction**

Referees: Prof. Dr. Markus Hecker

Prof. Dr. Marc Freichel

Contents

ABBREVIATIONS.....	1
1. ZUSAMMENFASSUNG	3
1. SUMMARY	5
2. INTRODUCTION	7
2.1 Diabetes mellitus.....	7
2.2 Cardiovascular complications of diabetes.....	8
2.3. Diabetes is an inflammatory disease	8
2.3.1. Association of obesity with type 2 diabetes and cardiovascular complications	9
2.3.2. Signaling pathways linking insulin resistance and inflammation in diabetes..	10
2.4. The fate of the endothelial cells in type 2 diabetes	11
2.4.1. Role of the endothelium in maintaining normal physiological conditions	12
2.4.2. Endothelial dysfunction in type 2 diabetes	12
2.5. CD40 signaling and endothelial activation	15
2.5.1. Impact of CD40 signaling on β -cell function, inflammation, and progression of vascular complications associated with diabetes.....	16
2.5.2. The T-1C <i>CD40</i> single nucleotide polymorphism.....	18
2.6. Aim(s) of the study.....	19
3. MATERIALS	20
3.1. Buffers and Solutions.....	20
3.2. Chemicals and reagents	21
3.3. Cell culture reagents	22
3.4. Consumables.....	22
3.5. Kits.....	22
3.6. Stimulants, siRNAs, and inhibitors.....	23
3.7. Oligonucleotides	23
3.7.1. Primers	23

3.7.2.	Decoy ODNs.....	24
3.8.	Antibodies	24
3.8.1.	Primary antibodies	24
3.8.2.	Secondary antibodies	25
3.8.3.	Miscellaneous Equipment.....	25
4.	METHODS.....	27
4.1.	Diabetes patient samples	27
4.2.	Isolation of DNA, RNA, and protein from patient and control samples.....	27
4.3.	<i>CD40</i> SNP genotyping.....	28
4.3.1.	Tetra-arms PCR	28
4.3.2.	Agarose gel electrophoresis	29
4.4.	ELISA	29
4.5.	Cell isolation and culture	30
4.5.1.	Human umbilical vein endothelial cells (HUVEC)	30
4.6.	Cell culture designs	30
4.6.1.	Sample preparation for RNA-Seq analysis.....	30
4.6.2.	Diabetic model	30
4.6.3.	NFAT5 siRNA transfection	31
4.6.4.	Treatment with KRN2 inhibitor.....	31
4.6.5.	Treatment with NFAT5 oligonucleotide decoy	31
4.7.	Collection of conditioned medium.....	32
4.8.	Quantitative measurement of proteins in the medium supernatant of cultured HUVEC.....	32
4.9.	RNA extraction from cells	32
4.9.1.	RNA extraction for gene expression analysis.....	32
4.9.2.	RNA extraction for RNA-sequencing.....	32
4.10.	Quantification of RNA quality.....	33

4.10.1. A260/A280 absorbance ratio	33
4.10.2. Native RNA gel electrophoresis	33
4.10.3. Bioanalyzer	34
4.11. Reverse transcription and cDNA synthesis	35
4.12. Real-time quantitative reverse transcription-polymerase chain reaction (RT-qPCR).....	35
4.13. Preparation of whole-cell lysate.....	36
4.14. Protein quantification and sample preparation for Western blot	36
4.15. SDS Polyacrylamide gel electrophoresis and protein transfer	37
4.16. Immunostaining procedure and band intensity analysis	38
4.17. Immunocytochemistry.....	38
4.18. Data analysis	39
4.18.1. RNA-Seq.....	39
4.18.2. Analysis of NFAT5 cytoplasmic and nuclear abundance.....	39
4.19. Statistical analysis	40
5. RESULTS	41
5.1. Prevalence of the T-1C SNP of the <i>CD40</i> gene in patients with type 2 and type 1 diabetes	41
5.2. Comparison of plasma levels of sCD40 and sCD40L between patients with T1D, T2D, and healthy individuals	42
5.3. Association of the T-1C SNP of the <i>CD40</i> gene with the plasma levels of sCD40 and sCD40L in patients with diabetes	43
5.4. Results of RNA-Seq analysis.....	45
5.5. Impact of a diabetes-like microenvironment on pro-inflammatory gene expression in CC-genotyped HUVECs.....	49
5.6. Analysis of soluble factors released into the supernatant of CC-genotype HUVECs subjected to a diabetes-like microenvironment	51
5.6.1. Soluble forms of surface adhesion molecules.....	51

5.6.2.	Cytokines, chemokines, and growth factor.....	52
5.6.3.	Matrix metalloproteinases.....	53
5.7.	Analysis of TNF Receptor Associated Factors (TRAF) mRNA expression....	54
5.8.	Impact of diabetes-like microenvironment on HUVEC morphology	55
5.9.	Impact of diabetes-like microenvironment conditions on TGF- β expression in the CC-genotype HUVECs	55
5.10.	Analysis of endothelial-to-mesenchymal transition (EndMT)-associated marker gene expression	56
5.10.1.	Markers specific for endothelial or mesenchymal origin	56
5.10.2.	Extracellular matrix mRNA expression	57
5.10.3.	Gene expression of transcription factors associated with EndMT	58
5.10.4.	Impact of diabetes-like microenvironment on NFAT5 mRNA levels	59
5.10.5.	Impact of a diabetes-like microenvironment on the abundance of NFAT5 protein in the cytoplasm and in the nucleus.....	60
5.10.6.	Effect of NFAT5 downregulation on SM22 α protein expression in HUVECs subjected to a diabetes-like microenvironment	61
6.	DISCUSSION.....	63
6.1.	Analysis of a SNP in the <i>CD40</i> gene and plasma levels of sCD40/sCD40L in patients with diabetes.....	63
6.1.1.	Association of the T-1C SNP of the CD40 gene (rs1883832) with diabetes	63
6.1.2.	Circulating sCD40 and sCD40L as indicators of the inflammatory status in patients suffering from diabetes.....	65
6.1.3.	Association of the T-1C SNP of the CD40 gene (rs1883832) with sCD40L and sCD40 plasma levels of patients with diabetes.....	66
6.1.4.	Impact of the T-1C SNP of the CD40 gene on differential gene expression in sCD40L stimulated CC- and TT-genotype HUVEC	67
6.2.	Effect of the diabetes-like microenvironment on the CC-genotype HUVECs	69
6.2.1.	Establishment of a diabetes-like cell culture model	69

6.2.2.	Limitations of the proposed diabetes-like culture model.....	69
6.2.2.1.	Analysis of the impact of the diabetes-like microenvironment on the cellular metabolism.....	70
I.	Glucose metabolism.....	70
II.	Glutamine metabolism.....	72
6.2.2.2.	Additional mediators of endothelial dysfunction in diabetes	72
I.	Lipotoxicity.....	73
II.	Oxidative stress.....	73
III.	Endoplasmic reticulum stress	74
IV.	Osmotic stress.....	74
V.	Other pro-inflammatory mediators	75
6.2.3.	Pro-inflammatory gene expression in a diabetes-like microenvironment	75
I.	Impact on the expression of markers facilitating leukocyte recruitment and transmigration	75
II.	Impact on the expression of additional pro-inflammatory mediators.....	76
6.2.4.	Influence of a diabetes-like microenvironment on CD40 downstream signaling.....	78
6.2.5.	The diabetes-like microenvironment promotes EndMT.....	79
6.2.6.	Potential role of NFAT5 in the pathogenesis of diabetes	80
6.2.6.1.	NFAT5 mediates progression of diabetes and contributes to the associated vascular complications.....	80
6.2.6.2.	Impact of NFAT5 on NF- κ B-induced downstream signaling	81
6.2.6.3.	NFAT5 expression and abundance in the diabetes-like cell culture model	81
6.3.	Limitations	82
6.4.	Summary and future perspectives	83
7.	REFERENCES.....	86
7.1.	Websites	86

7.2. Publications	86
8. SUPPLEMENTARY DATA	112
8.1. Supplementary figures	112
8.2. Supplementary tables	114
9. ACKNOWLEDGEMENTS	118

List of Figures

Figure 1: Prevalence of diabetes in Germany in the year 2019.....	7
Figure 2: Immune cell modulation and inflammatory status of an obese adipose tissue. 9	
Figure 3: Inflammatory pathways activated by the diabetes-associated metabolic stress factors	10
Figure 4: Endothelial dysfunction in diabetes.....	13
Figure 5: Biological role of CD40 signaling in different cell types.....	15
Figure 6: CD40-CD40L signaling is employed at several stages of atherosclerotic initiation and progression	17
Figure 7: Position of the T-1C SNP of the <i>CD40</i> gene and its effect on CD40 protein turnover.....	18
Figure 8: Additional purification steps applied to the isolated DNA, RNA, and protein samples	27
Figure 9: RNA quality analysis post isolation.....	34
Figure 10: Comparison of the allele frequency of the <i>CD40</i> SNP amongst a control cohort and patients with T2D and T1D	41
Figure 11: Association of the T-1C SNP of the <i>CD40</i> gene with susceptibility to CHD, T2D, and T1D.....	42
Figure 12: Comparison of sCD40 and sCD40L plasma levels in healthy individuals and patients with diabetes	43
Figure 13: Association between sCD40/sCD40L plasma levels and the T-1C SNP of the <i>CD40</i> gene in healthy controls and in patients with diabetes.....	44
Figure 14: Correlation of the sCD40 and sCD40L plasma levels in the CC-genotype T1D and T2D patients.....	45
Figure 15: Differentially expressed genes in sCD40L stimulated CC vs. TT- genotype HUVECs.....	45
Figure 16: Pro-inflammatory mediators with/without hyperglycemia upregulate pro-inflammatory mRNA expression in HUVECs	50
Figure 17: Soluble forms of surface adhesion molecules are enhanced in the supernatant of HUVECs exposed to pro-inflammatory mediators.	51
Figure 18: Impact of pro-inflammatory mediators with/without glucose on the release of cytokines, chemokines, and growth factors by the HUVECs.	53

Figure 19: Matrix metalloproteinases released by HUVECs in the presence of pro-inflammatory mediators with/out hyperglycemia	54
Figure 20: Effect of pro-inflammatory stimulants with/out glucose on TRAF adaptor molecules mRNA levels in HUVECs.....	54
Figure 21: HUVECs undergo morphology changes upon exposure to pro-inflammatory mediators in presence and absence of glucose	55
Figure 22: Impact of pro-inflammatory mediators with/out glucose on the mRNA and protein levels of TGF- β family members	56
Figure 23: HUVECs exposed to pro-inflammatory microenvironment with/out glucose undergo partial EndMT.	57
Figure 24: Impact of pro-inflammatory mediators in presence or absence of hyperglycemia on extracellular matrix mRNA expression in HUVECs.....	58
Figure 25: Impact of pro-inflammatory stimuli with/out glucose on the EndMT-associated transcription factor mRNA expression in HUVECs	59
Figure 26: Impact of pro-inflammatory mediators with/out hyperglycemia on HUVEC NFAT5 mRNA expression	60
Figure 27: Impact of pro-inflammatory microenvironment with/out hyperglycemia on NFAT5 abundance.....	61
Figure 28: NFAT5 decoy ODN inhibits SM22 α gene expression in HUVECs subjected to pro-inflammatory mediators under hyperglycemia.....	62

List of supplementary figures

Figure S1: Impact of siRNA-based silencing of NFAT5-on-NFAT5 mRNA levels in HUVECs treated with TNF- α and high glucose.....	112
Figure S2: Impact of pro-inflammatory mediators with/out glucose on the mRNA expression of endothelial markers in HUVECs.....	112
Figure S3: Impact of KRN2 inhibitor on NFAT5 mRNA expression of HUVECs exposed to pro-inflammatory mediators with high glucose	112
Figure S4: Human E-selectin promoter sequence	113

List of tables

Table 1: Composition of buffers and solutions used in this study	20
Table 2: List of chemicals and reagents used in this study	21
Table 3: List of cell culture reagents used in this study	22
Table 4: List of materials utilized in this study	22
Table 5: List of kits used in this study.....	22
Table 6: List of stimulants and inhibitors used in this study.....	23
Table 7: List of primers used in this study	23
Table 8: List of ODN decoys used in this study.....	24
Table 9: List of primary antibodies used in this study for Western blot (WB) and Immunocytochemistry (ICC).....	24
Table 10: List of secondary antibodies used in this study for Western blot (WB) and Immunocytochemistry (ICC).....	25
Table 11: Miscellaneous equipment utilized.....	25
Table 12: Composition of the reaction mixture for PCR	28
Table 13: PCR program for the genotyping of the -1C/T SNP of the <i>CD40</i> gene.....	29
Table 14: Composition of the reaction mixture for RT-qPCR	35
Table 15: Composition of the reaction mixture for RT-qPCR	36
Table 16: SDS gel components	38

List of supplementary tables

Table S1: Pathway analysis for the upregulated gene products in sCD40L stimulated CC-genotype HUVECs.	114
Table S2: Pathway analysis for the downregulated gene products in sCD40L stimulated CC-genotype HUVECs.	114
Table S3: Pathway analysis for the upregulated gene products in sCD40L stimulated TT-genotype HUVECs.	116
Table S4: Pathway analysis for the downregulated gene products in sCD40L stimulated TT-genotype HUVECs.....	116

ABBREVIATIONS

BMI	Body mass index
CHD	Coronary heart disease
COL1 α 1/COL3 α 1	Collagen 1A1/Collagen 3A1
DM	Diabetes mellitus
ECM	Extracellular matrix
EndMT	Endothelial to mesenchymal transition
ERK	Extracellular signal-regulated kinase
FCGR3A	Fc Gamma Receptor IIIa
FN1	Fibronectin
GPX	Glutathione Peroxidase
HUVEC	Human umbilical vein endothelial cells
ICAM-1	Intercellular Adhesion Molecule 1
IL	Interleukin
KTN1	Kinectin 1
MAPK	Mitogen-activated protein kinase
MCP-1	Monocyte chemoattractant protein-1
MMP	Matrix metalloproteinase
NFAT	Nuclear factor of activated T-cells
NF- κ B	Nuclear factor kappa B
NLRP3	NLR family pyrin domain containing 3
NOS3	Nitric Oxide Synthase 3
ODN	Oligonucleotide
RAC1	Ras-related C3 botulinum toxin substrate 1
RNA-Seq	RNA sequencing
sCD40/sCD40L	Soluble CD40/ligand
SM22 α	Smooth Muscle Protein 22-Alpha
SNAI1/2	Snail Family Transcriptional Repressor 1/2
SNP	Single nucleotide polymorphism
STAT	Signal transducer and activator of transcription
T1D	Type 1 diabetes
T2D	Type 2 diabetes
TGF- β	Transforming growth factor-beta

TNF- α	Tumour necrosis factor alpha
TRAF	tumour necrosis factor receptor-associated factor
VCAM-1	Vascular cell adhesion protein 1
WASP	Wiskott-Aldrich syndrome protein
WAVE	WASP-family verprolin-homologous protein
ZEB2	Zinc Finger E-Box Binding Homeobox 2
α -SMA	Alpha smooth muscle actin

1. ZUSAMMENFASSUNG

Der CD40-Signalweg ist ein wichtiger Modulator immunologischer Reaktionen und erfüllt mehrere biologische Funktionen in verschiedenen Organen. Während sein Hauptzweck die Wiederherstellung der Homöostase ist, führt seine unregulierte Aktivierung zu verschiedenen immunmodulierten pathologischen Erkrankungen. Seine Rolle bei der Entwicklung von Insulinresistenz und dem Fortschreiten von Diabetes ist gut dokumentiert. Die Beteiligung der CD40-Signalübertragung führt zu einer Verstärkung der systemischen Entzündungsreaktion bei Diabetes und zur Entstehung von Gefäßkomplikationen.

Der funktionelle Einzelnukleotid-Polymorphismus (SNP) in der Kozak-Region des *CD40*-Gens (T-1C, rs1883832) wirkt sich auf die CD40-Translationseffizienz aus und wird mit mehreren immun- und entzündungsbedingten Krankheiten in Verbindung gebracht. Angesichts der Rolle der CD40-Signalübertragung bei der Entstehung von Diabetes und systemischen Entzündungen liegt dieser Arbeit die Hypothese zugrunde, dass dieser SNP ein Risikofaktor für Diabetes ist.

Diese Hypothese wurde untersucht, indem die Verteilung des T-1C SNP bei Patienten mit Typ 1 (T1D) und Typ 2 Diabetes (T2D) verglichen wurde. Die Ergebnisse zeigen eine starke Assoziation des C-Allels mit T2D (Odds Ratio = 1,43; 95% Konfidenzintervall: 1,09-1,86). T2D-Patienten wiesen zudem höhere Plasmaspiegel des schützenden löslichen CD40-Rezeptors (sCD40) auf. Dieser ist dafür bekannt, CD40-Ligand (CD40L) zu binden und dessen pro-inflammatorische Reaktionen zu neutralisieren. Daher ist der CD40-Signalweg verstärkt bei T2D-Patienten aktiv, was durch eine verstärkte Bildung des sCD40 nachweisbar ist.

Die Auswirkung des T-1C SNP auf die Genexpression wurde mit sCD40L-stimulierten humanen kultivierten Endothelzellen (HUVECs) vom CC- und TT-Genotyp mit Hilfe der RNA-Sequenzierung untersucht und verglichen. CC-Genotyp-HUVECs wiesen generell ein höheres Maß an Genexpression auf. Ausserdem waren in diesen Zellen Gene verstärkt aktiviert, die eine Rolle bei Entzündungsreaktionen, dem Recycling von Insulinrezeptoren und dem Übergang von Endothel- zum Mesenchymzelltyp (EndMT) spielen. Die ruhenden TT-Genotyp-HUVECs waren vor diesen Veränderungen geschützt. Weiterhin wurden die Auswirkungen eines pro-diabetischen Kultivierungsmilieus auf die proinflammatorischen CC-Genotyp-HUVECs untersucht.

Diese zeigten eine erhöhte Expression von Mediatoren, die Entzündung, Atherosklerose und EndMT fördern. Darüber hinaus zeigten diese Zellen morphologische Veränderungen und wiesen einen teilweise EndMT-ähnlichen Phänotyp auf. Die Genexpression des osmoadaptiven Transkriptionsfaktors Nuclear Factor of Activated T-Cells (NFAT) 5 und seine Lokalisation im Zellkern waren unter diesen pro-diabetischen Bedingungen ebenfalls erhöht.

Die Blockierung der DNA-Bindung von NFAT5 in diesen Zellen durch ein neutralisierendes Konsensus-NFAT5-Decoy-Oligonukleotid verringerte die Expression des mesenchymalen SM22 α -Markergens signifikant. Eine in silico-Analyse konnte benachbarte NF- κ B/NFAT5-Doppelbindungsstellen in Promotorregionen von Genen nachweisen, die an der Progression von Atherosklerose und EndMT beteiligt sind. Während NF- κ B nachweislich Entzündungen und EndMT in HUVECs induziert, ist über die Rolle von NFAT5 bei der Modulation dieser Prozesse weniger bekannt. Die aktuelle Studie liefert neue Erkenntnisse über die Rolle von NFAT5 bei der Verstärkung NF- κ B-vermittelter Entzündung und EndMT unter pro-diabetischen Bedingungen.

1. SUMMARY

CD40 signaling is a key modulator of immunological responses and serves several biological functions across multiple organs. While its primary purpose is restoring homeostasis, its unregulated activation drives various immune-modulated pathological conditions. Its role in the development of insulin resistance and the progression of diabetes is well documented. A further contribution of CD40 signaling in escalating systemic inflammation in diabetes leads to the initiation of vascular complications.

The functional single nucleotide polymorphism (SNP) in the Kozak region of the *CD40* gene (T-1C, rs1883832) impacts CD40 translation efficiency and is associated with several immune and inflammation-modulated diseases. Given the role of CD40 signaling in the progression of diabetes and systemic inflammation, this SNP may also represent a genetic risk factor for diabetes.

This hypothesis was investigated by examining the distribution of the T-1C SNP in patients with type 1 (T1D) and type 2 diabetes (T2D). There was, in fact, a strong association of the C-allele with T2D (odds ratio = 1.43; 95% confidence interval: 1.09-1.86). T2D patients also revealed higher plasma levels of the presumably protective soluble CD40 receptor (sCD40), which is known to neutralize the CD40 ligand (CD40L) and its pro-inflammatory capacity. Hence, in T2D patients, CD40 signaling seems to be switched on, leading to an upregulation of the compensatory sCD40 in the blood.

The possibility that the T-1C SNP differentially affects the genome of sCD40L-stimulated CC and TT-genotype human cultured endothelial cells (HUVECs) was examined through RNA sequencing. The CC-genotype HUVECs exhibited a higher degree of gene expression in general and in particular of genes involved in escalating inflammation, insulin receptor recycling, and driving endothelial to mesenchymal transition (EndMT). The quiescent TT-genotype HUVECs seemed to be protected against such changes. The impact of a pro-diabetic microenvironment on the pro-inflammatory CC-genotype HUVECs was further studied. Under these conditions, they revealed an increased expression of mediators promoting inflammation, atherosclerosis, and EndMT. In addition, they showed morphological changes characteristic of a partial EndMT-like phenotype.

Expression of the osmoadaptive transcription factor nuclear factor of activated T-cells (NFAT) 5 and its nuclear abundance was also increased under these conditions. Blocking

NFAT5 DNA-binding in the CC-genotype HUVECs by using a neutralizing consensus NFAT5 decoy oligonucleotide significantly reduced the expression of the mesenchymal marker SM22 α . Several nuclear factor κ B (NF- κ B)/NFAT5 dual binding sites are located in promotor regions of genes involved in the progression of atherosclerosis and EndMT. While NF- κ B is known to drive inflammation and EndMT in HUVECs, less is known about the role of NFAT5 in modulating these processes. This work provides novel insights into the role of NFAT5 in enhancing NF- κ B mediated vascular inflammation and EndMT under pro-diabetic conditions.

2. INTRODUCTION

2.1 Diabetes mellitus

Diabetes mellitus (DM) is a chronic metabolic disease classified by high blood glucose - which after a prolonged duration, contributes to the development of other health complications (https://www.who.int/health-topics/diabetes#tab=tab_1, accessed on 26.06.2022). The global prevalence of this disease had almost doubled from the observed incidence rate of 4.7% in 1980 to 8.5% in 2014, accounting for 422 million adults who have diabetes worldwide (WHO global reports on Diabetes 2016, p. 2). The prevalence of diabetes in Germany in 2019 is outlined in Figure 1.

Total number of German patients suffering from diabetes



New cases of diabetes that were reported in Germany in 2019



Figure 1: Prevalence of diabetes in Germany in the year 2019: The images represent the total number of German citizens affected with diabetes (left) and the new cases of diabetes (right) reported in 2019 in Germany. The image was modified from the news article published by the German Diabetes Center on 07.02.2019 (<https://www.dzd-ev.de/en/latest/news/news/article/number-of-people-with-type-2-diabetes-projected-to-increase-to-12-million-in-germany-by-2040/index.html>, accessed on 25.08.2022)

Based on its pathophysiology, DM can be classified into three forms: type 1 DM (T1D), type 2 DM (T2D), and gestational diabetes (*NATIONAL DIABETES SURVEILLANCE REPORT 2019 Diabetes in Germany*, p.13). The prevalence of T2D has drastically increased in the last three decades and accounts for 95% of the total documented cases of diabetes (<https://www.who.int/news-room/fact-sheets/detail/diabetes>, accessed on 26.06.2022). A certain degree of heterogeneity in terms of clinical characteristics of the disease, its progression, and the risk of the associated complications is evident in the T2D patient cohort. Based on these factors, T2D can be further classified into further subtypes (Ahlqvist et al., 2020). These subtypes include severe insulin-resistant diabetes (SIRD), mild obesity-related diabetes (MOD), and mild age-related diabetes (MARD) (Ahlqvist et al., 2020). The risk factors associated with T2D can be categorized into modifiable and

non-modifiable categories. The non-modifiable factors include ethnicity, genetic predisposition to diabetes, and a previous case of gestational diabetes. In contrast, the modifiable ones consist of obesity, unhealthy eating habits, low levels of physical activity, and smoking (Glovaci et al., 2019).

2.2 Cardiovascular complications of diabetes

Uncontrolled diabetes leads to diabetic-specific secondary diseases, classified as microvascular and macrovascular complications. Microvascular complications caused by the damages incurred to the small blood vessels include diabetic retinopathy, diabetic nephropathy, and diabetic neuropathy (Forbes & Cooper, 2013). Complications arising from injuries caused to large blood vessels are termed macrovascular complications (Forbes & Cooper, 2013), including atherosclerotic cardiovascular diseases (ASCVDs) such as coronary heart disease (CHD), peripheral artery disease (PAD), and stroke (Dal Canto et al., 2019).

A systematic review analyzed the prevalence of cardiovascular diseases (CVD) in 4,549,481 patients with T2D (Einarson et al., 2018). The study reported CVD as the major cause of mortality in patients with T2D, accounting for 50% of all deaths. Moreover, these patients have a 10% higher risk of developing CHD, 53% higher risk of sustaining myocardial infarction, 58% elevated incidence of stroke, and 112% higher chances of heart failure. Thus, T2D is a significant risk factor for developing CVD and accelerating its complications.

2.3. Diabetes is an inflammatory disease

Several pro-inflammatory markers are detectable in the plasma of patients with diabetes, which serve as indicators of the systemic low-grade inflammation experienced by these patients (Al-Dahr, 2016; Meigs et al., 2004; Pradhan et al., 2001). The most important factors and processes responsible for escalating inflammation under pro-diabetic conditions are explained in the following sections.

2.3.1. Association of obesity with type 2 diabetes and cardiovascular complications

Adipose tissue is crucial for regulating metabolism and inflammation in patients with T2D (van Greevenbroek et al., 2013). The β -cells of the pancreas are highly responsive to the nutrient composition of their surrounding microenvironment. Long-term exposure to elevated glucose and free fatty acids subjects these cells to tremendous stress, causing β -cell dysfunction and death. The depletion of β -cell mass results in impaired insulin synthesis and the development of insulin resistance (IR) in the long run (Hudish et al., 2019). Insulin is essential in regulating adipocyte cellular expansion and lipid metabolism (Haczeyni et al., 2018). In the absence of insulin and upon exposure to an excessive nutrient load, adipocytes become stressed. (Hameed et al., 2015). These stressed cells undergo hypertrophy and secrete several chemokines and cytokines that attract immune cells to adipose tissue. The infiltrated immune cells further contribute in escalating the pre-existing inflammation. Moreover, the persistent lipid accumulation polarizes the resident anti-inflammatory M2 macrophages toward pro-inflammatory M1 macrophages (Wu & Ballantyne, 2020)

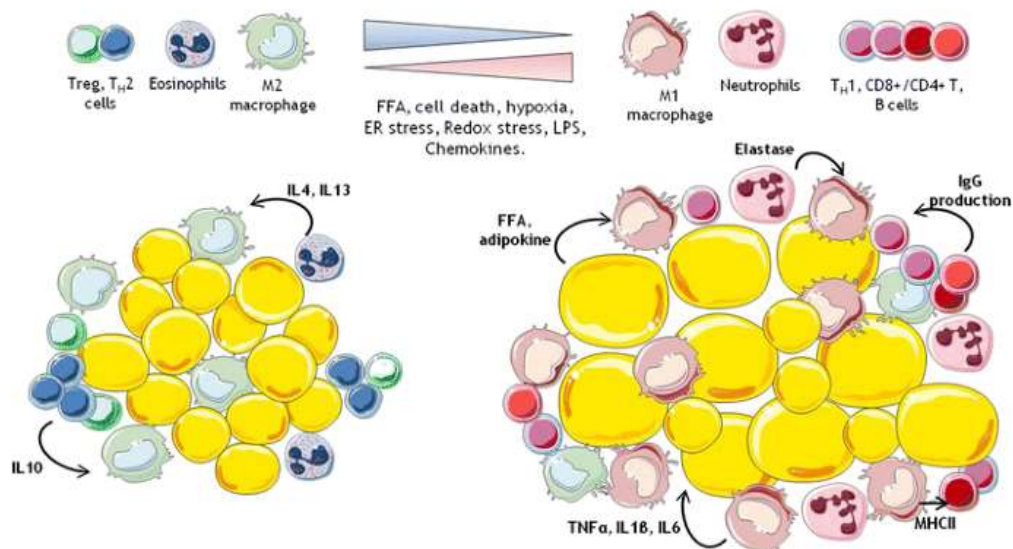


Figure 2: Immune cell modulation and inflammatory status of an obese adipose tissue. An obese adipose tissue is subjected to hypertrophy, immune cell infiltration, and enhanced inflammation, whereas the lean adipose tissue comprises of resident immune cells that mitigate inflammation. Image modified from Kammoun et al., Rev Endocr Metab Disord. 2014 Mar;15(1):31-44.

Around 65-80% of the new cases of T2D in Europe are reported from obese and overweight individuals (<https://www.who.int/europe/news-room/factsheets/item/diabetes>, accessed on 26.06.2022). Additionally, studies have reported a

positive correlation between obesity and prevalence rates of CVD in patients with T2D (Bhatti et al., 2016; Glogner et al., 2014; Tamba et al., 2013). An increased incidence of CHD with increasing body mass index (BMI) has been documented in T2D patients. A five-fold difference in CHD occurrences was observed between the lowest (BMI <25 kg/m² (normal)) and the highest (BMI>40 kg/m² (severely obese)) BMI categories (Wentworth et al., 2012). These findings suggest that obesity is not only a risk factor for diabetes but also seems to aggravate its cardiovascular complications.

2.3.2. Signaling pathways linking insulin resistance and inflammation in diabetes

Large amounts of metabolic stress factors are generated during the progression of insulin insensitivity and adipose tissue enlargement. These stress factors include glucotoxicity, lipotoxicity, oxidative stress, endoplasmic reticulum stress, and pro-inflammatory mediators (Donath & Shoelson, 2011).

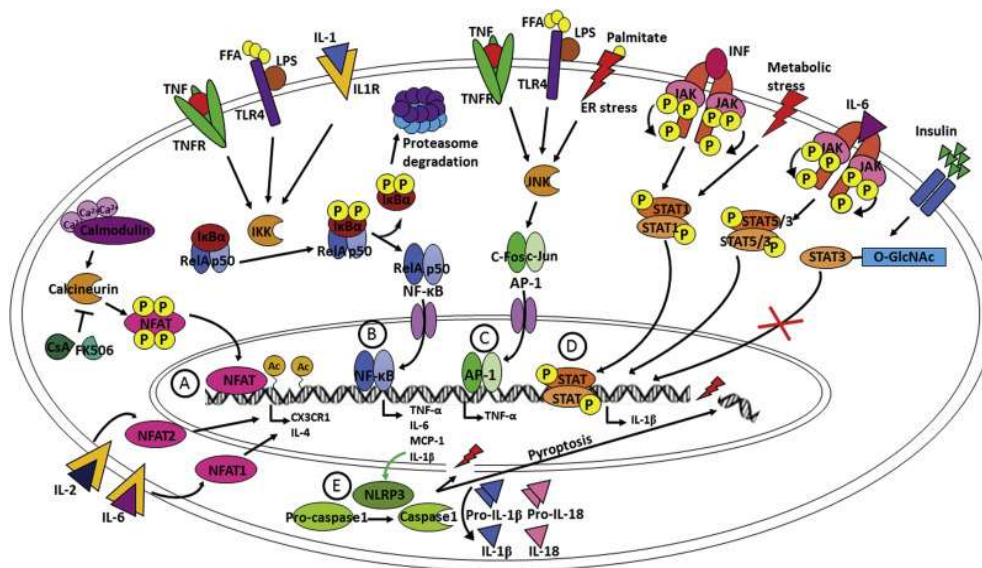


Figure 3: Inflammatory pathways activated by the diabetes-associated metabolic stress factors. Metabolic stressors generated during insulin resistance initiate several signaling pathways that enhance pro-inflammatory gene expression and promote low-grade systemic inflammation in diabetes. Image courtesy: Gonzalez et al., BBA - Molecular Basis of Disease 2018, 1864:3805–3823.

Most of these metabolic stress factors are shown to mediate insulin resistance and inflammation in T2D (Domingueti et al., 2016). They activate pathways such as c-Jun N-terminal kinase (JNK) and NF-κB, promoting the expression of pro-inflammatory genes, e.g. TNF α , IL-6, IL-1 β , and MCP-1, throughout different organs (Lontchi-Yimagou et al., 2013; Yung & Giacca, 2020). The activation of the STAT family of transcription factors which regulate cell growth, survival, and differentiation, is also enhanced during

diabetes (Gurzov et al., 2016). Furthermore, the STAT transcription factors promote inflammation by co-interacting with other transcription factors also activated in diabetes. For example, STAT1 and NF- κ B drive the synthesis of IL-1 β in its precursor form. In addition, the metabolic stress factors also activate NLRP3 inflammasomes that further process this precursor into active IL-1 β (L. L. Gonzalez et al., 2018; Oguntibeju, 2019). STAT3 is responsible for enhancing IL-6 expression, which positively regulates the SOCS proteins responsible for the ubiquitinylation of the insulin receptor substrate proteins (L. L. Gonzalez et al., 2018; Lontchi-Yimagou et al., 2013; Rehman & Akash, 2016).

The release of several pro-inflammatory cytokines is also enhanced in the blood flow of patients who have diabetes (Assar et al., 2016; Hegazy et al., 2020). Few of these chemokines play an essential role in regulating the activity of the transcription factors that belong to the NFAT family. The cytokine IL-2 induces the binding of NFAT2 to the CX3CR1 (Fractalkine) chemokine promoter, leading to its increased expression (Barlic et al., 2004). Fractalkine modulates inflammation by participating in the recruitment and adhesion of the leukocytes to the inflamed tissue site (Shah et al., 2011). Additionally, IL-6 activates NFAT1 transcription, which causes augmented IL-4 synthesis (L. L. Gonzalez et al., 2018). Figure 3 depicts various inflammatory pathways initiated upon exposure to stress factors generated during diabetes.

A plethora of overlapping and cooperating pro-inflammatory pathways are activated upon exposure to diabetes-associated metabolic stress factors. As a result, the expression of several cytokines and chemokines is enhanced, triggering a positive feedback loop of pro-inflammatory signaling cascades. This subjects patients with diabetes to low-grade systemic inflammation.

2.4. The fate of the endothelial cells in type 2 diabetes

The endothelium comprises endothelial cells arranged as a thin monolayer that coats the inner surfaces of blood vessels, forming a barrier between the circulating blood and the tissues. The following sections provide a deeper understanding of its physiological functions and impairment caused by diabetes.

2.4.1. Role of the endothelium in maintaining normal physiological conditions

By its location, endothelial cells act as initial regulators of the bi-directional flux of nutrients, hormones, and macromolecules from the circulating blood into the surrounding tissues and vice versa (Kolka & Bergman, 2012; Yazdani et al., 2019). A glycocalyx on its surface further imparts selectivity to this mechanism (Villalba et al., 2021). The endothelium senses mechanical forces like shear stress or other factors from the blood flow and responds via acute vasoregulation of the blood vessels. Vasodilation is performed by the expression of factors like nitric oxide (NO), endothelium-derived hyperpolarization factor (EDHF), and prostaglandins (PGI₂/PGE₂) (Sena et al., 2013). Its ability to secrete vasoconstrictor endothelin-1 (ET-1) is also a vital step of vasoregulation (Sena et al., 2013). The endothelium not only controls inflammation caused by the recruitment of leukocytes in a regulated manner but also plays a crucial role in wound healing and tissue remodeling (Domingueti et al., 2016; Velnar & Gradisnik, 2018). It further releases fibrinolytic regulators in the blood flow to limit its clotting and avoid the formation of a platelet thrombus (Yau et al., 2015).

2.4.2. Endothelial dysfunction in type 2 diabetes

The metabolic and inflammatory mediators mentioned before impede endothelial cell function. Hampered endothelial nitric oxide synthase (eNOS) (also known as nitric oxide synthase 3 (NOS3)) activity reducing the availability of NO is the hallmark of endothelial dysfunction (ED), along with the impairment of one or more endothelial cell functions (Sena et al., 2013). Endothelial dysfunction is observed from the onset of T2D and is closely related to further micro and macrovascular complications (Schalkwijk & Stehouwer, 2005).

NO is the most vital vasodilator that is produced by NOS3 mainly in response to increased unidirectional shear stress but also to some hormone-like factors circulating in the blood. It facilitates vascular smooth muscle cell relaxation and inhibits inflammation and atherogenesis (Cyr et al., 2020). Stimulation of insulin receptors on endothelial cells leads to the phosphorylation of NOS3, followed by the release of NO (Grandl & Wolfrum, 2018). As mentioned in the above sections, the inflammatory kinases IKK and JNK, activated during insulin resistance, cause impaired insulin signaling at several steps and hamper NO synthesis (Eringa et al., 2013). Moreover, the availability of the essential NOS3 co-factor tetrahydrobiopterin and the NO substrate L-arginine is severely reduced

during diabetes (Shi & Vanhoutte, 2017). Reduced amounts of NO accompanied by enhanced levels of NOS3 inhibitor asymmetric dimethylarginine (AMDA) and NO scavenging free radicals increase the production of vasoconstrictors (Shi & Vanhoutte, 2017). These vasoconstrictors include endothelin-1 (ET-1) and cyclo-oxygenase-dependent contracting factors (EDCF) such as endoperoxides, thromboxane A₂, and prostaglandin E₂ (Shi & Vanhoutte, 2017).

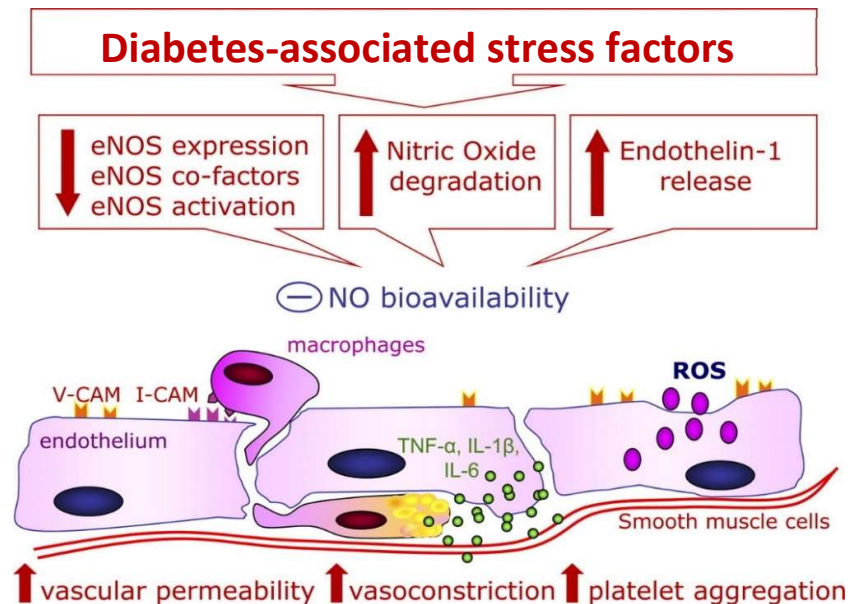


Figure 4: Endothelial dysfunction in diabetes. The metabolic stress factors associated with diabetes lead to endothelial dysfunction majorly by hampering nitric oxide synthesis and availability, which further increases vasoconstriction. The synthesis of pro-inflammatory cytokines and chemokines is enhanced, causing activation and recruitment of leukocytes from the blood. An increased abundance of adhesion molecules such as ICAM and VCAM aids the binding of the leukocytes to the endothelium, and supports their transmigration. Reduced availability of NO causes platelet hyperactivity and aggregation. The image was modified from Potenza et al., *Am J Physiol Endocrinol Metab* 2009;297: E568–E577.

Low-grade systemic inflammation observed during diabetes further activates the endothelial cells to express chemokines like MCP-1 and adhesion molecules/ligands such as VCAM-1, ICAM-1, and E-selectin. These factors attract the circulatory leukocyte to the endothelial surface, further facilitating their attachment and transmigration through the monolayer (La Sala et al., 2019). The infiltrated immune cells escalate the pre-existing inflammation and promote tissue remodeling (La Sala et al., 2019). These events mark the start of atherosclerosis. Pro-inflammatory cytokines such as TNF- α and IL-6 stimulate the expression of the blood-thickening coagulant factors like von-Willebrand factor (VWF), plasminogen activator inhibitor-1 (PAI-1), and surface tissue factor (TF)

(Domingueti et al., 2016). Moreover, these cytokines inhibit the synthesis of anti-coagulant factors such as thrombomodulin and fibrinolytic agents (Domingueti et al., 2016).

Diabetic metabolic stress factors also cause changes in endothelial morphology and extracellular matrix homeostasis. These changes include loss of the glycocalyx, basement membrane thickening, and remodeling modulated by elevated transforming growth factor-beta (TGF- β) (Bakker et al., 2009; Dogné et al., 2018). Additionally, the activation of the transcription factor STAT3 by IL-6 downregulates endothelial cells' tight junction proteins, causing vascular leakage. (Yun et al., 2017). Endothelial cells in a diabetic microenvironment further lose their polygonal morphology and transform into elongated, needle-shaped cells. This morphological change is a sign of endothelial-to-mesenchymal transition (EndMT). The expression of endothelial-specific cell markers is reduced, whereas those typical for mesenchymal lineage cells are upregulated during this phenomenon (Peng et al., 2016; Zhang et al., 2020).

Endothelial cells build the first line of barrier between the tissue and the blood flow. This confers endothelial cells with essential functions ranging from nutrient transport to regulating inflammation and tissue remodeling. The low-grade systemic inflammation and several other stress factors from the diabetic microenvironment lead to injury of the endothelial cell monolayer. They further hinder the functioning of defensive and repair mechanisms employed by the endothelium against such stress factors (Patel et al., 2019; Sena et al., 2013). Prolonged exposure to diabetic conditions causes epigenetic modifications in endothelial cells. These modifications give rise to a hyperglycemic and metabolic memory, inhibiting these cells from reverting to a healthy state even after the stress factors are removed (Paneni et al., 2013; Testa et al., 2017). This endothelial dysfunction not only leads to the onset of vascular complications but also accelerates their progression.

2.5. CD40 signaling and endothelial activation

The CD40 receptor and its ligand CD40L belong to the tumour necrosis factor receptor superfamily and modulate several biological processes. CD40 is expressed on the surface of immune cells (B cells, dendritic cells, and macrophages) as well as non-immune cells (endothelial cells, vascular smooth muscle cells, and fibroblasts) (Michel et al., 2017). CD40L is expressed on the cell membrane of T cells and activated platelets (Aloui et al., 2014). In addition to the membrane-bound form, CD40L is also known to be present in a soluble form (sCD40L) after cleavage from the surface of these cells (Aloui et al., 2014). Approximately 90% of the total amount of circulating sCD40L is released by platelets (Erez et al., 2008).

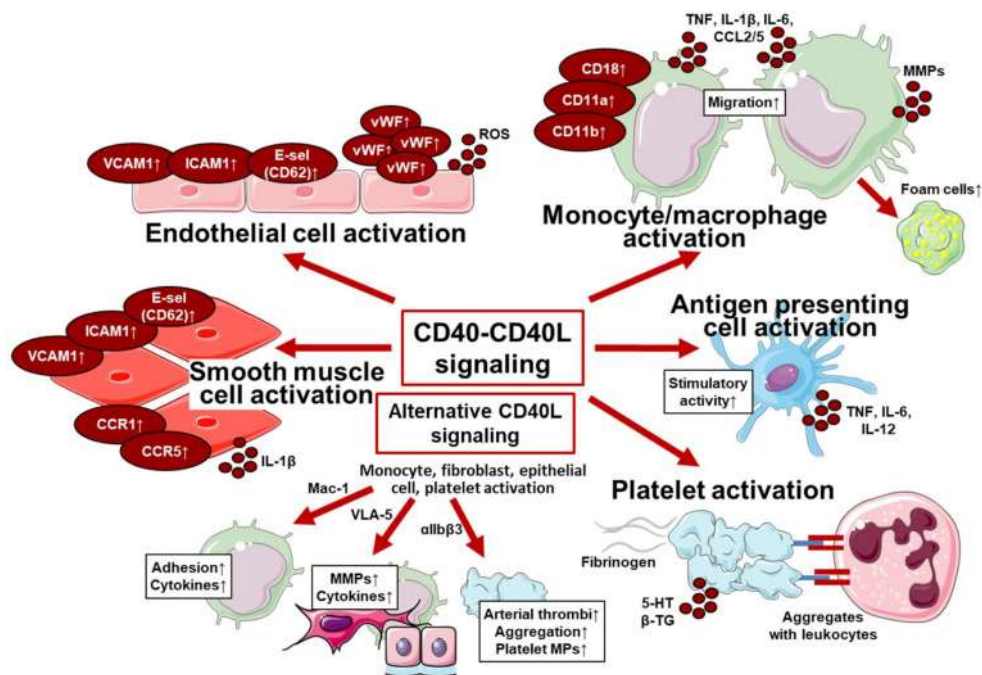


Figure 5: Biological role of CD40 signaling in different cell types. CD40-CD40L promotes activation and subsequent downstream signaling in endothelial cells, smooth muscle cells, platelets, and immune cells. Image courtesy: Daub et al., *Int J Mol Sci.* 2020;21(22):8533.

Engagement of the receptor with the ligand leads to CD40 trimerization and initiation of the downstream signaling cascade. Due to the absence of intrinsic kinase activity in the CD40 receptor, tumour necrosis factor receptor-associated factors (TRAF2/3/5/6) are recruited to the proximal and/or distal end of the CD40 receptor (Hayden & Ghosh, 2014). This results in the activation of different downstream pathways, such as NF- κ B, JNK, or the MAP kinases, depending on the type of recruited TRAF family member (Daub et al.,

2020). While CD40 signaling plays a vital role in inflammation, its function depends on the nature of the host cell type. An illustration of the different biological functions of CD40 signaling in different cell types is presented in Figure 5.

2.5.1. Impact of CD40 signaling on β -cell function, inflammation, and progression of vascular complications associated with diabetes

As mentioned above, obesity and T2D enhance the secretion of pro-inflammatory cytokines in the blood flow. Cytokines such as IL-1 β , IL-6, and TNF- α hamper the viability of the β -cells of the pancreas to a great extent (C. Wang et al., 2010). These cytokines upregulate CD40 surface expression in the β -cells of the pancreatic islet. The co-stimulation of these receptors with CD40L expressed by the infiltrating immune cells activates NF- κ B mediated downstream signaling, which induces the expression of several chemokines and cytokines (Seijkens et al., 2013). These pro-inflammatory mediators escalate pancreatic inflammation impairing β -cell insulin synthesis and release (Seijkens et al., 2013). Additionally, the activation of transcription factors- NF- κ B and STAT-1 by hyperglycemia and hyperlipidemia- further induces β -cell death (Bagnati et al., 2016).

CD40 receptor expressed in adipocytes plays a vital role in adipose tissue inflammation and remodeling. Positive correlations between the adipose tissue CD40 mRNA levels and BMI of lean and obese individuals have been reported (Poggi et al., 2009). The expression of CD40 on the surface of human adipocytes is enhanced during their differentiation (Poggi et al., 2009). The ligation of the CD40 receptor with CD40L instigates cytokine production and mitigates insulin signaling in these cells (Seijkens et al., 2014). Subsequently, infiltrating T-cells further impair adipocyte function by employing the CD40-CD40L pathway (Poggi et al., 2009).

CD40-CD40L signaling is one of the most critical stimuli responsible for the onset of diabetic macrovascular complications (Daub et al., 2020). A graphical representation of the documented CD40-CD40L inter/intracellular interactions and their role in promoting vascular complications is shown in Figure 6.

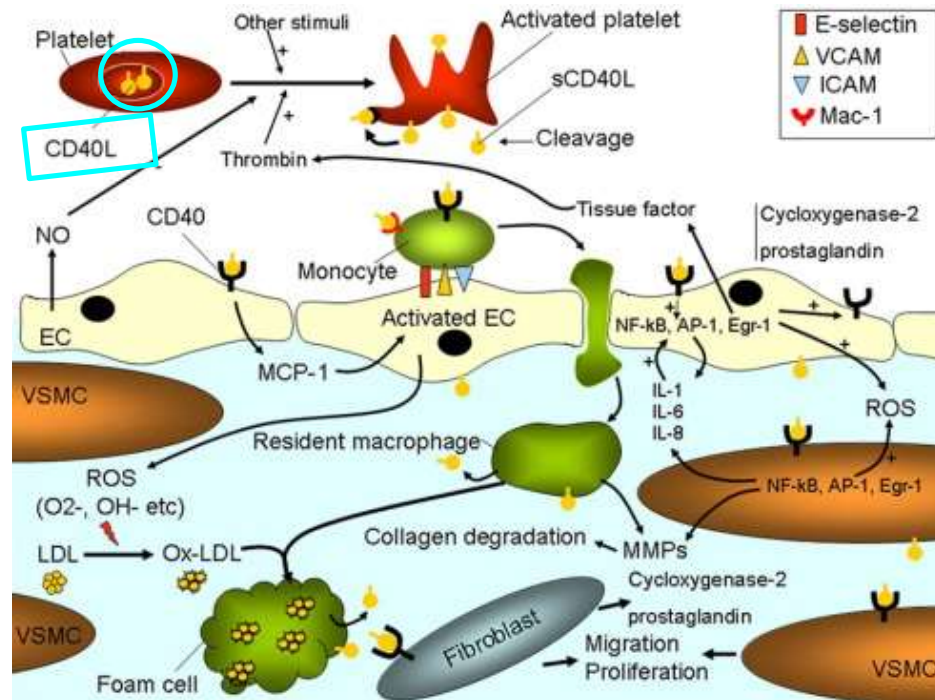


Figure 6: CD40-CD40L signaling is employed at several stages of atherosclerotic initiation and progression. CD40 receptor is expressed by the endothelial cell, vascular smooth muscle cells, immune cells, and platelets. Activation of the CD40 in these cells by the membrane-bound and soluble CD40L upregulates mechanisms such as cell activation, inflammation, and extracellular matrix remodeling, all of which promote atherosclerosis. Modified from *J Am Coll Cardiol* 2009;54(8):669-77

Various signaling pathways that are activated in T2D additionally promote platelet hyperactivity in patients (Cornelius et al., 2019; El Haouari & Rosado, 2008; Kaur et al., 2018). Surface platelet CD40L can bind to CD40 on other platelets, immune cells, and the endothelium (Lordan et al., 2021; Seijkens et al., 2013). Stimulating the endothelial CD40 receptor upregulates the expression of surface adhesion molecules that promote leukocyte adhesion and further aid their transmigration. Stimulating these infiltrated immune cells with CD40L synthesizes pro-inflammatory chemokines such as MCP-1, MIP-1 α/β , and RANTES (Lordan et al., 2021; Seijkens et al., 2013). These steps mark the initiation of atherosclerosis. Through the ligation of CD40, activated macrophages amplify the pre-existing inflammatory conditions in advanced plaques by increasing the expression of cytokines like IL-1 β , IL-2, IL-6, and TNF- α (Jansen et al., 2016). The CD40-CD40L interaction also enhances MMP expression, mediating plaque destabilization leading to plaque rupture and resulting arterial occlusion (Bosmans et al., 2021; Seijkens et al., 2013).

The stress factors upregulated during diabetes promote insulin resistance and upregulate CD40-induced downstream signaling in different cell types. This leads to an enhanced expression of the pro-inflammatory mediators that further contribute to the pre-existing inflammatory conditions. In addition, it also controls cell activation, proliferation, and ECM remodeling in these cells. An ability to modulate such processes entitles CD40-CD40L mediated downstream signaling as a critical player in the initiation and progression of atherosclerosis.

2.5.2. The T-1C *CD40* single nucleotide polymorphism

The most common source of genetic variation in the human genome is the substitution of a single nucleotide with another. This mutation form is called single nucleotide polymorphism (SNP) (D. G. Wang et al., 1998). The knowledge of SNPs can be employed for evolutionary studies, gene discovery, drug response prediction, and as prognostic markers for several diseases (Shastry, 2002). The position of a SNP dictates its potential impact on gene transcription and translation. Therefore, the positioning of the T-1C *CD40* SNP (Rs 1883832) in the Kozak region affects the translational activity and CD40 protein abundance to a great extent (Robert & Pelletier, 2018).

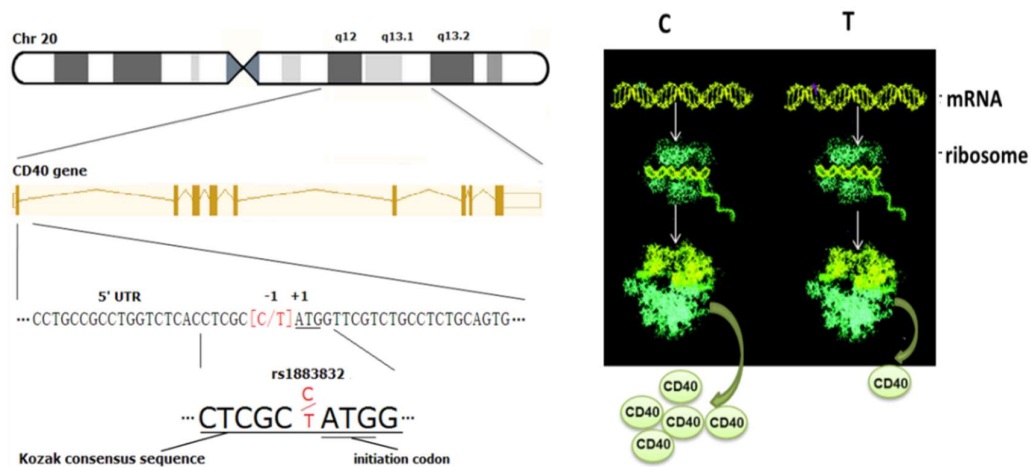


Figure 7: Position of the T-1C SNP of the *CD40* gene and its effect on CD40 protein turnover. The *CD40* gene is situated at the q12-q13.2 loci of chromosome 20 (left image). A base upstream of the start codon could either contain a cytosine or thymine. This SNP of the *CD40* gene is denoted as the T-1C *CD40* SNP or Rs 1883832. 5'UTR refers to 5'-untranslated region. This SNP affects the binding efficiency of the ribosome to *CD40* mRNA (right image), resulting in enhanced CD40 turnover in the C allele than in the T allele. The images are modified from Jacobson et al., *Endocrinology* 146(6):2684–2691 and Yun et al., *PLoS ONE* 9(5): e97289.

The homozygosity for the C allele has been associated with increased susceptibility to CHD (Sultan et al., 2020). Moreover, CC-genotype human cultured endothelial cells revealed augmented secretion of pro-inflammatory cytokines and chemokines (Sultan et al., 2020). Furthermore, a higher surface abundance of pro-inflammatory adhesion molecule VCAM-1 and ligand E-selectin led to increased leukocyte adhesion to their surface (Sultan et al., 2020).

2.6. Aim(s) of the study

As CD40-induced inflammation is known to promote insulin resistance and its vascular complications in diabetes, we hypothesize an association of the T-1C SNP of the *CD40* gene with diabetes mellitus. The allele frequencies of this particular SNP in healthy individuals and patients with T1D and T2D were compared to examine this hypothesis. Furthermore, the amounts of the soluble form of the CD40 ligand in the plasma of the healthy controls and diabetic patients were analyzed. We further hypothesize a more substantial degree of gene expression regulation in the pro-inflammatory CC-genotype HUVECs than in the quiescent TT-genotype cells. To test this hypothesis, RNA sequencing was performed on samples of quiescent and activated CC vs. TT genotype HUVECs. This study further aims at investigating the effects of a long-term diabetes-like microenvironment on the CC-genotype HUVECs.

The main aims of this study are outlined below:

- A. Examine the distribution of the T-1C SNP of the *CD40* gene in healthy individuals and patients with diabetes.
- B. Investigate if the T-1C SNP of the *CD40* gene acts as a risk factor for diabetes.
- C. Analyze *CD40* SNP mediated differential gene expression in sCD40L stimulated CC vs. TT-genotyped HUVECs.
- D. Investigate the effect and mediators involved in endothelial dysfunction in a long-term diabetes-like microenvironment.

3. MATERIALS

3.1. Buffers and Solutions

Table 1: Composition of buffers and solutions used in this study

Buffer/Solution	Composition
Agarose gel electrophoresis	
Loading buffer	10 mM Tris HCl, pH 7.5 10 mM EDTA, pH 8.0 30% Glycerol 0.01% Bromophenol blue 0.01% Xylene green
Running buffer	450 mM Tris 450 mM Boric acid 20 mM EDTA, pH 8.0
Protein extraction	
Lysis buffer (whole-cell extract)	10 mM Hepes, pH 7.9 10 mM KCl 0.1 mM EDTA 0.1 mM EGTA 0.1 M DTT 50 µM Pefabloc 25 µM Protease inhibitors
Pefabloc	15 mM HEPES buffer, pH 7 4 4 % Pefabloc®-SC
Protease inhibitor mixture	1 % Pepstatin A in 20 DMSO
Protease inhibitor mixture	80 % 15 mM Hepes, pH 7.4 1 % Leupeptin in 20 % DMSO 80 % 15 mM Hepes, pH 7.4
Phosphate-buffered Saline (PBS)	8.0 g NaCl 0.2 g KCl 1.44 g Na ₂ HPO ₄ 0.2 g KH ₂ PO ₄
SDS-PAGE	
Blocking buffer	5% milk powder in TBST
Running buffer	248 mM Tris-HCl, pH 8.7 192 mM Glycine 35 mM SDS in 2 L water
Stripping buffer	0.2 M NaOH
Transfer buffer	25 mM Tris 192 mM glycine, pH 8.3
Tris-buffered saline (TBS)	248 mM Tris-HCl pH 8.3

TBS-T	192 mM glycine dissolved in 2 litres H ₂ O TBS+0.05% Tween [®] 20
Decoy ODNs solubilization TEN buffer	40 mmol/L Tris-HCl pH 7.5 1mmol/L EDTA pH 8.0 150 mmol/L NaCl

3.2. Chemicals and reagents

Table 2: List of chemicals and reagents used in this study

Chemicals and reagents	Supplier
Agar-Agar	Carl Roth
Ammonium persulfate	Carl Roth
Bovine Serum Albumin	Carl Roth
β-mercaptoethanol	Sigma-Aldrich
Blotto milk powder	ChemCruz
Bradford solution	Sigma-Aldrich
Chloroform	VWR
Dispase	Gibco, Thermo Fisher Scientific
dNTP	BIORON
Dithiothreitol (DTT)	Carl Roth
DNA ladders and loading dye	Thermo Fisher Scientific
RNA ladder and loading dye	BioLabs
D-Glucose	Merck Millipore
DEPC treated water	Carl Roth
Ethanol	Honey well
Ethidium bromide	Carl Roth
L-mannitol	Sigma-Aldrich
Luminata [™] and Luminata [™] Forte	Merck Millipore
Methanol	Honey well
Oligo dT	Sigma-Aldrich
Pefabloc	Sigma-Aldrich
Pepstatin A + Leupeptin protease inhibitor	Sigma-Aldrich
Polyacrylamide	Carl Roth
Precision Plus Protein Standard [™]	Bio-Rad
RNase away	Molecular BioProducts
RNase free water	Qiagen, Carl Roth
Sodium dodecyl sulfate (SDS)	SERVA
TEMED (Tetramethylethylenediamine)	Sigma-Aldrich
Tween 20	Carl Roth
Tris	Carl Roth
Triton-X 100	Sigma-Aldrich
Trizol	Sigma-Aldrich
Taq Polymerase	BIORON

3.3. Cell culture reagents

Table 3: List of cell culture reagents used in this study

Chemicals and reagents	Supplier
Dimethyl sulfoxide (DMSO)	Sigma-Aldrich
D-Phosphate-buffered saline solution	Gibco, Thermo Fisher Scientific
Endothelial cell growth medium	PromoCell
Endothelial cell growth supplements	PromoCell
Fungizone	Gibco, Thermo Fisher Scientific
Gelatin	Sigma-Aldrich
Heat inactivated fetal bovine serum	Gibco, Thermo Fisher Scientific
MATra-si	IBA Lifesciences
Opti-MEM I	Gibco
Penicillin + Streptomycin	Gibco, Thermo Fisher Scientific
Trypsin	Gibco, Thermo Fisher Scientific

3.4. Consumables

Table 4: List of materials utilized in this study

Materials	Company
60 mm cell culture dishes	Sarstedt
6-well plates	Cell-star
Cell scraper	Sarstedt
PCR tubes	
Pipette tips	
Serologic pipettes	
PVDF Transfer membranes	
RT-PCR tubes and caps	Qiagen

3.5. Kits

Table 5: List of kits used in this study

Kit	Catalogue Number	Supplier
Omniscript RT Kit	205113	Qiagen
QuantiTect SYBR Green R PCR kit	95.064.981	Bio&SELL
RNA Isolation (RNeasy Mini Kit)	74104	Qiagen
Human bone metabolism array Cs1	AAH-BMA-1-2	RayBiotech
NucleoSpin® TriPrep	740966.250	MACHEREY-NAGEL
Agilent RNA 6000 Nano Kit	5067-1511	Agilent Technologies

3.6. Stimulants, siRNAs, and inhibitors

Table 6: List of stimulants and inhibitors used in this study

Recombinant protein	Concentration applied	Company
Soluble trimeric CD40Ligand recombinant MEGACD40L [®] , human	200 ng/ml	Enzo Life Sciences
TNF- α	250 (RNA) and 200 (Protein) U/ml	Biomol GmbH
KRN2 inhibitor	0.5 μ M and 1 μ M	MedChemExpress
NFAT5 siRNA	3 μ g	Santa Cruz Biotechnology, Inc.
Scrambled siRNA	3 μ g	Qiagen

3.7. Oligonucleotides

3.7.1. Primers

Table 7: List of primers used in this study

Gene product	Primer sequence (Direction 5' to 3')	Annealing Temperature
α -SMA	For: GCTTTGCTGGGGACGATGCT Rev: GTCACCCACGTAGCTGCTTT	61° C
CD31	For: GTGAGGGTCAACTGTTCTGT Rev: GTGACCAGTTCACTCTTGGT	63° C
COL1A1	For: CTGGAGAGGCTGGTACTGCT Rev: AGCACCAAGAAGACCCTGAG	65° C
COL3A1	For: CTGGACCCCAGGGTCTTC Rev: CATCTGATCCAGGGTTTCCA	62° C
E-selectin	For: TTCGCCTGTCCTGAAGGATG Rev: TCAGTTGAAGCCGTCCTTG	60° C
FNN1	For: CTGGCCGAAAATACATTGTA Rev: CCACAGTCGGGTCAGGAG	60° C
MCP-1	For: CAAACTGAAGCTCGACTCTCGCC Rev: CAAAGACCCTCAAACATCCCAGG	63° C
NFAT5	For: AATGGAAGTAACAGCAGAA Rev: GGAAGATGATGGTGTGAA	55° C
RPL32	For: AGGCATTGACAACAGGGTTC Rev: GTTGCACATCAGCAGCACTT	60° C
TGF β 2	For: ATAGACATGCCGCCCTTCTT Rev: CTCCATTGCTGAGACGTCAA	57° C
TRAF2	QT00093800 (QuantiTect Primer Assay)	55° C
TRAF6	QT00062888 (QuantiTect Primer Assay)	55° C
VCAM-1	For: CATGGAATTCGAACCCAAACA Rev: GACCAAGACGGTTGTATCTCTG	53° C
VE-cadherin	For: AAGCCTCTGATTGGCACAGT	65° C

	Rev: CTGGCCCTTGTCACTGGT	
ZEB2	For: AAGCCAGGGACAGATCAGC Rev: CCACACTCTGTGCATTTGAACT	60° C
Genotyping primer		
CD40 (T-1C SNP)	Forward outer: GGACCGCGATTGGTCTTTGAAGACCCCG Reverse outer: CACCCACCTCCTGCCCCACAAAAATC T_forward_inner: TGGTCCTGCCGCCTGGTCTCACCTCTCT C_reverse_inner: GACGCACTGCAGAGGCAGACGAACCCTG	62° C

3.7.2. Decoy ODNs

Table 8: List of ODN decoys used in this study

Decoy ODN	Primer sequence (Direction 5' to 3')
NFAT5 forward	CAGTGGAAAATTACGTGCT
NFAT5 reverse	AGCACGTAATTTTCCACTG
NFAT mut	AGTTTAAACATGTTTAAACT

3.8. Antibodies

3.8.1. Primary antibodies

Table 9: List of primary antibodies used in this study for Western blot (WB) and Immunocytochemistry (ICC)

Target	Dilution	Provider/Catalogue number	Application
α -SMA	1:1000	Cell Signaling #19245S	WB
α -SMA	1:100	Abcam # ab5694	ICC
β -actin	1:200	Abnova MAB8232	WB
CD31	1:1000	Cell Signaling #3528S	WB
CD31	1:20	DAKO JC70A	ICC
CD40	1:1000	Abcam ab13545	WB
GPX-1	1:1000	GeneTex GTX116040	WB
GPX-4	1:1000	Abcam ab125066	WB

NFAT5	1:50	Novus Bio sc-13035	ICC
NOS3	1:2500	BD Biosciences Pharmingen #610296	WB
SM22 α	1:1000	GeneTex GTX629078	WB
VCAM-1	1:2000	Abcam #ab134047	WB

3.8.2. Secondary antibodies

Table 10: List of secondary antibodies used in this study for Western blot (WB) and Immunocytochemistry (ICC)

Secondary antibody	Dilution	Provider/Catalogue number	Application
Donkey IgG- Alexa 647 (Anti-mouse)	1:100	Jackson ImmunoResearch #715-606-150	ICC
Donkey IgG- Cy5 (Anti-mouse)	1:100	Jackson ImmunoResearch	ICC
Goat IgG- HRP (Anti-rabbit)	1:3000	Sigma-Aldrich A6154	WB
Goat IgG- HRP (Anti-mouse)	1:5000	Sigma-Aldrich A4416	WB

3.8.3. Miscellaneous Equipment

Table 11: Miscellaneous equipment utilized

Equipment	Model	Supplier
Agarose gel electrophoresis power supply	EV231	peQLab
CO2 incubator	VIOS160i	HERACell
Centrifuge	Universal 32	Hettich
Digital Imaging System	ImageQuant LAS 4000 mini	GE Healthcare
Dry block heater	HBT-1131	Haep Labor Consult
Fluorescence microscope	Axio observer Z1 Inverted Microscope	Carl Zeiss
Gel electrophoresis chamber		Self-made
Image analyzer	Gel Doc [®] XR Imager	Bio-Rad
Lab pH meter	pH 720	InoLab [®]
Laminar flow	HS18 Hera safe	Heraeus Instruments
Light microscope	Axiovert 25	Carl Zeiss

Microplate spectrophotometer	PowerWave XS	Bio Tek Instruments
Mini transfer chamber	Mini Trans-Blot®	Bio-Rad
NanoDrop spectrophotometer	ND-One	Thermo Fisher Scientific
PCR cycler	Mastercycler personal	Eppendorf
Rotor geneQ	2PLEX	Qiagen
SDS-PAGE system	Mini-Protean® Tetra Cell	BioRad
Water bath	SU1811	Sunlab
Weighing scale	Entris II	Sartorius

4. METHODS

4.1. Diabetes patient samples

White blood cell samples from 203 type 2 diabetes (T2D), 49 type 1 diabetes (T1D) patients, and 80 healthy individuals were obtained from Dr. Stefan Kopf (Department of Medicine I, Endocrinology and Clinical Chemistry, University Hospital Heidelberg). The average ages of the control cohort and patients with T1D and T2D were 55 years, 49 years, and 63 years respectively.

4.2. Isolation of DNA, RNA, and protein from patient and control samples

DNA, RNA, and protein were isolated from the patient and control white blood cell samples using the NucleoSpin® TriPrep kit. This kit consists of specialized lysis buffers containing chaotropic ions that immediately inactivate all the degrading enzymes in almost all biological materials while creating appropriate binding conditions, favouring RNA and DNA adsorption to the silica membrane. The protein is collected in the flow-through, which can be further precipitated.

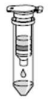




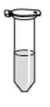


DNA and RNA Purification (both bound to the silica membrane)		Protein Purification (protein in the column flow-through)	
6	Wash silica membrane		1 st and 2 nd wash each: 500 µL <i>DNA Wash</i> 1 min, 11,000 x <i>g</i>
7	Dry membrane		RT, 3 min (with open lid)
8	Elute DNA		100 µL <i>DNA Elute</i> Incubate 1 min 1 min, 11,000 x <i>g</i>
9	Digest residual DNA		95 µL DNase reaction mixture RT, 15 min
10	Wash and dry silica membrane		1 st wash 200 µL RA2 2 nd wash 600 µL RA3 30 s, 11,000 x <i>g</i> 3 rd wash 250 µL RA3 2 min, 11,000 x <i>g</i>
11	Elute highly pure RNA		60 µL H ₂ O (RNase-free) 1 min, 11,000 x <i>g</i>
12	Precipitate protein		10–700 µL flowthrough 1 vol PP RT, 10 min 5 min, 11,000 x <i>g</i>
13	Wash protein pellet		500 µL ethanol (50%) 1 min, 11,000 x <i>g</i>
14	Dry protein pellet		RT, 5–10 min
15	Prepare protein sample		20–100 µL PSB-TCEP 3 min, 95–98 °C 1 min, 11,000 x <i>g</i>

Figure 8: Additional purification steps applied to the isolated DNA, RNA, and protein samples. The image on the left outlines the steps performed to obtain purified nucleic acid. The image on the right represents the steps performed to obtain purified protein. Image modified from <https://www.mn-net.com/media/pdf/a0/12/3b/Instruction-NucleoSpin-TriPrep.pdf>, accessed on 02.08.2022.

RP1 buffer supplemented with 1% β -mercaptoethanol was added to the frozen cell pellets and vortexed vigorously. This solution was pipetted onto the NucleoSpin[®] Filter, followed by centrifugation at 11,000 rpm for 1 min. An equal volume of 70% ethanol was added to the flow-through. After a series of quick vortexing steps, it was applied to the NucleoSpin[®]TriPrep silica Column. The protein was collected in the flow-through following a short centrifugation step while the RNA and DNA were embedded in the silica membrane. The steps further performed to obtain purified DNA, RNA, and protein samples are described in detail in Figure 8.

4.3. *CD40* SNP genotyping

4.3.1. Tetra-arms PCR

The tetra-primer amplification refractory mutation system-polymerase chain (ARMS-PCR) reaction was performed to identify the T-1C *CD40* genotypes of the cells obtained from the diabetic patients and the HUVEC donors. This method consists of outer forward and outer reverse primers amplifying the area flanking the SNP, producing non-allele-specific control amplicons and acting as an internal control for the PCR. Another set of forward inner and forward outer primers generate allele-specific amplicons of different lengths that can be separated via agarose gel electrophoresis. The composition of the PCR mixture and the amplification parameters are elaborated in Tables 12 and 13, respectively.

Table 12: Composition of the reaction mixture for PCR

Component	Volume (μ l)
PCR buffer (10X)	5
dNTPs (10mM)	1
Forward primer	2
Reverse primer	
T forward inner primer	
C reverse inner primer	
Taq polymerase	0.25
RNAse free water	32.75
DNA	3
Total	50

Table 13: PCR program for the genotyping of the T-1C SNP of the *CD40* gene

Step	Temperature (°C)	Time
Pre-denaturation	95	5 min
Denaturation	95	60 s
Annealing	62	45 s
Synthesis	72	60 s
Extension	72	5 min

4.3.2. Agarose gel electrophoresis

Agarose gel electrophoresis applies an electric field to migrate the negatively charged DNA to the positive electrode through agarose gel that acts as a molecular sieve separating the DNA fragments for their sizes. The amplified PCR products obtained from tetra-arms PCR were analyzed via this method. Agarose gel with a density of 2% (w/v) was prepared by dissolving 3 g agarose in 150 ml TBE buffer and was briefly cooked in the microwave for approximately 2 min. This solution was supplemented with 3 µl of ethidium bromide to visualize DNA. The gel solution was poured into the gel chamber and incubated at room temperature until polymerized. DNA samples mixed with 10 µl of 6X loading dye and standard DNA ladders were loaded into the respective wells of the gel. Electrophoresis was performed at 120 V for 60 min. The resolved samples were visualized using the Gel Doc XR+ system and the Quantity One software (Version 4.6.9, Bio-Rad Germany).

4.4. ELISA

Enzyme-linked immunosorbent assay (ELISA) was performed to detect the soluble amounts of CD40 receptor and ligand present in the plasma samples of diabetic patients. The steps were executed according to the manufacturer's protocol. Samples were added to the respective assay diluents in the ratios of 1:5 and 1:4 for detecting sCD40R and sCD40L, respectively. Afterwards, they were incubated on an orbital shaker for 2 hr at room temperature. After a series of washing steps, the samples were incubated with the conjugates provided in the respective kits for 2 hr at room temperature. Washing steps were performed to remove the unbound conjugate, and samples were incubated with substrate solution for 30 min in the dark. The reaction was terminated by adding the stop solution. After that, the optical density was determined at 450 nm using a colorimetric

plate reader. Standard curves were generated with standards provided by the manufacturer.

4.5. Cell isolation and culture

4.5.1. Human umbilical vein endothelial cells (HUVEC)

Human umbilical vein endothelial cells (HUVECs) were isolated from freshly collected umbilical cords provided by the surrounding hospitals with the consent of the local Ethics Committee (S-383/2013). A cannula was inserted into the ends of the umbilical veins, which D-PBS was then flushed through until the outcoming PBS was free of residual blood. Dispase (3.1 g/l) solution was added to the veins through the cannula with its ends closed and incubated for 30 min at 37°C. It was then collected into a falcon and centrifuged at 1000 rpm for 5 min. The resulting cell pellet was resuspended in HUVEC growth medium containing supplements provided in the kit (except hydrocortisone), antibiotics, and antimycotic agents. These cells were seeded onto a 2% (w/v) pre-gelatinized polystyrene 60 mm dishes and stored in a CO₂ incubator at 37°C until further use.

4.6. Cell culture designs

4.6.1. Sample preparation for RNA-Seq analysis

One set of cell culture experiments aimed at identifying differential gene expression between *CD40* SNP CC- and TT-genotype HUVEC. Upon reaching confluence in P1, the cells were stimulated with sCD40L (200 ng/ml) for 12 hr.

4.6.2. Diabetes-like cell culture model

Another set of cell culture experiments aimed to create a simulated ‘diabetes-like microenvironment’ where the HUVECs with CC-genotype were cultured in high glucose (25 mmol/L) medium supplemented with TNF- α (250 U/ml for mRNA and 200 U/ml for protein) for three days. The medium was changed after every 1.5 days to compensate for the half-life of TNF- α (<https://www.geneandcell.com/blogs/molecular-biology-methods/human-tnf-alpha-stability-testing>, accessed on 08.09.2022). The cells were then stimulated with sCD40L and collected after 8 hr for RNA isolation and 16 hr for protein and cell medium supernatant isolation. TNF- α concentration was determined to its corresponding range reported in the plasma of diabetic patients (Y. Gonzalez et al., 2012; Qiao et al., 2017).

4.6.3. NFAT5 siRNA transfection

CC-genotype HUVECs were transfected with NFAT5 and scrambled siRNA upon reaching 40-50% confluence in P1. Cells were washed with +/+ PBS and incubated with 2 ml of Opti-MEM I during the preparation of the transfection medium. The transfection medium was prepared by diluting 3 µg of respective siRNAs in Opti-MEM I. Then, 3 µL of MATra-si reagent was added to constitute a final volume of 200 µL for a single well of a 6-well plate. This medium was incubated at room temperature for 20 min, during which it was thoroughly vortexed at regular intervals and then added to the cells. The 6-well plate was incubated for 30 min on a magnetic plate at 37°C, after which the medium was replaced with the regular HUVEC medium. Further stimulation, as mentioned in section 4.6.2, was performed 24 hr post-transfection.

4.6.4. Treatment with KRN2 inhibitor

CC-genotype HUVECs were subjected to the abovementioned diabetic conditions in the presence of the KRN2 inhibitor. The stock inhibitor solution was diluted 10-folds in DMSO to obtain a 1 mM solution, out of which 1 µl and 2 µl were added to a single well of a 6-well plate to reach a final concentration of 0.5 µM and 1 µM, respectively. DMSO with a final concentration of 0.01% was added to the control conditions to compensate for any effects that the DMSO could cause. This was performed during each medium change, as described in section 4.6.2.

4.6.5. Treatment with NFAT5 oligonucleotide decoy

Lyophilized human NFAT5 forward and reverse ODNs were dissolved in the TEN buffer. After that, they were heated at 95°C for 7 min in equal volumes, followed by a cooling phase to obtain a hybridized decoy solution. The resulting double-stranded molecule was confirmed by resolving on a 2.5% agarose gel with a low molecular weight marker.

CC-genotype HUVECs at a confluency of around 50% were incubated with a final concentration of 10 µM NFAT5 ODNs for 2 hr before subjecting them to the diabetic microenvironment. They were additionally treated with the ODNs during each medium change, as described in section 4.6.2.

4.7. Collection of conditioned medium

Conditioned medium from the cultured cells was collected 16 hr after sCD40L stimulation of CC-genotype HUVECs cultured under the aforementioned diabetes-like conditions. It was centrifuged at 1000 rpm for 5 min. The resulting supernatant medium was isolated, and the dead cell debris pellet was discarded. The isolated supernatant was then snap-frozen in liquid nitrogen and stored at -80°C until further use.

4.8. Quantitative measurement of proteins in the conditioned medium of cultured HUVEC

Cytokines and growth factors secreted into the conditioned medium by the CC-genotype HUVECs under the diabetes-like cell culture model were detected via the Quantibody[®] Human Bone Metabolism array. The Quantibody[®] array is a multiplexed sandwich ELISA-based quantitative array platform that screens for 31 specific cytokines and growth factors simultaneously. RayBiotech provided the quantification and screening services. RNA extraction from cells

4.8.1. RNA extraction for gene expression analysis

To isolate RNA from adherent cells, they were gently washed twice with ice-cold ++ D-PBS and lysed using 350 µl RNA lysis buffer supplemented with 1% β-mercaptoethanol. An equal amount of 70% absolute ethanol was added to the cells. Further steps were carried out according to the manufacturer's instructions described in the Qiagen RNEasy extraction kit. Column silica membranes act as the binder of RNA in this process. The cell/lysis buffer/ethanol suspension was eluted via these column membranes. A series of washing steps using the different buffers provided in the kit and centrifugation formed the basis of the next few steps. DNA/cellular components-free RNA obtained in the end was eluted in 30 µl of RNase-free water.

4.8.2. RNA extraction for RNA-Seq

A Series of additional steps were applied to the abovementioned protocol to increase the RNA purity and yield obtained from the cells marked for RNA-Seq. The RNA bound to the column silica membranes was eluted in 100 µl RNase-free water. Equal amounts of TRIZOL and 1/5th of chloroform were added to this eluted RNA and centrifuged at 13,000 rpm at 4°C for 20 min. TRIZOL is a monophasic solution of phenol and guanidine isothiocyanate, facilitating the disruption and dissolution of cell components while

maintaining RNA integrity. Further addition of chloroform aids in the phase-based separation of RNA, DNA, and protein, wherein RNA forms the top aqueous phase. RNA was isolated from this aqueous phase and mixed with equal amounts of n-isopropanol. After a freeze and thaw cycle, the samples were centrifuged at 10,000 rpm for 10 min at 4°C. The resulting pellet was subjected to 75% ethanol washing followed by centrifugation. RNA was condensed into an air-dried pellet and resuspended in 50 µl of RNase-free water. The heating of samples at 60°C for 10 min was performed to dissolve the pellet into a homogenous RNA solution.

4.9. Quantification of RNA quality

4.9.1. A260/A280 absorbance ratio

Nucleic acids have a maximum absorbance at 260 nm, and proteins at 280 nm. The ratio of A260/A280 of the RNA sample indicates the presence of residual organic solvents and proteins resulting from the isolation process. Therefore, the purity of the eluted RNA was determined by calculating the ratio of absorbance readings at 260 and 280 nm (A260/A280) spectrophotometrically. Samples with A260/A280 falling within the range of 1.9 to 2.1 were used for further procedures.

4.9.2. Native RNA gel electrophoresis

As RNA quality is essential for a highly sensitive technique such as RNA-Seq. The purity of the samples was measured via native agarose gel electrophoresis and Bioanalyzer and the basic A260/A280 ratio. For a pure and intact RNA sample, the ratio of the molecular weights and fluorescence band intensities between the separated 28S and 18S rRNA are equal to 2:1, respectively.

Agarose gel with a density of 1% (w/v) was prepared as described in section 4.3.2. RNA samples were diluted with respective volumes of RNase-free water to reach a final concentration of 2 µg in a total volume of 10 µl. They were then supplemented with 3.33 µl of 3X sample loading buffer. RNA ladder was constituted by adding 16 µl of 2X loading dye to 4 µl of RNA ladder. The samples and the ladder were denatured at 65°C for 10 min. Electrophoresis was thereby performed at 180 V for 16 min. The resolved samples were visualized using the Gel Doc XR+ system and the Quantity One software (Version 4.6.9, Bio-Rad Germany). An exemplary image of the results obtained at the end of electrophoresis is presented in Figure 9A.

4.9.3. Bioanalyzer

Bioanalyzer is a sample-specific chip-based method that applies the principle of microfluidics to analyze DNA, RNA, protein, and cells. Samples are mixed with a fluorescent dye and pipetted on the wells located on a chip. Upon initiating the Bioanalyzer device, the samples are processed through the gel matrix located in the microchannels and further separated by electrophoresis. The separated samples are detected by fluorescence, generating an electropherogram and gel-like image. Furthermore, a score termed RNA Integrity Number (RIN) is generated that signifies the purity and intactness of the RNA sample. The highest RIN score of 10 indicates completely intact RNA, whereas a RIN score of 0 represents degraded RNA.

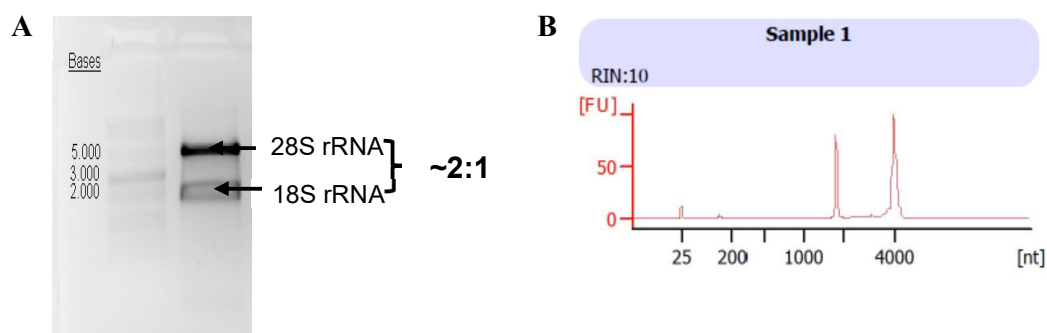


Figure 9: RNA quality analysis post isolation. The exemplary pictures depict post-isolation RNA quality which was analyzed via (A) native gel electrophoresis and (B) Agilent 2100 Bioanalyzer. The 2:1 ratio (28S:18S) is a good indication that the RNA is completely intact. RIN: RNA Integrity Number is the score generated by the Agilent 2100 Bioanalyzer to denote the quality of RNA. A RIN score of 10 represents intact non-degraded RNA.

The loading gel matrix was prepared by adding 550 μ l of Agilent 6000 Nano gel matrix to a spin filter and centrifuged for 10 min at 1500 rpm. RNA 6000 Nano dye in the ratio 1:65 was added to the above gel matrix and centrifuged at 13,000 rpm for 10 min. A volume of 9 μ l of this mixture was loaded on the RNA Nano chip and allowed to polymerize, and then further plunged to form a sample loading well. RNA samples were diluted with RNase-free water to reach 100 ng/ μ l and denatured at 70°C for 2 min. RNA 6000 Nano marker was added to each well, to which 1 μ l of RNA sample and RNA ladder was added to their respective wells. The chip was then vortexed at high speed to form a homogenous sample and fluorescent dye mixture. This chip was placed into the Agilent 2100 Bioanalyzer and further assessed according to the manufacturer's protocol. An exemplary image of the RIN score generated after the run is over is provided in Figure 9B.

4.10. Reverse transcription and cDNA synthesis

RNA with a total amount of 1 µg was reverse transcribed to cDNA using the Qiagen Omniscript® Reverse Transcription Kit in a final reaction volume of 20 µl. For this purpose, appropriate amounts of the RNA samples were added to RNase-free water to form a solution of 12 µl. 8 µl of master mix comprising reverse transcriptase (RT) enzyme, RT buffer, RNase inhibitor, dNTPs, and random primers was added (Table 14). Added primer cocktail ensured transcription of all regions of sample RNA, including the untranslated regions. The samples were then incubated at 37°C for 1 hr for reverse transcription. After cooling, the resulting cDNA was diluted 1:5 using RNase-free water and stored at -20°C until further use.

Table 14: Composition of the reaction mixture for RT-qPCR

Component	Volume (µl)
Oligo-dT primer	2
dNTP	2
10X RT buffer	2
RNase inhibitor	1
Reverse transcriptase	1
RNA 10 µg	12

4.11. Real-time quantitative reverse transcription-polymerase chain reaction (RT-qPCR)

Gene expression analysis was performed to determine the expression status of the target genes (Table 9) using QuantiTect SYBR Green® Kit (Qiagen, Germany) with the LightCycler 1.5 instrument (Roche Diagnostics, Germany). The reaction mixture consisted of 15 µl of the gene expression master mix comprised of SYBR green, forward, and reverse primers and 5 µl of cDNA to make up a final volume of 20 µl. The recipe of the above master mix is depicted in table 15. The real-time qPCR program started with a heating step at 95°C for 15 min, followed by denaturation at 95°C for 15 seconds. The following annealing of the primers depended on the temperature listed in Table 9 and lasted for 25 sec. The subsequent extension step was executed at 72°C for 10 sec. The last three steps were repeated for 39 cycles for all analyzed genes. The housekeeping gene RPL32 was also quantified with the target genes for internal endogenous control. Samples were pipetted in duplicates that served as technical replicates. The specificity of the amplified product was assessed by the production of a single melting peak positioned

outside that of the negative control. The cycle threshold value (Ct) is generated at the end of the analysis, referring to the cycle number required to overcome the fluorescence threshold caused by background noise. Fold changes in the target gene expression were computed by applying $2^{-\Delta\Delta CT}$ formula stated below:

$$ratio = \frac{(E_{target})^{\Delta CP_{target}(control-sample)}}{(E_{ref})^{\Delta CP_{ref}(control-sample)}}$$

E_{target}, E_{ref} = amplification efficiencies of the target and reference gene

CP_{target}, CP_{ref} = fluorescence crossing points

Table 15: Composition of the reaction mixture for RT-qPCR

Component	Volume (µl)
5X Evagreen	4
Forward primer	1
Reverse primer	1
RNase free water	9
cDNA	5

4.12. Preparation of whole-cell lysate

Cultured HUVECs were gently washed twice with ice-cold ++ DPBS and harvested using a cell scraper. The cell suspension was centrifuged at 3000 rpm for 5 min at 4°C, and the supernatant was discarded. The remaining cell pellet was dissolved in 30 µl of RNase-free water. The nitrogen decompression method disrupted the cell membrane to extract cellular proteins. For this purpose, the cell suspension was exposed to 5 cycles of freeze and thaw, wherein the cell pellet was snap-frozen in liquid nitrogen followed by thawing at 37°C. Upon completing these five cycles, two-fold concentrated homogenization I buffer containing protease inhibitors (Pepstatin, Leupeptin, and Pefabloc) and DTT as a reducing agent were added in an equal volume to the cell suspension. Finally, centrifugation at 3000 rpm for 5 min at 4°C was performed. The supernatant was transferred to a new Eppendorf tube and stored at -80°C.

4.13. Protein quantification and sample preparation for Western blot

To ensure that an equal protein amount was loaded in each well, it was necessary to determine the initial protein concentrations of the samples. Bradford assay was performed for this purpose. This assay is based on the degree of color change observed

in Coomassie blue dye upon binding to proteins, which is directly proportional to the protein content of the sample.

Bradford solution was diluted 5-folds and was added to the wells of a 96-well plate in a volume of 200 μ l. BSA standards with protein concentrations ranging from 0-30 μ g/ml were pipetted into the wells containing Bradford solution. These standards with known protein concentrations were employed to generate a standard linear curve, from which the total protein concentrations of the sample could be interpolated. Diluted protein samples (dilution depended on confluence before cell harvesting) were also added to the Bradford solution. Protein amounts were measured at 595 nm using a microplate spectrophotometer.

Protein samples were diluted with appropriate volumes of RNase-free water to obtain a final loading concentration of 20 μ g. The samples were then heated up to 95°C for 5 min in the presence of respective volumes of 4X sample loading buffer and stored at -80°C until further use.

4.14. SDS Polyacrylamide gel electrophoresis and protein transfer

Separation of protein samples based on their molecular weights was achieved via denaturing sodium dodecyl sulfate-polyacrylamide gel electrophoresis (SDS-PAGE). This method employs protein separation in an electric field using two types of denaturing gels. These gels differ in pore sizes and ionic strengths, facilitating proteins to form specific bands according to their molecular weight, irrespective of their loading properties and tertiary structures.

Denaturing gels with a density of 12% overlaid with 4% stacking gel in a gel chamber of 1.5 mm thickness were prepared as mentioned in table 16 and were incubated for polymerization. Denatured protein samples with a total concentration of 20 μ g and a dual-color protein marker with defined molecular weights were pipetted into the respective well of the stacking gel. Electrophoresis using a vertical system was performed at 80V for 30 min, upon which the dye front crossed the stacking-resolving gel interface. The voltage was increased to 120V until the dye front reached the end of the resolving gel. A standard sandwich assembly consisting of sponges, filter papers, resolved gel, and pre-activated PVDF membrane (0.45 μ M, activated with methanol incubation) was constructed. Electrotransfer that applies emersion of electrodes into cold transfer buffer

was performed at 350 A for 60-90 min resulting in the transfer of proteins from gel to PVDF membrane.

Table 16: SDS gel components

Component	Separating gel (12%)	Stacking gel (4%)
1.5M Tris-HCl (pH 8.8)	4 ml	-
1.5M Tris-HCl (pH6.8)	-	0.38 ml
SDS (10%)	100 μ l	30 μ l
APS (10%)	100 μ l	30 μ l
Acrylamide (30%)	4.08 ml	0.4 ml
TEMED	6 μ l	3 μ l
Water	1.72 ml	2.2 ml
Total	10 ml	3 ml

4.15. Immunostaining procedure and band intensity analysis

After protein transfer, the PVDF was briefly washed with Millipore water and incubated with a solution of 5% (w/v) blotto milk powder in TBS-T as a blocking reagent for 1 hr on a shaker. This step ensured the elimination of any unspecific binding activities. Afterwards, the membrane was cut into fragments corresponding to the molecular weights of the protein of interest and incubated with primary antibodies (Table 9) prepared in blocking solution overnight on a speed rotator at 4°C. The next day, the membranes were washed thrice with TBS-T for 5 min each to remove any weakly bounded or unbound antibodies. The membranes were then incubated with horseradish peroxidase-conjugated secondary antibodies specific to primary antibodies for 1 hr at room temperature. The following steps consisted of washing the membrane three times with TBS-T for 5 min each and then with TBS for 10 min to remove residual detergents.

4.16. Immunocytochemistry

CC-genotype HUVECs cultured under the diabetic cell culture model were fixed with ice-cold methanol for 30 min at 4°C. After that, methanol was discarded, and the cells were air-dried to remove residual methanol. After two washing steps with PBS, cells were blocked with 10% goat serum and 7% BSA in PBS, including 0.1% TritonX100 for 1 hr, and subsequently incubated overnight with respective primary antibodies at 4°C. The next day three PBS washing steps of 5 min each were performed to remove unbound antibodies. The cells were then incubated with respective secondary antibodies for 1 hr in the dark. Information about the antibodies is outlined in Table 9 and Table 10. After

additional washing steps, the nuclei of the cells were stained with DAPI solution (Invitrogen, 1:1250 - 1:2500 in PBS) for 8 min in the dark. After two PBS washing steps of 10 min each, the stained regions were covered with coverslips using 13.3% (w/v) Mowiol (Calbiochem, La Jolla, CA, solved in 0.2 M Tris-HCl, pH 8.5, and 33.3% (w/v) glycerine) as the mounting medium. The cells were finally imaged via Axio observer Z1 inverted fluorescence microscope and viewed on TissueFax Viewer7.10.

4.17. Data analysis

4.17.1. RNA-Seq

Data obtained from RNA-Seq experiments were analyzed with Dr. Eugen Rempel and Olga Ermakova (The Centre for Organismal Studies Heidelberg, Stem cell Biology, Department headed by Prof. Dr. Jan Lohmann). The sample sizes consisted of 5 CC and 3 TT-genotype control and sCD40L-stimulated HUVEC pairs. Two TT-genotype HUVEC pairs were eliminated from the analysis as they were outliers in the principal component analysis (PCA). The gene targets that were differentially regulated significantly ($P > 0.05$) were further analyzed using Reactome online analysis tool. The top twenty curated pathways were documented.

4.17.2. Analysis of NFAT5 cytoplasmic and nuclear abundance

Three regions of interest (ROI): one at the center and others near the circumference of the well of a 6-well plate containing the cells stained for NFAT5 protein were randomly selected. A minimum of 49 images were recorded from each of these ROI for all the treatment groups. Analysis of the NFAT5 nuclear and cytoplasmic abundances of the cells in these ROI was kindly performed by Dr. Holger Lorenz (Head of imaging facility, ZMBH). To analyze Cy5-labeled protein signal intensities inside and outside nuclear areas of cells, DAPI was used as a nuclear counterstain. Binary mask images were created from both the Cy5 and the DAPI images, and subtraction of the DAPI mask images from the corresponding Cy5 mask images created Cy5 mask images exclusive of nuclear regions. For correct masks, 1-pixel-radius linear mean and median filters were applied to the input images to eliminate pixel outliers. Also, empirically-determined size exclusions were used to avoid incorrect background and nuclei area sizes. The appropriate sets of mask images were subjected to segmentation, i.e., nuclear regions only vs. everything else but nuclear regions. The foreground areas were redirected to the rolling ball background-subtracted Cy5 micrographs for intensity measurements. To automate the

whole process, a macro, IntensityAnalysis_final.ijm, was created for both the data analyses and the recording of all analysis parameter settings, including log files, results tables, ROI (region-of-interest) lists and all processed images. The macro allowed for selecting image data sets from multiple folders and guaranteed fully quantitative analyses in a comparable and reproducible manner. The mean intensities of the Cy5-labeled protein signals were taken directly from the results tables and grouped and averaged for comparisons of the individual conditions. All image processing, image analyses, and macro generation were performed with FIJI (Schindelin et al., 2012).

4.18. Statistical analysis

Data were initially tested for normal Gaussian distribution by applying the Shapiro-Wilk test. Since all the other experimental groups were normalized to the control group, the fold-change value for this group was always set at 1 or 100%. Therefore, a comparison between the control and treated groups was performed using a one-sample t-test. Comparison between two groups was performed by unpaired t-test for normally distributed data and Mann-Whitney test for not normally distributed data. Differences amongst three or more groups were computed via ordinary one-way ANOVA (Gaussian distribution) and the Kruskal-Wallis ANOVA test (non-Gaussian distribution). All experiments (except immunocytochemistry) consist of n=7-8 biological replicates. A high degree of variability in response to treatment was visible in individual preparations due to their genetic makeup. Considering this factor, uncorrected Fischer's LSD posthoc test was performed for normally distributed data, whereas uncorrected Dunn's test was performed for not normally distributed data. GraphPad Prism version 9.2 (GraphPad Software, USA) was used to analyze all experiments. Data are represented as mean \pm standard deviation unless stated otherwise.

5. RESULTS

5.1. Prevalence of the T-1C SNP of the *CD40* gene in patients with type 2 and type 1 diabetes

An association of the T-1C SNP of the *CD40* gene with CHD has been previously documented (Sultan et al., 2020). The association of this particular SNP with diabetes was further investigated in this study. For this purpose, DNA samples of 203 patients with T2D, 49 patients with T1D, and 80 healthy individuals were genotyped for the T-1C SNP of the *CD40* gene through tetra-arms PCR. One hundred and ten of 203 T2D patients were homozygous for the C allele, 6 for the T allele, and 87 were heterozygous carriers (Figure 10B). However, the distribution of *CD40* SNP genotypes in T1D was different than the trend observed in the population with CDH and T2D, with the highest percentage of CT carriers. Seventeen of 49 T1D patients were homozygous for the C allele, 1 for the T allele, and 31 were heterozygous (Figure 10C).

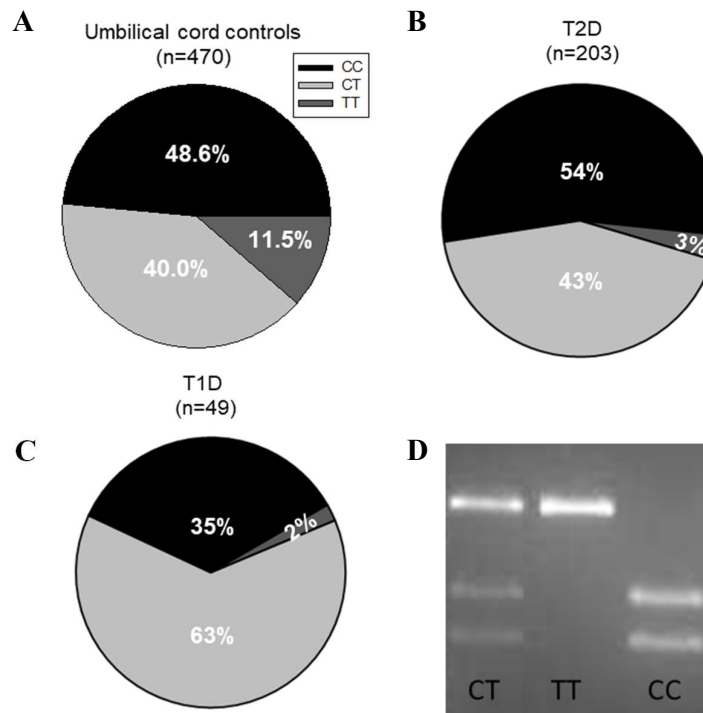


Figure 10: Comparison of the allele frequency of the *CD40* SNP amongst a control cohort and patients with T2D and T1D: Pie chart denoting the *CD40* SNP genotype in (A) umbilical cord controls with 49% CC-genotype as compared to 54% in the T2D (B) and (C) 35% in the T1D patient cohorts. (D) Representative gel electrophoresis image of 3 genotypes of the T-1C SNP of the *CD40* gene.

Chi-square analysis was used to verify a statistically significant association of the genotype with T2D, as previously published for patients with CHD (Figure 11). Homozygosity for the T allele conferred a 4.3-fold lower risk of developing T2D as

compared to that for the C allele (P=0.0002). These data suggest that the T-allele confers a certain degree of protection against T2D.

A	CHD Patients (%) n=346	Controls (%) n=470	Odds Ratio 95% CI	P value
C	521 (75.3)	644 (68.5)	Reference	
T	171 (24.7)	296 (31.5)	1.38 (1.11-1.71)	0.0031
Genotype				
CC	194 (56.1)	228 (48.5)	Reference	
CT	133 (38.4)	188 (40.0)	-	
TT	19 (5.5)	54 (11.4)	2.22 (1.31-3.75)	0.0028
CC	194 (56.1)	228 (48.5)	Reference	
CT+TT	152 (43.9)	242 (51.5)	1.35 (1.03-1.77)	0.0331

B	T2D Patients (%) n=203	Controls (%) n=470	Odds Ratio 95% CI	P value
C	307 (76)	644 (68.5)	Reference	
T	99 (24)	296 (31.5)	1.43 (1.09-1.86)	0.0091
Genotype				
CC	110 (54)	228 (48.5)	Reference	
CT	87 (43)	188 (40.0)	1.043 (0.74-1.46)	0.8620
TT	6 (3)	54 (11.4)	4.342 (1.90-9.66)	0.0002
CC	110 (54)	228 (48.5)	Reference	
CT+TT	93 (46)	242 (51.5)	1.26 (0.91-1.75)	0.1802

C	T2D Patients (%) n=203	T1D Patients (%) n=49
C	307 (76)	65 (66)
T	99 (24)	33 (34)
Genotype		
CC	110 (54)	17 (35)
CT	87 (43)	31 (63)
TT	6 (3)	1 (2)
CC	110 (54)	17 (35)
CT+TT	93 (46)	32 (65)

Figure 11: Association of the T-1C SNP of the *CD40* gene with susceptibility to CHD, T2D, and T1D. The tables represent the allele frequencies and genotype distribution in total n-numbers and percentages among the CC, CT, and TT genotypes in patients with (A) coronary heart disease and healthy controls (Sultan et al., 2020), with (B) type 2 diabetes and healthy controls, and between (C) type 1 diabetes and type 2 diabetes cohorts. The populations are in accordance with the Hardy–Weinberg equilibrium. Odds ratios were calculated via Fisher’s exact test. n: number of subjects examined; CI: confidence interval.

5.2. Comparison of plasma levels of sCD40 and sCD40L between patients with T1D, T2D, and healthy individuals

Patients with diabetes are subjected to enhanced CD40 downstream signaling due to significantly increased levels of soluble CD40L (sCD40L) shed by hyperactive platelets (Jinchuan et al., 2004; Yngen, 2005). Plasma levels of sCD40L in healthy individuals and patients with T1D and T2D were analyzed by ELISA. Soluble CD40L plasma levels were 1.7-fold and 2.2-fold higher in the patients with T2D than in the healthy and T1D cohorts (Figure 12B). There was no significant difference in plasma sCD40L levels between the healthy control group and the T1D group.

The C-allele of the *CD40* SNP provokes a pro-inflammatory endothelial cell phenotype which can be compensated by the soluble form of the CD40 receptors (sCD40). Soluble

CD40 receptor obtained by the shedding of membrane CD40 and alternative splicing of CD40 transcript is shown to bind and thereby neutralize the pro-inflammatory effects of sCD40L (Esposito et al., 2012; Tang et al., 2021). To examine the existence of this compensatory mechanism in diabetes, sCD40 plasma levels of healthy control and patient cohorts were detected through ELISA.

The abundance of sCD40 in the plasma of patients with T1D and T2D was 1.3-fold elevated compared to the healthy individuals (Figure 12A). Furthermore, the plasma sCD40 content of patients with T2D was significantly increased than those suffering from T1D. Hence, it can be inferred that patients with diabetes are subjected to enhanced sCD40 production to mitigate the pro-inflammatory effects of increased sCD40L amounts.

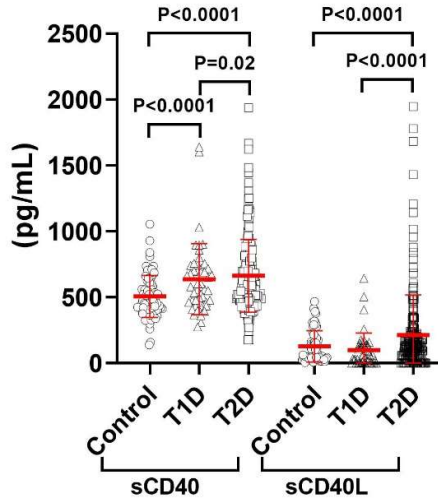


Figure 12: Comparison of sCD40 and sCD40L plasma levels in healthy individuals and patients with diabetes. The amounts of sCD40 (left) and sCD40L (right) in the plasma of healthy individuals (n=78), patients with T1D (n=48), and T2D (n=192) are depicted in the scatter plots. Two outliers from control, 1 outlier from T1D and 11 outliers from T2D were excluded respectively, after performing the Grubb's test. Data are represented as means \pm SD.

5.3. Association of the T-1C SNP of the *CD40* gene with the plasma levels of sCD40 and sCD40L in patients with diabetes

Plasma sCD40L and sCD40 levels of healthy individuals and those suffering from diabetes were further characterized according to their *CD40* SNP. This was done to visualize any genotype-based differences in these entities. No significant differences were observed in the sCD40L and sCD40 plasma levels between the CC vs. TT-genotype individuals in the healthy control and T1D patient cohorts (Figures 13A and 13B). CC-genotype T2D patients revealed a 1.5-fold higher sCD40 level than their TT-genotype

counterparts (Figure 13C). Comparing sCD40 levels among the other genotypes in this group of patients depicted trends but did not reach statistical significance (Figure 13C). Plasma levels of sCD40L were unaffected by the T-1C SNP of the *CD40* gene.

These findings suggest that the *CD40* SNP has a prominent effect on the sCD40 production under T2D conditions. However, it is difficult to draw any conclusions regarding the impact of this SNP under normal physiology and T1D owing to insufficient numbers of TT-genotype samples.

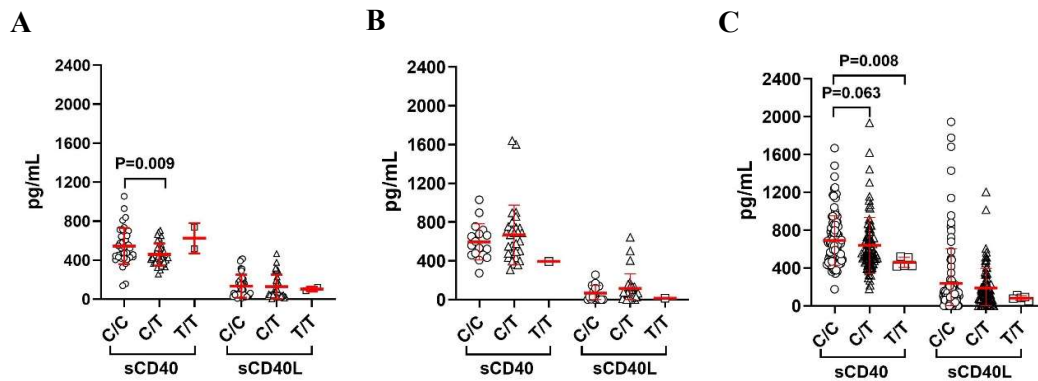


Figure 13: Association between sCD40/sCD40L plasma levels and the T-1C SNP of the *CD40* gene in healthy controls and in patients with diabetes. Plasma sCD40 and sCD40L protein abundances of (A) Healthy control (n=78), and patients with (B) T1D (n=48), and (C) T2D (n=192) are represented according to their T-1C SNP genotypes. Two outliers from control, 1 outlier from T1D, and 11 outliers from T2D were excluded respectively, after performing the Grubb's test. Data are represented as mean (for CC-genotype control and T1D cohort samples control and means \pm SD.

Next, Pearson's correlation matrix was generated to detect genotype-based correlations between sCD40L and sCD40 levels in the three genotypes. A moderate positive correlation could be detected between sCD40 and sCD40L levels in the plasma of CC-genotype patients with T1D (Figure 14A). Similarly, a weak positive correlation between sCD40 and sCD40L was also evident in the CC-genotype T2D patient cohort (Figure 14B).

No correlation was observed between sCD40 and sCD40L plasma levels in the CT-genotype T1D patients ($r=0.201$, $p=0.296$) or in the CT-genotype ($r=0.113$, $p=0.314$) and TT-genotype patients with T2D ($r=0.110$, $p=0.318$). CC-genotype cells demonstrate higher CD40 surface abundance than their TT-genotype counterparts (Sultan et al., 2020). Increased levels of sCD40L, as seen in patients with diabetes, subject these cells to an enhanced degree of activation. Hence, the CC-genotype patients with diabetes are rescued by the increased availability of the sCD40 receptor, as suggested by the positive correlations between their sCD40L and sCD40 levels.

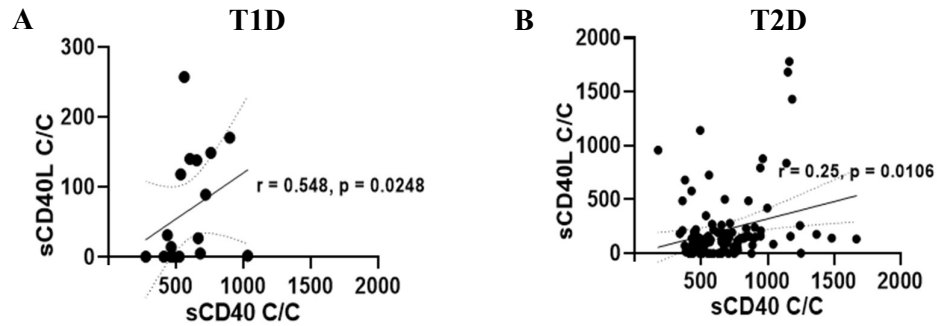


Figure 14: Correlation of the sCD40 and sCD40L plasma levels in the CC-genotype T1D and T2D patients. The graphs designate a Pearson’s correlation matrix between the soluble CD40 receptor and ligand plasma contents in the CC-genotype patients with (A) T1D and (B) T2D.

5.4. Results of RNA-Seq analysis

A higher surface abundance of CD40 receptor drives enhanced CD40 downstream signaling in CC-genotype HUVECs compared to TT-genotype cells (Sultan et al., 2020). As a result, CC-genotype HUVECs possibly depict a higher expression of the mediators and their target genes involved in downstream CD40 signaling in these cells (Sultan et al., 2020). Genome-wide comparison of the RNA samples obtained from CC vs. TT-genotype HUVECs stimulated with sCD40L for 12hr was performed. This was done to gain deeper insights into the genes differentially expressed between these two genotypes.

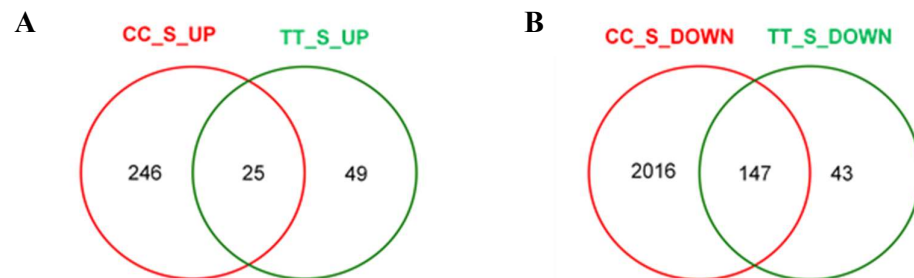


Figure 15: Differentially expressed genes in sCD40L stimulated CC vs. TT- genotype HUVECs. The Venn diagrams illustrate the number of genes differentially (A) upregulated and (B) downregulated in sCD40L stimulated CC (n=5) vs. TT (n=3) genotype HUVECs.

Stimulation with sCD40L depicted a higher degree of transcriptional regulation in the CC-genotype HUVECs than in the TT-genotype counterpart. Around 3.7-fold higher number of genes were upregulated in the sCD40L-stimulated CC-genotype HUVECs. A few of these upregulated genes that are relevant in driving endothelial dysfunction and cardiovascular complication are highlighted in Table 17. The upregulated gene products in the sCD40L-stimulated CC-genotype HUVECs were assigned to 13 signaling

pathways (Supplementary Table S1), most of which participate in escalating inflammation. The number of genes downregulated in these cells was much higher than that of the genes upregulated by sCD40L stimulation. Some downregulated gene products contribute toward selenocysteine synthesis, scavenging hydrogen peroxide molecules and nitric oxide synthesis. The significantly downregulated gene products are listed in Table 18. The pathways associated with the downregulated gene products are recorded in the supplementary table S2.

Table 17: List of differentially upregulated gene products in the sCD40L stimulated CC-genotype HUVECs

Family/Function	Gene name		Log2 Fold change	Adjusted P-value
Pro-inflammatory mediators	CCL2	C-C motif chemokine ligand 2	2.22	7.79 x 10 ⁻³¹
	VCAM1	Vascular cell adhesion molecule 1	3.15	1.66 x 10 ⁻⁶
	TNFRSF4	TNF receptor superfamily member 4	2.48	1.71 x 10 ⁻⁶
	IRAK2	Interleukin 1 receptor associated kinase 2	0.695	5.57 x 10 ⁻⁴
	CX3CL1	C-X3-C motif chemokine ligand 1	0.962	0.042
	IFNGR1	Interferon gamma receptor 1	0.974	0.011
Involved in insulin signaling	INSR	Insulin receptor	0.816	6.72 x 10 ⁻⁴
Mediating NF-κB downstream signaling	MAP3K14	Mitogen-activated protein kinase kinase kinase 14	0.776	7.52 x 10 ⁻⁴
	NFKB1	Nuclear factor kappa B subunit 1	0.579	0.005
	TRAF3	TNF receptor associated factor 3	0.753	0.002
	TNFSF10	TNF superfamily member 10	0.814	0.013
Extracellular matrix proteins and their regulators	MMP1	Matrix metalloproteinase 1	0.757	4.88 x 10 ⁻⁵
	ADAMTS9	ADAM metalloproteinase with thrombospondin type 1 motif 9	0.566	0.029
	LAMC1	Laminin subunit gamma 1	0.401	0.027

	COL4A1	Collagen type IV alpha 1 chain	0.403	0.017
Mediators of EndMT	JAG1	Jagged canonical Notch ligand 1	0.834	8.24×10^{-5}
	PSEN1	Presenilin 1	0.479	0.024

Table 18: List of differentially downregulated gene products in the sCD40L stimulated CC-genotype HUVECs

Family/Function	Gene name		Log2 Fold change	Adjusted P-value
Selenocysteine synthesis	RPS5	Ribosomal protein S5	-0.5	9.99×10^{-4}
	RPLP0	Ribosomal protein lateral stalk subunit P0	-0.423	0.005
	RPL10	Ribosomal protein L10	-0.435	0.002
	FAU	FAU ubiquitin like and ribosomal protein S30 fusion	-0.418	0.01
Selenoaminoacid metabolism	QARS1	Glutaminyl-tRNA synthetase 1	-0.445	5.22×10^{-4}
	RPS15	Ribosomal protein S15	-0.398	0.005
	AHCY	Adenosylhomocysteinase	-0.434	0.01
Mediating NF-κB downstream signaling	TRAF7	TNF receptor associated factor 7	-0.453	9.9×10^{-4}
	NKIRAS2	NFKB inhibitor interacting Ras like 2	-0.344	0.008
	TRAF4	TNF receptor associated factor 4	-0.463	0.003
	NFKBID	NFKB inhibitor delta	-0.626	0.023
	CD40	CD40 molecule	-0.334	0.018
H2O2-scavenging enzymes	GPX3	Glutathione peroxidase 3	-0.652	7.28×10^{-4}
	GPX4	Glutathione peroxidase 4	-0.419	0.003
	GPX1	Glutathione peroxidase 1	-0.426	0.011
Nitric oxide synthesis	NOS3	Nitric oxide synthase 3	-0.573	5.87×10^{-4}

Compared to the CC-genotype, only a few genes were differentially regulated in the sCD40L-stimulated TT-genotype HUVECs. Most of the upregulated gene products, as denoted in Table 19, were protective against inflammation, endothelial dysfunction, and EndMT. On the other hand, the mediators of inflammation, thrombosis, and endothelial dysfunction were downregulated in these cells (Table 20). An overview of the pathways attributed to the differentially up/downregulated gene products in the sCD40L-stimulated TT-genotype HUVECs is provided in the supplementary tables S3 and S4, respectively.

Table 19: List of differentially upregulated gene products in the sCD40L stimulated TT-genotype HUVECs

Family/Function	Gene name		Log2 Fold change	Adjusted P-value
Anti-inflammatory	RHBDF2	Rhomboid 5 homolog 2	0.377	0.04
	SUMO1	Small ubiquitin like modifier 1	0.57	0.04
	ANXA1	Annexin A1	0.547	0.016
Inhibitor of EndMT	NCOA7	Nuclear receptor coactivator 7	0.903	4.78 x 10 ⁻³
Adaptation to stress factors	HMGB1	High mobility group box 1	0.52	0.011
	NPM1	Nucleophosmin 1	0.397	0.020
	NAMPT	Nicotinamide phosphoribosyltransferase	0.885	0.029
Regulation of endothelial function	ZEB1	Zinc finger E-box binding homeobox 1	0.876	0.028
Inhibition of VEGF-induced hyper-permeability	TNFSF15	TNF superfamily member 15	0.751	0.020

Table 20: List of differentially downregulated gene products in the sCD40L stimulated TT-genotype HUVECs

Family	Gene name		Log2 Fold change	Adjusted P-value
Pro-inflammatory	GRAMD4	GRAM domain containing 4	-0.533	9.96 x 10 ⁻³
	CAMK2N1	Calcium/calmodulin dependent protein kinase II inhibitor 1	-0.661	0.0103
Mediators of endothelial dysfunction	TXNIP	Thioredoxin interacting protein	-1.19	60.3 x 10 ⁻⁴
	BMP4	Bone morphogenetic protein 4	-0.455	4.78 x 10 ⁻³
	CPT1A	Carnitine palmitoyltransferase 1A	-0.372	0.028
	DLGAP4	DLG associated protein 4	-0.348	0.014
Pro-thrombotic	PEAR1	Platelet endothelial aggregation receptor 1	-0.369	5.13 x 10 ⁻³
	TSPAN18	Tetraspanin 18	-0.341	0.022

Extracellular matrix proteins and their regulators	COL3A1	Collagen type III alpha 1 chain	-0.508	1.52 x 10 ⁻⁴
	HTRA1	HtrA serine peptidase 1	-0.34	0.04
	TIMP2	TIMP metalloproteinase inhibitor 2	-0.362	0.022

The result obtained from RNA-Seq analysis document the TT-genotype as the protective one with upregulation of protective biological processes and downregulation of those driving endothelial dysfunction. In contrast, the CC-genotype seems highly susceptible to inflammation, endothelial dysfunction, and EndMT. This data supports the previous findings made by our working group (Sultan et al., 2020).

5.5. Impact of a diabetes-like microenvironment on pro-inflammatory gene expression in CC-genotype HUVECs

CD40-CD40L induced downstream signaling in endothelial cells enhances the expression of surface adhesion molecules and the release of chemokines facilitating recruitment of circulating immune cells and their extravasation. Prominent marker gene products include E-selectin, VCAM-1, and MCP-1 (Sultan et al., 2020). The C-allele of the T-1C SNP of the *CD40* gene showed a strong association with T2D. Hence, the effects of a microenvironment comprised of hyperglycemia and pro-inflammatory mediators were studied with CC-genotype HUVECs.

In this study, HUVECs were exposed to 25 mM glucose (G) for 80 hr and 96 hr for RNA and protein isolation, respectively. In addition, HUVECs were also subjected to pro-inflammatory mediators: TNF- α and sCD40L (T+L) in the absence or presence of glucose (G+T+L) for the duration mentioned above.

E-selectin mRNA expression was enhanced 1.4-fold in HUVECs exposed to high glucose (group G vs. control; Figure 16A). Exposure to sCD40L with or without hyperglycemia increased the expression of E-selectin about 116-fold (group L vs. G+L; Figure 16A). Co-treatment with TNF- α and sCD40L (T+L) upregulated E-selectin mRNA expression 737-fold compared to control (Figure 16A). Under hyperglycemic conditions (G+T+L), this effect was further augmented by a factor of 1.4 (Figure 16A).

Incubation of HUVECs with high glucose led to a 1.2-fold increased *MCP-1* mRNA levels (G vs. control; Figure 16B). *MCP-1* mRNA levels were further enhanced 13-fold upon treatment with sCD40L with or without hyperglycemia (group L vs. G+L; Figure 16B). TNF- α /sCD40L combined treatment raised *MCP-1* mRNA expression by 32-fold

(control vs. T+L; Figure 16B), which was further upregulated by 1.3-fold upon inclusion of high glucose (T+L vs. G+T+L; Figure 16B).

Interestingly, there was no effect of hyperglycemia on the mRNA expression of *VCAM-1* and *CD40*, irrespective of the exposure to sCD40L or TNF α plus sCD40L (Figure 16C and 16 D).

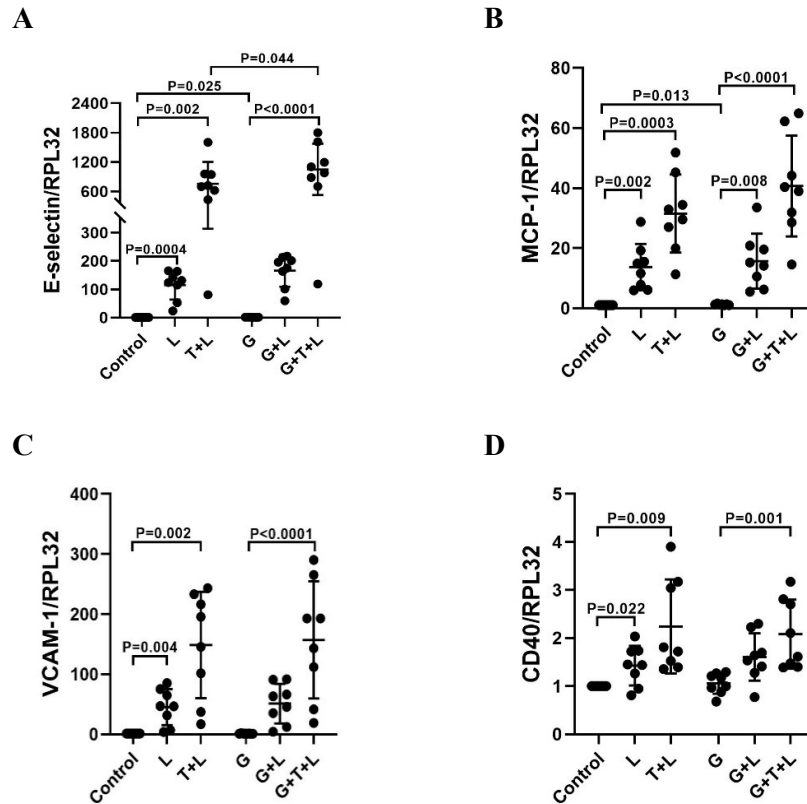


Figure 16: Pro-inflammatory mediators with/out hyperglycemia upregulate pro-inflammatory mRNA expression in HUVECs. The scatter plots represent the effect of single sCD40L (200 ng/ml), and sCD40L (200 ng/ml) /TNF- α (250 U/ml) combined stimulation with/out hyperglycemia (25 mM) on the mRNA expression of (A) E-selectin, (B) *MCP-1*, (C) *VCAM-1*, and (D) *CD40*. The cycle threshold values of the target genes were normalized to those of the RPL32 housekeeping gene. Data are represented as means \pm SD; n=8.

An enhancing effect of sCD40L with or without TNF- α co-incubation on HUVEC pro-inflammatory mRNA expression has been confirmed in this study. These observations are in line with the findings documented in the literature. However, glucose seemed to have a selective impact on the mRNA levels of certain pro-inflammatory genes, such as E-selectin and *MCP-1* but did not modulate *VCAM-1* and *CD40* mRNA expression to a great extent.

5.6. Analysis of soluble factors released into the supernatant of CC-genotype HUVECs subjected to a diabetes-like microenvironment

Systemic low-grade inflammation persists in diabetes, causing an enhanced release of several cytokines, chemokines, and soluble forms of adhesion molecules in the blood flow (Assar et al., 2016; Hegazy et al., 2020). Multiplex sandwich ELISA screening was performed to analyze amounts of such pro-inflammatory mediators released by the HUVECs upon exposure to a pro-inflammatory environment in the presence of high glucose.

5.6.1. Soluble forms of surface adhesion molecules

In addition to the surface expression of endothelial adhesion molecules there are also their soluble forms, which are shed from the luminal surface of the endothelium into blood (Herren, 2002).

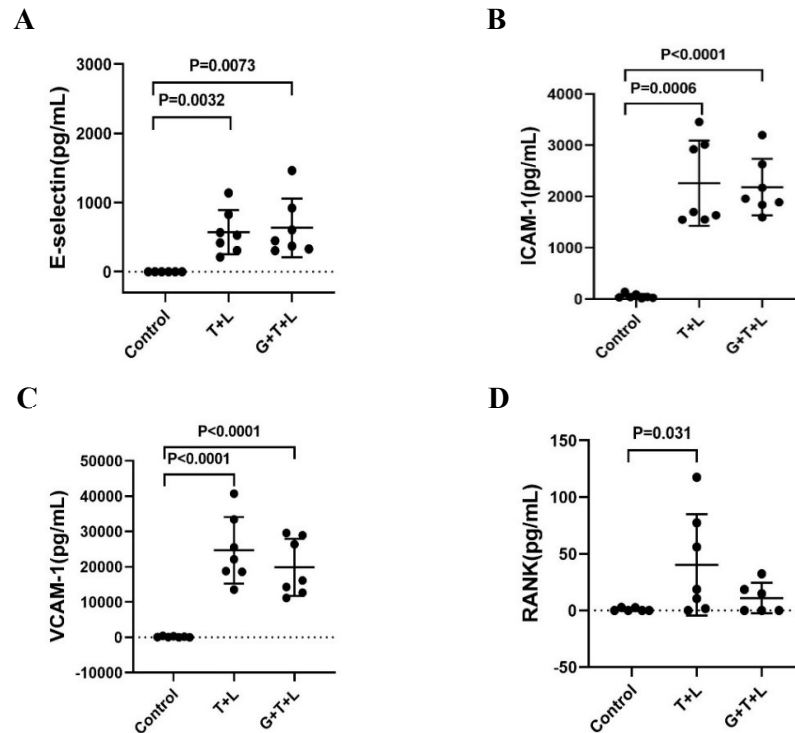
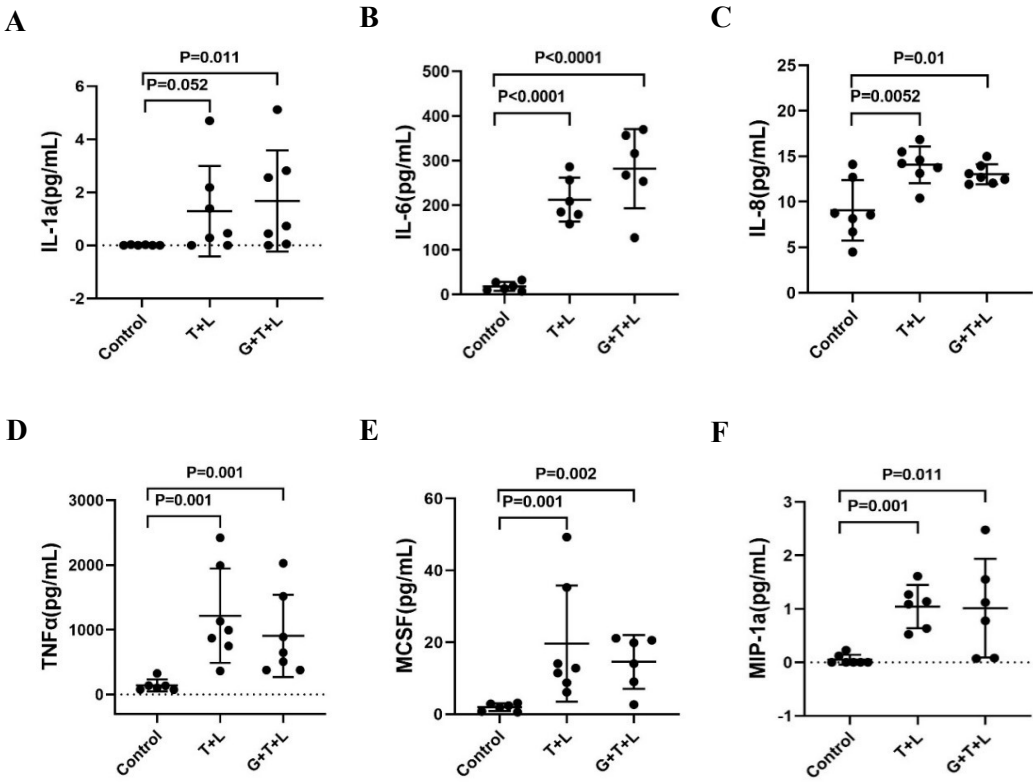


Figure 17: Soluble forms of surface adhesion molecules are enhanced in the supernatant of HUVECs exposed to pro-inflammatory mediators with/out glucose. The scatter plots represent the abundance of (A) E-selectin, (B) ICAM-1, (C) VCAM-1, and (D) RANK in the conditioned medium of HUVECs subjected to sCD40L/TNF- α co-stimulation in the presence or absence of high glucose. The quantitation of these entities was performed through multiplexed sandwich ELISA. Data are represented as means \pm SD; n=6-7.

Looking into this in the cultured HUVECs revealed that shedding of the soluble form of E-selectin was not significantly different between the T+L and G+T+L groups (Figure 17A). This was also true for the soluble forms of ICAM-1, VCAM-1, and RANK (Figure 17B-D).

5.6.2. Cytokines, chemokines, and growth factor

Several pro-inflammatory pathways are upregulated during the course of β -cell dysfunction and insulin resistance, leading to the release of various cytokines and chemokines (Y. Gonzalez et al., 2012). Conditioned medium collected from the cultured HUVECs was analyzed by multiplexed sandwich ELISA to detect the abundance of such cytokines and chemokines released by these cells.



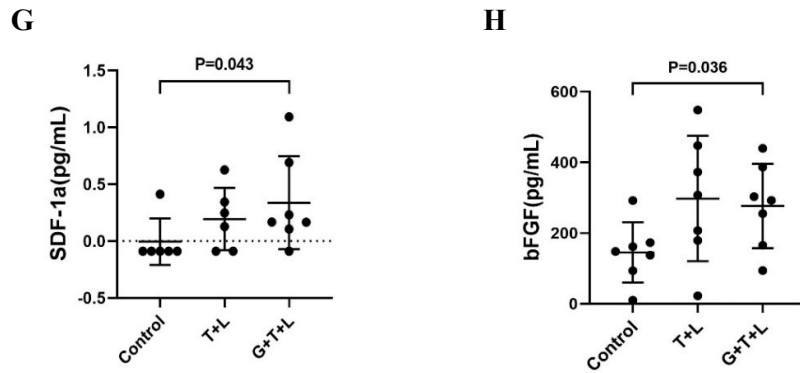


Figure 18: Impact of pro-inflammatory mediators with/out glucose on the release of cytokines, chemokines, and growth factors by the HUVECs. Soluble amounts of (A) IL-1 α , (B) IL-6, (C) IL-8, (D) TNF- α , (E) MCSF, (F) MIP-1 α , (G) SDF-1 α , and (H) bFGF detected in the medium supernatant of CC-genotyped HUVECs upon co-incubation of HUVECs with sCD40L/TNF- α with/out hyperglycemia. Data are represented as means \pm SD; n=6-7.

The abundance of interleukins IL-1 α , IL-6, and IL-8 was significantly upregulated upon exposure to pro-inflammatory components. However, the addition of high glucose to these pro-inflammatory mediators did not further impact these interleukins' levels (T+L vs. G+T+L; Figures 18A-C). A similar observation was also made for the amounts of TNF- α , MCSF, and MIP-1 α (T+L vs. G+T+L; Figures 18D-F). In contrast, the sCD40L and TNF- α combined incubation did not affect the amounts of SDF-1 α and bFGF to a great extent. However, the amounts of SDF-1 α and bFGF released by G+T+L treated HUVECs were 68-fold and 1.9-fold higher than those by the control group (G+T+L vs. control; Figure 18G-F).

5.6.3. Matrix metalloproteinases

The amounts of matrix metalloproteinases released by the HUVECs under current experimental settings were also examined. The levels of MMP-2 and MMP-9 detected in the supernatant of T+L vs. G+T+L treated cells did not differ much. However, long-term exposure of the HUVECs to TNF- α , sCD40L, and high glucose attenuated MMP-2 abundance (G+T+L vs. control; Figure 19A). TNF- α and sCD40L co-incubation enhanced the amounts of MMP-9 released by the HUVECs (T+L vs. control; Figure 19B).

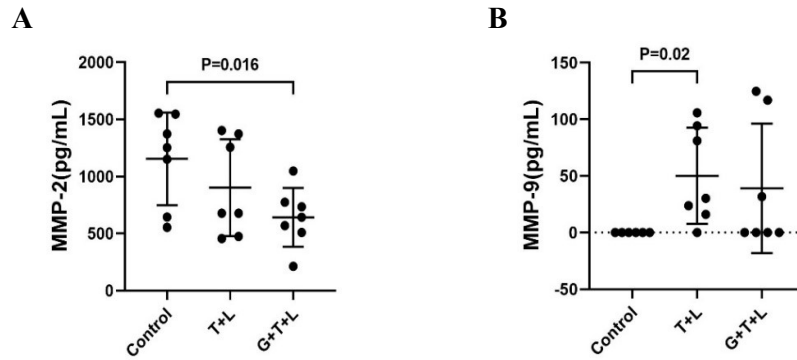


Figure 19: Matrix metalloproteinases released by HUVECs in the presence of pro-inflammatory mediators with/out hyperglycemia. (A) MMP-2 and (B) MMP-9 protein amounts detected in the supernatant of the CC-genotype HUVECs upon treatment with sCD40L/TNF- α co-stimulation in the absence or presence high glucose. Data are represented as means \pm SD; n=6-7.

5.7. Analysis of TNF Receptor Associated Factors (TRAF) mRNA expression

Since the CD40 receptor lacks an intracellular kinase domain, the recruitment of additional adaptor molecules like TNF receptor-associated factors (TRAFs) is required to initiate downstream signaling (Engel et al., 2009). In particular, TRAF2 and TRAF6 are involved in CD40-CD40L-induced signaling in endothelial cells (Lutgens et al., 2010; Sultan et al., 2020). To study the impact of the current experimental conditions on CD40-mediated downstream signaling, RT-qPCR was performed to examine the mRNA levels of TRAF2 and TRAF6. Analysis of their protein levels was not possible in our hands owing to the difficulty in finding target-specific primary antibodies which provide a unique signal with a minimum of signal to noise ratio.

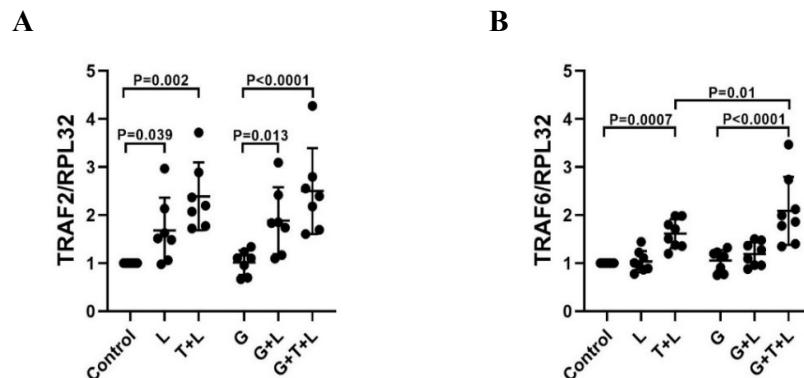


Figure 20: Effect of pro-inflammatory stimulants with/out glucose on TRAF adaptor molecules mRNA levels in HUVECs. Real-time qRT-PCR analysis of (A) *TRAF2* and (B) *TRAF6* mRNA levels of HUVECs cultured with sCD40L/TNF- α co-stimulation in presence or absence of hyperglycemia. Data are represented as means \pm SD; n=7-8.

In the absence or presence of TNF- α and sCD40L co-stimulation, hyperglycemic treatment did not affect the TRAF2 expression (G+T+L vs. T+L; Figure 20A). However, it amplified TRAF6 mRNA levels in HUVECs when added in combination with the mentioned pro-inflammatory mediators (G+T+L vs. T+L; Figure 20B). These data indicate that glucose and pro-inflammatory mediators significantly increased TRAF6-mediated CD40 downstream signaling more than TRAF2.

5.8. Impact of diabetes-like microenvironment on HUVEC morphology

An apparent change in the morphology was observed in the HUVECs exposed to pro-inflammatory mediators under a hyperglycemic microenvironment supplemented with pro-inflammatory mediators. The cells lost their polygonal cobblestoned appearance characteristic for endothelial cells and transformed into long spindle-shaped cells. These cells also lost the property of contact-dependent inhibition of proliferation and appeared to grow on top of the initial monolayer. These morphological changes are exemplified in Figure 22, where these cells also displayed a reduced abundance of CD31 protein in their cell membranes. The HUVECs, when exposed to such a microenvironment, therefore, seem to partially lose their endothelial lineage-specific properties and embark on the path toward cellular transformation.

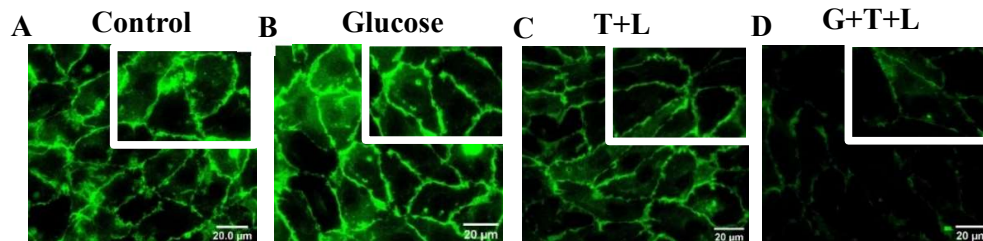


Figure 21: HUVECs undergo morphology changes upon exposure to pro-inflammatory mediators in presence and absence of glucose. The images illustrate CD31 abundance and morphology of CC-genotype HUVEC under (A) control conditions and upon exposure to (B) hyperglycemia, (C) TNF/sCD40L co-stimulation, and (D) hyperglycemia combined with TNF/sCD40L co-stimulation.

5.9. Impact of diabetes-like microenvironment conditions on TGF- β expression in the CC-genotype HUVECs

Hyperglycemia enhances the expression of TGF- β family members, which increases cell size (Lamouille & Derynck, 2007). Therefore, the expression status of the two prominent TGF- β family members, TGF- β 1 and TGF- β 2, was examined under these experimental settings.

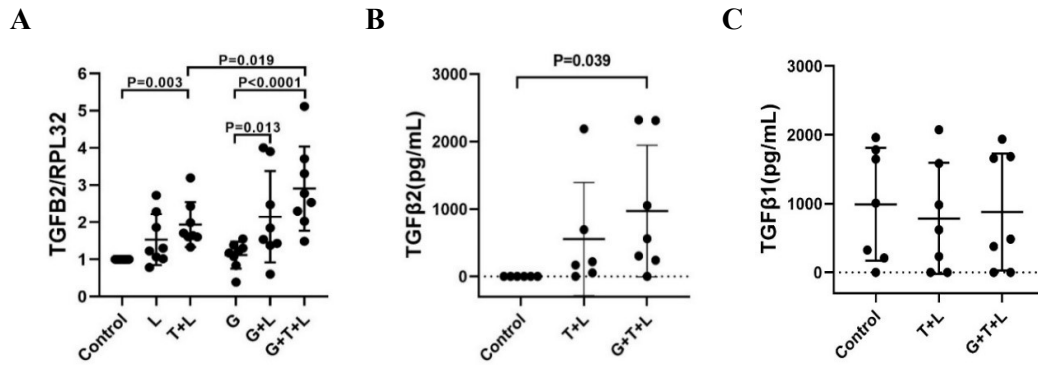


Figure 22: Impact of pro-inflammatory mediators with/out glucose on the mRNA and protein levels of TGF- β family members. (A) *TGFB2* mRNA and (B) TGF β 2 protein levels, and (C) TGF β 1 protein abundance of CC-genotype HUVECs subjected to sCD40L/TNF- α co-incubation with/out glucose. Data are represented as means \pm SD; n=6-8.

Stimulation of HUVECs with sCD40L alone did not impact *TGFB2* mRNA expression (L vs. Control; Figure 22A). However, it upregulated TGF β 2 mRNA levels by 1.9-fold under hyperglycemia (G+L vs. L; Figure 22A) and 2.6-fold with TNF- α co-stimulation (T+L vs. L; Figure 22A). Furthermore, adding high glucose to the sCD40L and TNF- α co-stimulation enhanced *TGFB2* expression by a factor of 1.5 (G+T+L vs. T+L; Figure 22A). Similarly, TGF- β 2 abundance was significantly higher in the conditioned medium of these cells (G+T+L vs. Control; Figure 22B). However, the amount of TGF- β 1 released by the HUVECs upon exposure to these pro-inflammatory mediators in the presence or absence of high glucose was unaffected (T+L/G+T+L vs. Control; Figure 22C). In conclusion, TGF- β 2 mediated downstream signaling, which seems to be augmented by hyperglycemia, contributes to the morphological changes of the HUVECs under the current experimental settings. Moreover, it may also play an important role in enhancing the expression of the above-mentioned pro-inflammatory markers in HUVECs subjected to a pro-inflammatory environment under high glucose conditions.

5.10. Analysis of endothelial-to-mesenchymal transition (EndMT)-associated marker gene expression

Considering the observed changes in morphology and the enhanced TGF- β 2 release, the expression of marker genes known to be associated with EndMT was analyzed next.

5.10.1. Markers specific for endothelial or mesenchymal origin

The HUVECs, when cultured under hyperglycemia and sCD40L/TNF- α co-incubation did not show any change in their α -SMA protein levels. However, adding pro-

inflammatory mediators to a hyperglycemic medium augmented α -SMA expression by 2-fold (G+T+L vs. Control; Figure 23C). On the other hand, no significant differences in the protein levels of SM22 α and NOS3 between T+L and G+T+L treatment groups were evident (G+T+L vs. T+L; Figure 23D-E). Enhanced expression of mesenchymal markers, along with the downregulation of endothelial NOS3 expression, is observed in the HUVECs subjected to pro-inflammatory conditions under hyperglycemia. These results suggest that the HUVECs demonstrate the initial signs of EndMT upon long-term exposure to such a microenvironment.

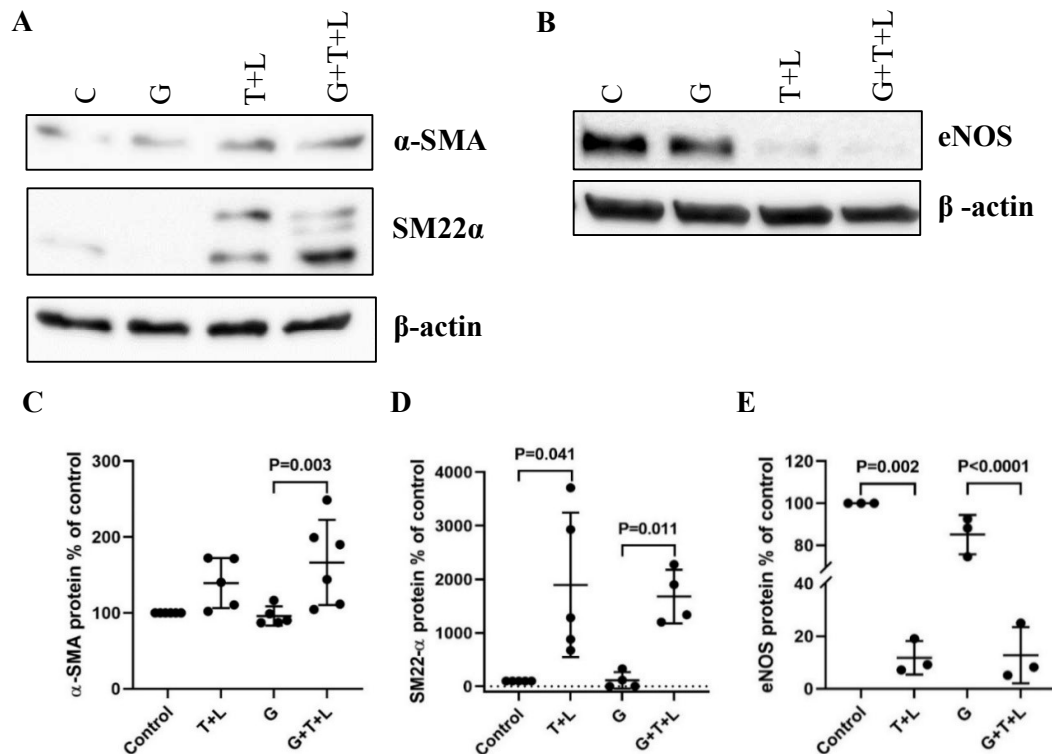


Figure 23: HUVECs exposed to pro-inflammatory microenvironment with/out glucose undergo partial EndMT. (A) mesenchymal markers (α -SMA and SM22 α), and (B) endothelial marker (eNOS) protein levels in the HUVECs cultured under sCD40L/TNF- α co-stimulation with/out glucose were analyzed by Western blot. The scatter plots depict the protein levels of (C) α -SMA, (D) SM22 α , and (E) eNOS normalized to β -actin in these cells. Data are represented as means \pm SD; n=3 (eNOS); n=4-6 (others).

5.10.2. Extracellular matrix mRNA expression

Cells undergoing EndMT also contribute to the remodeling of the extracellular matrix (Piera-Velazquez & Jimenez, 2019). Thus, mRNA levels of prominent extracellular matrix marker gene products COL1 α 1, COL3 α 1, and FN1 were examined by RT-qPCR method. These analyses were performed at the laboratory of our collaboration partner Dr.

Guido Krenning at the department of Pathology and Medical Biology, University Medical Center Groningen. Hyperglycemia downregulated *COL1A1* expression by 1.48-fold (G vs. Control; Figure 24A), but the other treatment groups failed to impact *COL1A1* mRNA expression. Also, no major differences in *COL3A1* mRNA levels were noted between T+L and G+T+L groups (G+T+L vs. T+L; Figure 24C).

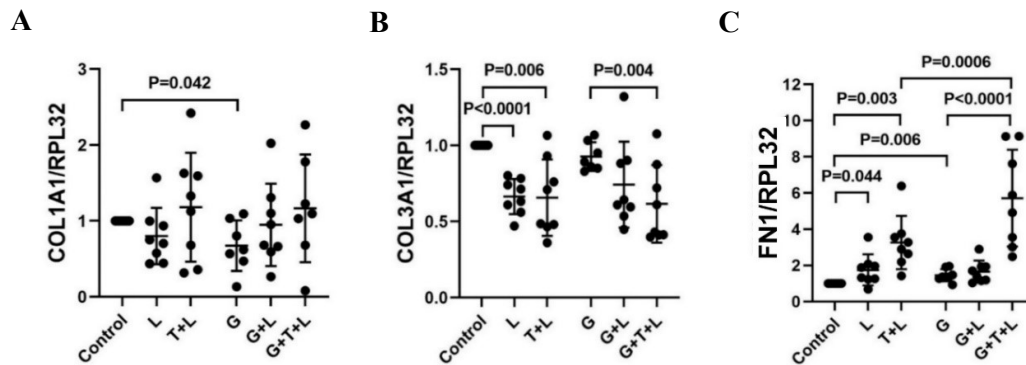


Figure 24: Impact of pro-inflammatory mediators in presence or absence of hyperglycemia on extracellular matrix mRNA expression in HUVECs. The scatter plots illustrate the mRNA levels of (A) *COL1A1*, (B) *COL3A1*, and (C) *FNI* in HUVECs treated with sCD40L/TNF- α co-incubation with/out glucose. Data are represented as means \pm SD; n=7-8.

Incubation of HUVECs with 25 mM glucose raised *FNI* mRNA expression by 1.5-fold (G vs. Control; Figure 24C). Stimulating these cells with sCD40L with or without hyperglycemia enhanced *FNI* mRNA levels by 2-fold (L/ G+L vs. Control; Figure 24C). Likewise, exposure of HUVECs to sCD40L and TNF- α upregulated *FNI* mRNA expression by 3-fold (T+L vs. Control; Figure 24C). Adding high glucose to these pro-inflammatory stimulants further boosted *FNI* mRNA levels by another 2-fold (G+T+L vs. T+L; Figure 24C).

The expression of *FNI*, an early EndMT marker, was upregulated by glucose to a great extent. The pro-inflammatory mediators amplified the effects of glucose furthermore. Changes in the extracellular matrix composition of the HUVECS under current experimental settings further support the notion of EndMT occurring in these cells.

5.10.3. Gene expression of transcription factors associated with EndMT

To acquire a deeper understanding of the signaling process underlying the morphological changes in the HUVECs, the following transcription factors known to play a role in driving EndMT under various experimental settings were evaluated at the laboratory of Dr. Guido Krenning at the department of Pathology and Medical Biology, University

Medical Center Groningen: Snail (*SNAIL*), Slug (*SNAIL2*), *TWIST1*, and *ZEB2* (Kovacic et al., 2019). *SNAIL2* mRNA decreased 2-fold upon sCD40L stimulation (L vs. Control; Figure 25A) and 4.2-fold upon sCD40L/TNF- α co-stimulation (T+L vs. control; Figure 25A). No significant changes were observed in the corresponding hyperglycemic groups. *ZEB2* mRNA expression of HUVECs subjected to co-stimulation with sCD40L and TNF- α was elevated by 1.5-fold with or without hyperglycemia (T+L/G+T+L vs. Control; Figure 25B). *SNAIL1* and *TWIST1* mRNA expression showed no significant differences (not shown).

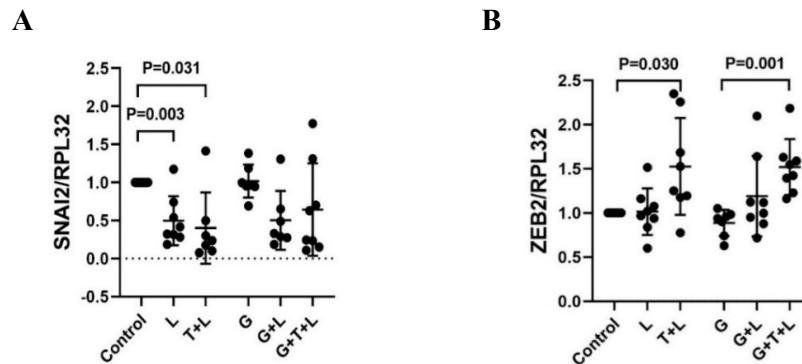


Figure 25: Impact of pro-inflammatory stimuli with/out glucose on the EndMT-associated transcription factor mRNA expression in HUVECs. (A) *SNAI2* and (B) *ZEB2* mRNA levels in HUVECs subjected to sCD40L/TNF- α co-stimulation with/out hyperglycemia were evaluated with RT-qPCR. Data are represented as means \pm SD; n=7-8.

5.10.4. Impact of diabetes-like microenvironment on NFAT5 mRNA levels

NFAT5 is involved in the pathologies of diseases associated with hyperosmolarity and inflammation (Neuhofer, 2010). Single sCD40L and/or glucose treatment did not seem to affect the mRNA expression of NFAT5 (L/G vs. Control; Figure 26). Nevertheless, the addition of TNF- α to sCD40L stimulation amplified NFAT5 mRNA expression by 1.4-fold (T+L vs. Control; Figure 26). These mRNA levels were boosted by another 1.3-fold upon the addition of high glucose (G+T+L vs. T+L; Figure 26). Hence, glucose seems to strongly impact NFAT5 mRNA expression in HUVECs under a pro-inflammatory microenvironment.

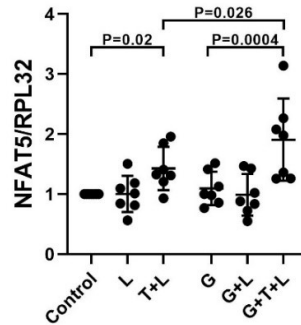


Figure 26: Impact of pro-inflammatory mediators with/out hyperglycemia on HUVEC NFAT5 mRNA expression. The scatter plot denotes NFAT5 mRNA levels in HUVECs exposed to sCD40L/TNF- α co-incubation with/out high glucose. Data are represented as means \pm SD; n=7.

5.10.5. Impact of a diabetes-like microenvironment on the abundance of NFAT5 protein in the cytoplasm and in the nucleus

Increased mRNA expression of NFAT5 indicates its possible involvement in pro-inflammatory gene expression in HUVECs under the current experimental settings. However, nuclear translocation is a prerequisite for NFAT5 to modulate the expression of its target genes (Cen et al., 2020). Hence, the abundance of NFAT5 protein in the cytoplasm and the nucleus of these cells was further investigated via immunocytochemistry. The resulting images were analyzed by Dr. Holger Lorenz (Head of imaging facility, ZMBH). The method section provides a detailed explanation of the regions of interest and analysis of the recorded images for NFAT5 nuclear and cytoplasmic abundance (4.17.2; page no. 40). In short, an image of the nuclei stained with DAPI was used as a mask to differentiate between the nuclear and cytoplasmic regions of the cell. After appropriate background subtraction, the mean fluorescence intensities of NFAT5-specific Cy5 signal in the cytoplasmic and nuclear areas were calculated. Only a small but significant increase in NFAT5 abundance was observed in the cytoplasm of HUVECs subjected to T+L and G+T+L treatments. However, NFAT5 abundance increased significantly in the nucleus of the G+T+L group, which was 1.3-fold (G+T+L vs. control; Figure 27C) and 1.2-fold higher than those in the control nuclei and T+L groups (G+T+L vs. T+L; Figure 27C) respectively. Overall, nuclear translocation of NFAT5 induced by the pro-inflammatory mediators was enhanced in the presence of hyperglycemia.

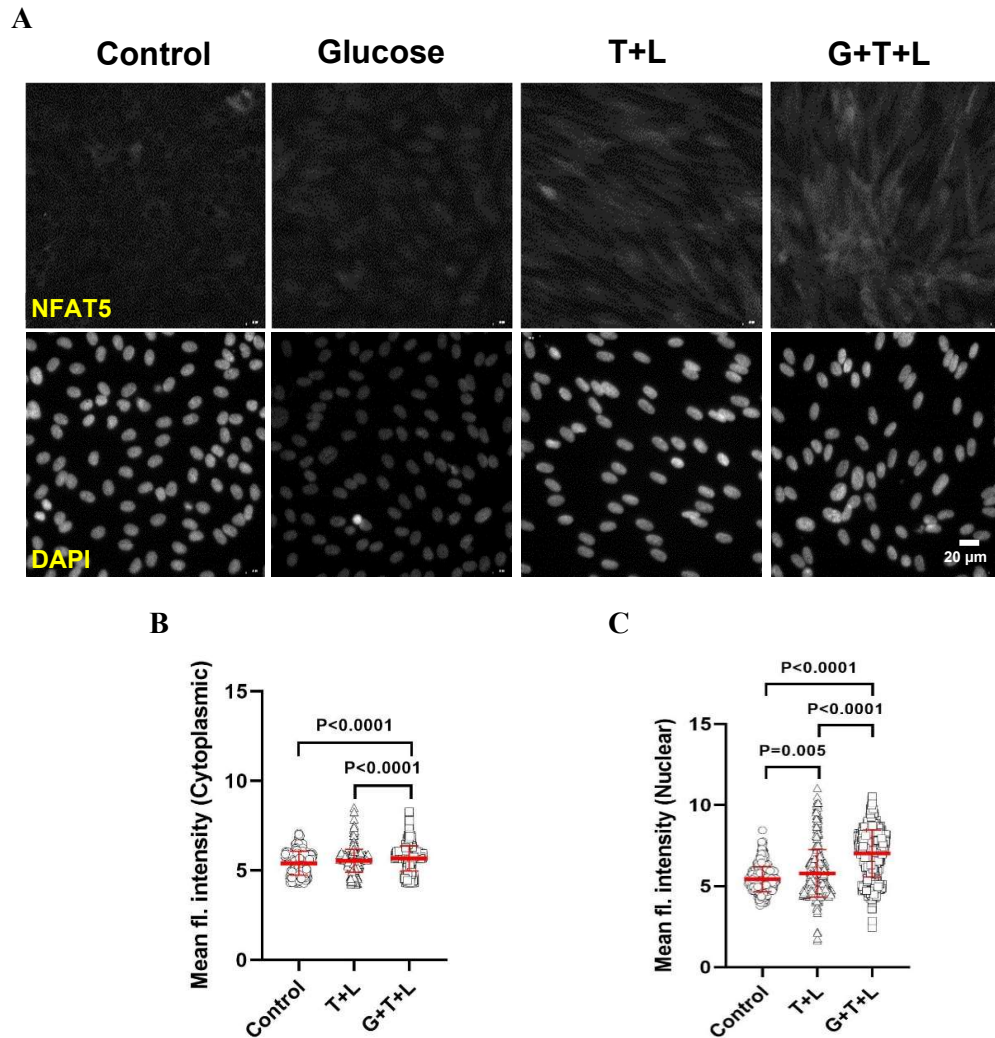


Figure 27: Impact of pro-inflammatory microenvironment with/out hyperglycemia on NFAT5 abundance. (A) Immunofluorescence-based detection and the mean fluorescence intensity of NFAT5 (B) in the cytoplasm and (C) in the nucleus of HUVECs exposed to sCD40L/TNF- α co-stimulation with/out high glucose. Data are represented as means \pm SD (n-numbers are as follows for cytoplasmic/nuclear abundance of NFAT5 protein: control=96/491; T+L=441/445; G+T+L=701/701).

5.10.6. Effect of NFAT5 downregulation on SM22 α protein expression in HUVECs subjected to a diabetes-like microenvironment

To understand the relevance of increased mRNA expression and nuclear translocation of NFAT5, inhibition of NFAT5 expression was further attempted. Therefore, experiments aiming at knocking down NFAT5 via siRNA-based silencing were performed. However, the knockdown efficiency was insufficient to proceed with further analysis (Supplementary figure S1). The HUVECs cultured in the presence of pro-inflammatory mediators and high glucose were also treated with KRN2, a selective NFAT5 inhibitor.

KRN2 is reported to partially downregulate NFAT5 expression by blocking the NF- κ B binding sites in the promoter region of the NFAT5 gene (Han et al., 2017). However, also KRN2 failed to downregulate NFAT5 expression significantly (Supplementary figure S2). Finally, NFAT5 neutralizing decoy ODN was applied to the HUVECs under current experimental settings. These ODNs are short double-stranded DNA molecules with a specific sequence of bases that typically match the target transcription factor's consensus DNA recognition motif (Hecker & Wagner, 2017).

This approach investigated the impact of enhanced NFAT5 expression and nuclear translocation observed in the HUVECs exposed to pro-inflammatory mediators in the presence of high glucose. Exposure to such a microenvironment augmented SM22 α protein levels by 7.1-fold (G+T+L vs. Control; Figure 28B). Pre-incubation with the NFAT5 neutralizing decoy ODN led to a significant 2.3-fold reduction of SM22 α expression in the HUVECs treated with G+T+L (G+T+L+NFAT5 vs. G+T+L; Figure 28B). When treated with the corresponding mutant control ODN, the cells also showed a decrease in SM22 α protein abundance, which was insignificant (G+T+L+mut vs. G+T+L; Figure 28B). These results indicate that NFAT5 is involved and is essential for the expression of SM22 α in HUVECs under the current experimental conditions.

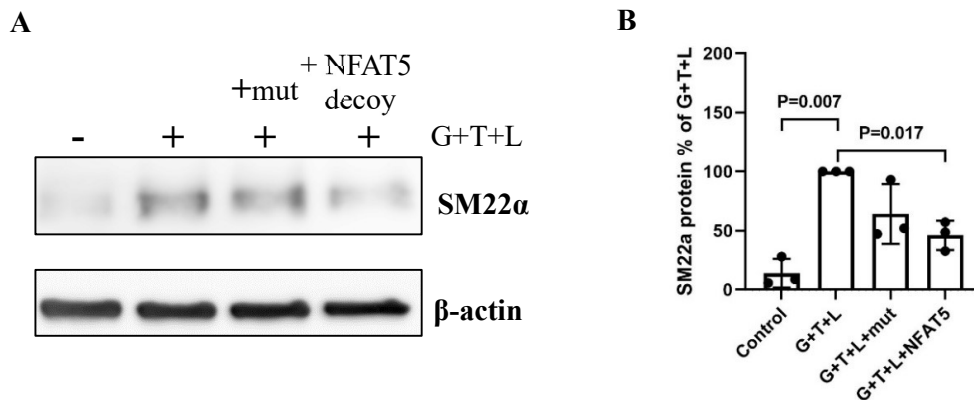


Figure 28: NFAT5 decoy ODN inhibits SM22 α gene expression in HUVECs subjected to pro-inflammatory mediators under hyperglycemia. (A) Exemplary western blot image, and (B) SM22 α protein levels in HUVECs incubated with NFAT5 decoy ODN (10 μ M) before and during co-stimulation with sCD40L/TNF- α under hyperglycemia. Data are represented as means \pm SD; n=3.

6. DISCUSSION

The associated micro- and macrovascular complications render diabetes one of the leading causes of health and economic damage. Systemic inflammation stemming from metabolic stress factors facilitates the onset and progression of these complications. The CD40 co-stimulatory receptor expressed in several cell types in different organs is a mediator of systemic inflammation in diabetes. CD40-CD40L interaction is an important trigger for endothelial dysfunction and the following vascular complications. This study investigated the allelic distribution of the T-1C SNP of the *CD40* gene, a possible risk factor for cardiovascular diseases, in patients with diabetes. In addition, the abundance of the soluble forms of CD40 and CD40L in the plasma of these patients was analyzed. Last but not least, this study investigated the effects of the pro-inflammatory diabetes-like microenvironment on endothelial cell properties and functions.

6.1. Analysis of a SNP in the *CD40* gene and plasma levels of sCD40/sCD40L in patients with diabetes

6.1.1. Association of the T-1C SNP of the *CD40* gene (rs1883832) with diabetes

CD40-induced downstream signaling is essential for initiating innate and adaptive immune responses against pathogenic infections. It also activates immune reactions in response to metabolic risk factors termed metabolism-associated danger signals (MADS) (Dai et al., 2017). MADS include the intermediates and products of glucose, lipids, amino acids, and nucleotides, among others (Dai et al., 2017). Therefore, unregulated CD40 expression or downstream signaling is associated with the progression of autoimmune, inflammatory, and thrombotic diseases (Chatzigeorgiou et al., 2009).

Single nucleotide polymorphisms are the most basic and frequent source of genetic mutations. They are linked with several diseases and disorders (Altshuler et al., 2008; Katsonis et al., 2014). Previous studies have reported an association of SNPs in the *CD40* gene with susceptibility to multiple sclerosis, Graves' disease, rheumatoid arthritis, systemic lupus erythematosus, and cancer (Dimitrakopoulos et al., 2021; Lee et al., 2015; Qin et al., 2017).

A T-1C SNP located in the Kozak region of the *CD40* gene (rs1883832) impacts the translation efficiency of CD40 mRNA and, thereby abundance of CD40 protein. Considering the potential significance of CD40 signaling in promoting diabetes and its vascular complications, the association of this SNP with diabetes was investigated. The

proportion of homozygous T-allele carriers was much less in the T2D patient cohort than in the control group. Moreover, the homozygosity for the C allele, in other words, an absence of the T allele, elevated the odds of developing T2D significantly. This odds ratio was even greater than that documented for CHD (Sultan et al., 2020). Hence, homozygous loss of the T alleles seems to act as a more significant risk factor for T2D, which plausibly contributes to the progression of diabetes-associated cardiovascular complications. The allele frequency observed in T1D revealed a different trend where most patients were heterozygous carriers of both the T and C alleles. However, the current number of patients analyzed is too small to conclude that this SNP of the *CD40* gene is associated with T1D.

To the best of our knowledge, this is the first study to report an association of the T-1C SNP of the *CD40* gene with T2D in a Caucasian population. Overall, only a very few studies provide insight into such an association. The association of the T-1C SNP of the *CD40* gene with T2D in the Iranian population has been examined (Erfanian et al., 2019). In contrast to our finding, the T allele frequency was higher in the Iranian T2D cohort than in healthy individuals. Similarly, an association of the T allele of the *CD40* gene SNP with diabetic nephropathy in the Egyptian population has been reported (Ghareeb et al., 2020). On the other hand, a higher frequency of the C allele in patients with T2D than in healthy individuals is documented by another Egyptian study (Moosad et al., 2015). However, the control group in this study consisted of only 62 individuals, which is a bit too small for a population-based characterization study. This factor, to some extent, might explain the different observations made in the Egyptian population by these two research groups.

Differences in the ethnicities of the study populations might explain the contradictory observations made by other research groups and us regarding this association. Vast population-based differences in the allele distribution of several disease-associated genes have been reported (Adeyemo & Rotimi, 2010). Moreover, a lack of correlation in allele frequencies between the Caucasian and non-Caucasian populations has also been confirmed (Adeyemo & Rotimi, 2010). These findings may explain the different observations made by us and the above groups concerning the association of the T-1C SNP of the *CD40* gene with T2D.

6.1.2. Circulating sCD40 and sCD40L as indicators of the inflammatory status in patients suffering from diabetes

CD40 receptor and CD40L exist in both membrane-bound and soluble forms. Membrane CD40L can be cleaved to a soluble form by ADAM10 and ADAM17 or MMP-2 (Hassan et al., 2022). Circulating levels of sCD40L have been linked with cardiovascular diseases, several forms of kidney diseases, inflammatory bowel disease, and multiple sclerosis, amongst others (Figueredo et al., 2017; Tousoulis et al., 2010; Xie et al., 2017; Yang et al., 2022). Moreover, sCD40L levels have been associated with the severity of these diseases (Lamine et al., 2020; Shami et al., 2021).

As evident in the case of CD40L shedding, more than one process is involved in the generation of sCD40. Alternative splicing of a single mRNA transcript leads to the membrane-bound and soluble form of CD40 (Esposito et al., 2012). Moreover, CD40 shedding by proteolytic cleavage of the membrane-bound extracellular receptor domain mediated by ADAM17 is also documented (Esposito et al., 2012). In clinical settings, increased sCD40 levels in patients suffering from immunity and inflammation-modulated diseases have been often reported, too (Leonetti et al., 2022; Meltzer et al., 2021; Schwabe et al., 1999).

In light of such findings, the plasma levels of sCD40L and sCD40 in patients with T1D and T2D were compared to those of healthy individuals. Plasma levels of both sCD40 and CD40L were significantly elevated in patients suffering from T2D, while only sCD40 abundance was substantially enhanced in the plasma of patients with T1D.

The soluble CD40 receptor acts in a fashion opposite to that of its membrane-bound form. While membrane-bound CD40 signals downstream in the host cells, sCD40 functions as a decoy receptor that neutralizes CD40L and thus abrogates its pro-inflammatory effects (Tang et al., 2021). As sCD40 rescues the cells from overstimulation under pro-inflammatory conditions, CD40 shedding serves as a compensatory mechanism during such circumstances. (Contin, Pitard, Itai, et al., 2003; Eshel et al., 2008). These findings are confirmed *in vivo*, where patients with restored kidney functions after hemodialysis presented with a rapid decrease in their serum sCD40 levels (Contin, Pitard, Delmas, et al., 2003).

While many studies document the protective role of sCD40, the biological function of sCD40L is not clearly defined in the literature. Some studies state that membrane-bound

CD40L but not sCD40L acts as the potent stimulus for driving CD40-mediated cell activation and apoptosis (Bachsais et al., 2020; Elmetwali et al., 2020; Ludewig et al., 1996; Salti et al., 2021). These studies describe membrane-bound CD40L shedding as a compensatory mechanism that attenuates CD40-CD40L signaling (Henn et al., 2001). On the contrary, sCD40L can bind to the CD40 receptor and integrin receptors on the surface of platelets, immune and endothelial cells, thereby promoting thrombosis and atherogenesis (Hassan et al., 2022; Pereira-da-Silva et al., 2020).

Plasma concentrations of the circulating forms of soluble CD40 and CD40L are elevated in immune-modulated diseases and therefore proposed to be a potential prognostic marker. Moreover, CD40-CD40L signaling is a major driver of insulin resistance and systemic inflammation during the progression of diabetes ((Seijkens et al., 2013). Hence, the levels of sCD40 and sCD40L could serve as potential prognostic markers to assess the inflammatory status of patients suffering from diabetes.

6.1.3. Association of the T-1C SNP of the *CD40* gene (rs1883832) with sCD40L and sCD40 plasma levels of patients with diabetes

The T-1C SNP of the *CD40* gene (rs1883832) is situated nearby the translation initiation codon and thereby impacts the CD40 protein turnover in the cells (Jacobson et al., 2005). As a result, the CC-genotype HUVECs exhibit a higher CD40 surface abundance than the TT-genotype cells (Sultan et al., 2020). The release of the potential decoy sCD40 receptor is enhanced in these cells, presumably to protect them from the risk of overstimulation (Sultan et al., 2020). The protein amounts of sCD40 were also elevated in the plasma of CC-genotype patients diagnosed with CHD as compared to the corresponding TT-genotype patients (Sultan et al., 2020).

Likewise, sCD40 levels were significantly higher in the plasma of CC-genotype patients suffering from T2D than in their TT-genotype counterparts. Moreover, medium and weak positive sCD40-sCD40L correlations were observed in patients with T1D and T2D, respectively. Genotype-dependent differences were not observed in healthy individuals with regard to both sCD40 and sCD40L plasma levels. Unlike sCD40, sCD40L plasma levels did not differ much amongst the three genotypes in patients with diabetes in general. Since the SNP in the *CD40* gene may not directly affect the formation of sCD40L, such genotype-dependent differences were in fact not expected.

Patients with diabetes are subjected to chronic systemic inflammation. Overall, this inflammation is further aggravated in homozygous carriers of the C allele. Endothelial cells from CC-genotype individuals harbor an enhanced risk of activation because of the increased abundance of CD40 on their surface. The formation of CD40L and sCD40L neutralizing sCD40 is increased in patients homozygous for the C allele, possibly to mitigate the augmented pro-inflammatory effects of enhanced CD40 downstream signaling.

6.1.4. Impact of the T-1C SNP of the *CD40* gene on differential gene expression in sCD40L stimulated CC- and TT-genotype HUVEC

CD40L-induced stimulation of the CD40 receptor leads to a higher degree of downstream signaling in CC-genotype as compared to TT-genotype HUVECs (Sultan et al., 2020). This activation enhances pro-inflammatory gene expression and monocyte adhesion in CC-genotype HUVECs to a greater extent (Sultan et al., 2020). To obtain a detailed overview of the differential gene expression occurring between these two genotypes in response to sCD40L stimulation, a genome-wide comparison of their gene expression profile was performed through RNA-Seq analysis.

Stimulation with sCD40L caused greater transcriptional regulation in CC-genotype HUVECs. This was evident by the greater number of up- and downregulated genes in these cells as compared to their TT-genotype counterparts. Closer inspection of the regulated genes revealed that the upregulated genes in the CC-genotype HUVECs encode mediators of inflammation, thrombosis, and EndMT. Moreover, the pathways significantly associated with these gene products included insulin receptor recycling. Recycling of insulin receptors contributes to insulin insensitivity and the progression of diabetes (Y. Chen et al., 2019). Downstream signaling of the receptor for advanced glycation endproduct (RAGE), which is involved in the manifestation of diabetes and its associated complications, was also enhanced in these cells (Egaña-Gorroño et al., 2020; Ramasamy et al., 2011).

Selenocysteine synthesis was significantly downregulated in the CC-genotype HUVECs upon stimulation with sCD40L. Selenocysteine is an amino acid required to synthesize selenoenzymes such as GPXs (Hariharan & Dharmaraj, 2020). Its downregulation causes decreased expression of GPX1, GPX3, and GPX4 in these cells. These selenoproteins comprise a central antioxidant defense system in various cell types (Hariharan &

Dharmaraj, 2020). Hence, without the availability of the GPXs, the CC-genotype HUVECs are subjected to enhanced oxidative stress upon activation with sCD40L. Moreover, expression of NOS3 providing the antioxidant and anti-inflammatory mediator nitric oxide was also attenuated in these cells. A redox imbalance leads to an atheroprone endothelial cell phenotype promoting vasoconstriction and inflammation (Theofilis et al., 2021).

Rho GTPases and their activators were also significantly downregulated in the CC-genotype HUVECs but were upregulated in TT-genotype cells upon sCD40L stimulation. Rho GTPases are known to regulate several different biological processes. While they modulate protective functions such as insulin synthesis and maintaining glucose homeostasis, they also cause vascular leakage and inflammation (Møller et al., 2019; Strassheim et al., 2019). Since they modulate a large spectrum of activities, a detailed study of their role in the current experimental setting is essential. In addition to the Rho GTPases family, gene products associated with IL-4 and IL-13 signaling were augmented in the sCD40L-stimulated TT-genotype HUVECs. These anti-inflammatory cytokines facilitate the differentiation of T cells and macrophages into immunomodulatory Th2 cells and M2 macrophages (Y. Chen et al., 2019; Junttila, 2018). On the other hand, the mediators of NOTCH and TGF- β downstream signaling were significantly reduced in the sCD40L-stimulated TT-genotype HUVECs. Both of these signaling pathways are known promoters of EndMT in HUVECs (Maleszewska et al., 2013; Tian et al., 2019).

These findings illustrate that the CC-genotype HUVECs are highly susceptible to inflammation, thrombosis, and endothelial dysfunction upon exposure to the pro-inflammatory sCD40L. In contrast, the TT-genotype HUVECs are relatively quiescent to sCD40L stimulation and thereby seemed to be protected against stress factors. Apparently, the strength of receptor-mediated activation determines whether signaling pathways are turned on or off (Wagner et al., 2015; Zikherman & Au-Yeung, 2015). Reports document that large CD40L clusters induce CD40-mediated ERK-1/2 downstream signaling, whereas smaller CD40L clusters drive p38MAPK activation (Nair et al., 2020). These findings might explain the effects of differential surface CD40 abundance on driving distinguished gene expression between the sCD40L-stimulated CC- and TT-genotype HUVECs. However, these findings derived from comparing transcription levels and need to be further confirmed on the protein level.

6.2. Effect of the diabetes-like microenvironment on the CC-genotype HUVECs

6.2.1. Establishment of a diabetes-like cell culture model

This study aimed to mimic a diabetes-like microenvironment to assess the fate of endothelial cells under similar conditions. As most of the examined patients with T2D were homozygous for the C allele of the T-1C SNP of the *CD40* gene and thus prone to enhanced inflammation, only CC-genotype HUVECs were used for this approach. Twenty-five mmol/L glucose was added to the medium to mimic the hyperglycemia of the diabetic conditions in contrast to the baseline concentration of 5.5 mmol/L (De Nigris et al., 2015). Moreover, most patients suffering from T2D are also reported to be overweight (<https://www.who.int/news-room/fact-sheets/detail/diabetes>, accessed on 26.06.2022). Enhanced immune cell infiltration into the adipose tissue of obese people as compared to lean people has been previously documented (Kammoun et al., 2014). These immune cells secrete cytokines and chemokines, leading to systemic inflammation (Donath & Shoelson, 2011). One of the most classical cytokines released from these immune cells is TNF- α (Kammoun et al., 2014; Ouchi et al., 2011). Belonging to the TNFR receptor family, the CD40 receptor-mediated downstream effects are highly impacted by TNF- α stimulation. Therefore, the endothelial cells were also exposed to TNF- α in addition to high glucose for an extended period. The final TNF- α working concentration was adopted from those documented in the serum of diabetic patients (Qiao et al., 2017). Moreover, the availability of CD40L is augmented in patients with diabetes (Santilli et al., 2015); therefore, sCD40L was added to the culture medium, too. Just for the sake of simplicity, the HUVECs exposed to the above culture conditions shall henceforth be termed as the diabetic group/diabetic HUVECs.

6.2.2. Limitations of the proposed diabetes-like culture model

Diabetes mellitus is a complex metabolic disease accompanied by other diseases, such as hypertension and dyslipidemia. Moreover, diabetes leads to the progression of macro- and microvascular complications in the long run (Forbes & Cooper, 2013). From an experimental point of view, it is impossible to mimic these conditions in any cell culture model. Thus, the model used in this study contains only a few aspects of an actual diabetes microenvironment. It fails to consider several additional metabolic stress factors contributing to the pathophysiology of diabetes. A detailed analysis of metabolic processes would possibly impact the results obtained by this study. A comprehensive overview of these limitations is provided in the following sections.

6.2.2.1. Analysis of the impact of the diabetes-like microenvironment on the cellular metabolism

I. Glucose metabolism

Endothelial cells rely on glycolysis for energy metabolism (Eelen et al., 2018). In addition to glycolysis, glucose can be metabolized by the polyol pathway, where it is initially converted to sorbitol and finally to fructose (A. Singh et al., 2022). This pathway consumes massive amounts of NADH, essential in maintaining glutathione (GSH) levels and activity (Ighodaro, 2018). GSH is a free radical scavenging tripeptide. Reduction or even absence of its antioxidant activity subjects cells to strong oxidative stress (A. Singh et al., 2022). NADPH is also an essential cofactor for the synthesis of NO from L-arginine. For these reasons, the polyol pathway metabolizes only a tiny proportion of cellular glucose (A. Singh et al., 2022). However, increased glycolytic flux generated during hyperglycemia drives higher amounts of glucose toward this pathway (A. Singh et al., 2022). In addition to the polyol pathway, other glycolytic side branches are activated under hyperglycemic conditions (Gero & Gero, 2017). The glycolytic intermediates serve as substrates for these side pathways contributing to the pathophysiology of diabetes (Gero & Gero, 2017).

Glucose is converted to glucose-6-phosphate (G-6-P) during the initial step of glycolysis and further reduced to fructose-6-phosphate. In parallel, G-6-P can also be reduced to a 5-carbon sugar via the pentose phosphate pathway (PPP), which is essential for synthesizing nucleic acids and nucleotides (Eelen et al., 2018). Like the polyol pathway, this glycolytic side branch also utilizes large amounts of NADPH, thereby enhancing oxidative stress (Ighodaro, 2018). Increased glycolytic flux observed during hyperglycemia produces saturating amounts of F-6-P that are then shunted to the hexosamine pathway (A. Singh et al., 2022). The enzyme glucosamine-fructose amidotransferase (GFAT) activated in this pathway metabolizes F-6-P to glucosamine-6-phosphate, which is finally reduced to uridine diphosphate-N-acetylglucosamine (UDP-GlcNAc) (Ighodaro, 2018). UDP-GlcNAc mediates protein and lipid glycosylation (Clyne, 2021). It also promotes post-translational modification of proteins in the presence of the enzyme O-glucosamine-N-acetyl transferase (Clyne, 2021). Furthermore, activation of the hexosamine pathways upregulates the expression of TGF- β family members, which are known mediators of endothelial dysfunction (Figueroa-

Romero et al., 2008). Overall, the toxic and pro-oxidative effects of the hexosamine pathway contribute to the progression of diabetes-associated complications (Buse, 2006).

Under normoglycemia, F-6-P is further reduced to glyceraldehyde-3-phosphate by glyceraldehyde-3-phosphate dehydrogenase (GAPDH) (Gero & Gero, 2017). Glyceraldehyde-3-phosphate is then metabolized to 1,3-diphosphoglycerate, and finally pyruvate is produced (Gero & Gero, 2017). However, the activity of GAPDH is stalled by the high amounts of reactive oxygen species (ROS) produced during the glycolytic side pathways upstream of this step (Chung et al., 2003). As a result, the overly abundant glyceraldehyde-3-phosphate is diverted toward the protein kinase C (PKC) pathway. Metabolites like methylglyoxal which are involved in the formation of advanced glycation end products (AGEs), are produced by activating this pathway (A. Singh et al., 2022). Such AGE-forming precursors promote endothelial dysfunction by modifying the intracellular and ECM proteins, thereby hampering their functions (Clyne, 2021). Similarly, they modify plasma proteins and facilitate their binding to RAGE (Clyne, 2021). RAGE-mediated downstream signaling has been reported to enhance inflammation via the activation of NF- κ B under hyperglycemia (Gero & Gero, 2017).

Glyceraldehyde-3-phosphate can also be transformed to diacylglycerol (DAG), a well-known activator of the protein kinase C (PKC) family (Giacco et al., 2010). The PKC family comprising 11 serine/threonine kinase isoforms, is the most prominent kinase family controlling the activities of other proteins (A. Singh et al., 2022). A few of the processes regulated by the members of this family include the activation of ET-1, VEGF, TGF- β , and NF- κ B (Way et al., 2001). All of these are significant effectors of endothelial dysfunction and diabetes-associated vascular complications.

Under normal physiological conditions, most intracellular glucose is metabolized via glycolysis. However, several pathological side pathways of glycolysis are activated during hyperglycemia, leading to the increased synthesis of pro-inflammatory mediators and reactive oxygen species. Such processes controlled by the glycolytic side pathways may have plausible direct or indirect effects on the HUVECs subjected to the cell culture model. However, the specific glycolytic side branches activated under the chosen cell culture conditions have not been analyzed. Moreover, an analysis of the downstream products arising from these metabolic pathways was not performed.

II. Glutamine metabolism

Glutamine is a non-essential amino acid and an important source of carbon and nitrogen atoms essential for endothelial metabolism (Eelen et al., 2018). It is the most abundant free amino acid in the plasma and a readily available source of energy (Du et al., 2021). Almost 90% of the extracellular glutamine is imported into endothelial cells, constituting 30% of the tricarboxylic acid (TCA) cycle carbons atoms (Du et al., 2021).

At the end of glycolysis, pyruvate is transported into the mitochondria and serves as a substrate for the TCA cycle (Martínez-Reyes & Chandel, 2020). The TCA cycle is one of the most important metabolic processes that generate intermediates essential for synthesizing macromolecules such as lipids and nucleotides (Martínez-Reyes & Chandel, 2020). Hence, it is necessary to keep this cycle replenished (Martínez-Reyes & Chandel, 2020). However, the activation of the glycolytic side branches by hyperglycemia hampers pyruvate synthesis, thereby reducing its supply to the TCA cycle. In such scenarios, glutamine serves as a prominent energy source for the cells, which is reduced to glutamate by glutaminase (GLS) (Martínez-Reyes & Chandel, 2020). Glutamate is metabolized to α -ketoglutarate and shuttled into the TCA cycle (Martínez-Reyes & Chandel, 2020). The activity of GLS documented in the endothelial cells is 20-fold higher than that in the lymphocytes, which exhibit high rates of glutaminolysis (Polet & Feron, 2013). In endothelial cells, glutamine regulates their proliferation and contributes to synthesizing nucleotides and proteins (Theodorou & Boon, 2018). Moreover, it also plays a role in the modulation of oxidative stress and inflammation in these cells (Theodorou & Boon, 2018). Therefore, glutamine metabolism might have some confounding effects on the results of this study.

6.2.2.2. Additional mediators of endothelial dysfunction in diabetes

The current culture model only mimics the hyperglycemic and pro-inflammatory aspects of the microenvironment observed during diabetes. However, several other metabolic stress factors promote endothelial dysfunction during the course of diabetes. The inability to include these factors in the proposed cell culture model marks another limitation of this study. A few of these factors and their role in causing endothelial dysfunction are highlighted in the following sections.

I. Lipotoxicity

The blood lipid concentrations of patients with diabetes are much higher than those of healthy individuals (Hirano, 2018). Augmented levels of lipids such as triglycerides, non-esterified fatty acids, and low-density lipoprotein cholesterol cause injuries to the vascular tissues (Petrie et al., 2018). The damaging effects of lipids are termed as lipotoxicity (Petrie et al., 2018). Lipotoxicity upregulates oxidative and endoplasmic reticulum stress in endothelial cells (Kim et al., 2012). It further promotes inflammation and mitochondrial dysfunction in these cells (Kim et al., 2012). Such molecular processes are significant drivers of endothelial dysfunction and trigger the initiation of vascular complications associated with diabetes.

II. Oxidative stress

Levels of reactive oxygen species (ROS) and reactive nitrogen species (RNS) are significantly enhanced during diabetes (Low Wang et al., 2016). These highly reactive molecules carry free electrons that interact with and modify cellular lipids, proteins, and DNA (Oguntibeju, 2019). As discussed above, the pathological glycolytic side branches produce a vast proportion of ROS, further upregulating these pathways (Paneni et al., 2013). In addition, leakage of electrons due to increased mitochondrial membrane potential is another cause of ROS generation during hyperglycemia (Halim & Halim, 2019). Peroxynitrite (ONOO^-) is a powerful oxidant produced from the reaction of NO and superoxide anions causing protein nitration (Paneni et al., 2013; Wagner et al., 2011). The conversion of NO to peroxynitrite reduces the availability of bioactive NO, further contributing to endothelial dysfunction (Paneni et al., 2013).

Moreover, ROS enhances inflammation via the activation of the transcription factors NF- κ B and activator protein-1 (AP-1) (Oguntibeju, 2019). In these ways, oxidative stress is prominent in causing endothelial dysfunction under several disease conditions, such as diabetes. The components involved in the current model are known producers of oxidative stress (Chakrabarti et al., 2005; Sandoval et al., 2018), which might influence the expression of the gene markers analyzed. However, the levels of oxidative stress factors were not examined.

III. Endoplasmic reticulum stress

The endoplasmic reticulum (ER) is involved in the synthesis, folding, and maturation of several cellular proteins (Oakes & Papa, 2015). Though the protein synthesis and folding mechanisms are tightly regulated, the success rate of protein folding is marginal (Oakes & Papa, 2015). The unfolded protein response (UPR) leads to misfolded proteins being disposed through ER-associated degradation (Smith et al., 2011). The cells experience ER stress when the synthesis of misfolded proteins overtakes the repair mechanisms occurring in the ER (Walter & Ron, 2011). ER stress is often observed during hyperglycemia when the ER is under extreme stress for synthesizing the enzymatic machinery for cellular metabolism due to an increased influx of glucose (Maamoun et al., 2019). An increased error rate and enhanced activation of the UPR is the consequence (Maamoun et al., 2019). Extended periods of UPR instigate inflammatory responses and pro-apoptotic pathways (Maamoun et al., 2019; Walter & Ron, 2011). Enhanced oxidative stress and upregulation of glycolytic side pathways are additional sources of ER stress in diabetes (Lemmer et al., 2021). ER stress further promotes NF- κ B activation and reduces NO availability (Agouni et al., 2014; Li et al., 2020). In such ways, ER stress hinders endothelial cell function and promotes atherosclerosis (X. Chen et al., 2019). Hence, investigating the impact of ER stress on endothelial dysfunction in the current cell culture approach is an interesting aspect for future studies.

IV. Osmotic stress

In addition to augmenting the above-mentioned stress factors, hyperglycemia is also involved in elevating osmotic stress. Upon exposure to a hyperosmotic environment, the cell activates several adaptive responses to restore the osmotic balance (Brocker et al., 2012). The initial and most prominent of these responses include the activation of the osmoadaptive transcription factor-nuclear factor of the activated T cells-5 (NFAT5) (Neuhofer, 2010). Upon its activation, NFAT5 translocates into the nucleus to drive the expression of its target genes, restoring cellular osmolarity (Cen et al., 2020). The target genes upregulated by NFAT5 include those regulating the synthesis and transport of osmolytes, antioxidant defense system, cytoskeleton remodeling, and molecular chaperones associated with UPR (Brocker et al., 2012). However, under persistent hyperosmotic conditions, NFAT5 assumes a pathological role rather than the protective one. NFAT5 upregulates the expression of pro-inflammatory mediators such as

lymphotoxin-(LT-) β , TNF- α , IL-1 β , IL-6, IL-8, and IL-18 (Brocker et al., 2012; Cen et al., 2020). Therefore, the hyperosmolarity-driven activity of NFAT5 is a potent mediator of endothelial dysfunction. An impact of the osmotic stress on endothelial dysfunction is also expected in the current model owing to high glucose concentrations. However, the absence of an appropriate osmotic control in this study makes it difficult to differentiate the biological effects of glucose from the osmotic ones.

V. Other pro-inflammatory mediators

The HUVECs in the current model were exposed to both sCD40L and TNF- α under conditions of hyperglycemia to mimic the pro-inflammatory environment observed during diabetes. However, the mere presence of these entities is not sufficient to replicate the low-grade systemic inflammation present in diabetes. Several other cytokines, such as IL-1, IL-6, IL-8, IL-22, and the chemokines MCP-1, fractalkine, and RANTES (Sena et al., 2018) are further amplified during diabetes. These additional pro-inflammatory mediators were not used in the current model due to the drastic effects of such a cytokine/chemokine cocktail on the viability of HUVECs under long-term exposure. Nevertheless, the chosen components hyperglycemia, TNF- α , and sCD40L, are significant drivers of endothelial dysfunction. Moreover, long-term exposure of HUVECs to these factors upregulated the expression of several genes involved in the progression of diabetes-associated vascular complications in vivo.

6.2.3. Pro-inflammatory gene expression in a diabetes-like microenvironment

I. Impact on the expression of markers facilitating leukocyte recruitment and transmigration

Endothelial cell function is highly compromised in patients with diabetes, which further causes the progression of vascular complications (Potenza et al., 2009). Surface adhesion molecules such as CD40, E-selectin, VCAM-1, ICAM-1, and the chemoattractant protein MCP-1 are a few prominent markers of endothelial dysfunction (Medina-Leyte et al., 2021; S. Singh et al., 2021).

Co-stimulation of the CD40 receptor with sCD40L induces the release and the formation of ultra-large von Willebrand factor (ULVWF) multimers on the surface of endothelial cells upon exposure to shear stress. (Möller et al., 2015). This is followed by the upregulation of adhesion molecules such as VCAM-1, ICAM-1, and E-selectin (Daub et al., 2020). In addition, CD40-CD40L signaling in endothelial cells also induces the

synthesis/release of the chemotactic protein MCP-1 (Sultan et al., 2020). MCP-1 attracts leukocytes from the flowing blood towards the activated endothelial cells (Lin et al., 2014). Circulating Monocytes interact with activated platelets attached to the highly adhesive ULVWF multimers. This ULVWF multimer–platelet string formation mediated trapping of monocytes on the endothelial cell surface facilitates the transmigration through the endothelial cell monolayer despite high shear stress (Popa et al., 2018). These steps constitute the initial and most crucial phase of atherosclerosis.

Exposure to a pro-inflammatory microenvironment with high glucose significantly boosted the mRNA levels of E-selectin, MCP-1, VCAM-1, and CD40. Hyperglycemia alone had almost no effect on *VCAM-1* or *CD40* expression. In contrast, E-selectin and *MCP-1* mRNA levels were significantly increased in response to hyperglycemia alone. In addition, *SELE* and *MCP-1* transcript levels were considerably augmented upon adding the pro-inflammatory mediators TNF- α and sCD40L. These findings suggest that glucose exhibits selective effects on the expression of genes associated with vascular complications. Nevertheless, it establishes a primary low-grade pro-inflammatory environment, further amplified by TNF- α and/or sCD40L.

The soluble forms of E-selectin, ICAM-1, and VCAM-1 were also significantly abundant in the conditioned medium of the HUVECs cultured under a pro-inflammatory environment combined with hyperglycemia, which has also been documented in the case of patients diagnosed with diabetes (Derosa & Maffioli, 2016; Hegazy et al., 2020; Muris et al., 2012). In addition, the circulating levels of these soluble adhesion molecules showed a positive correlation with cardiovascular diseases in these patients (Hegazy et al., 2020).

These results demonstrate that hyperglycemia, along with pro-inflammatory mediators, is a potent inducer of endothelial dysfunction. They further support the reports documenting diabetes as an associated risk factor for developing vascular complications (Einarson et al., 2018).

II. Impact on the expression of additional pro-inflammatory mediators

The pro-inflammatory pathways activated by metabolic stress factors and the immune cells infiltrating into the adipose tissue serve as the primary sources of chemokines and cytokines observed in patients with diabetes. These chemokines and cytokines further contribute to pre-existing inflammation.

The secretion of interleukins IL-1 α , IL-6, and IL-8 was significantly elevated under the diabetes-like culture conditions. IL-1 α acts as a nuclear protein that translocates into the nucleus and mediates the expression of other interleukins, such as IL-6 and IL-8 (Ballak et al., 2015; Dinarello, 2018). It also acts as a danger signal generated by the necrotic cells and instigates inflammation in the necrotic core of atherosclerotic lesions (Pfeiler et al., 2019). Increased levels of IL-6 have been reported in patients with diabetes and are strongly associated with a high incidence of T2D (Bowker et al., 2020). In diabetes, the action of IL-6 is linked with the destruction of β -cells of the pancreas and, thus, the development of insulin resistance (Kreiner et al., 2022). The expression of IL-6 in endothelial cells is upregulated in response to inflammation, leading to vascular permeability and coagulation (Kreiner et al., 2022). IL-8 mediates acute inflammatory responses by recruiting monocytes and neutrophils and mediating their adhesion to the endothelium (Apostolakis et al., 2009). Hence, it contributes to the initial stages of atherogenesis. Higher IL-8 circulating levels were noted in the serum of patients with T2D and were associated with worsened inflammatory and cardiometabolic profiles (Cimini et al., 2017).

The abundance of cytokines and chemokines such as TNF- α , MCSF-1, MIP-1 α , and SDF-1 α was also increased in the supernatant of the HUVECs exposed to the pro-inflammatory mediators in the presence of hyperglycemia.

TNF- α is a highly potent pro-inflammatory cytokine as it regulates the activity of many multifunctional pathways such as JNK and NF- κ B (Akash et al., 2018) promoting β -cell apoptosis, systemic inflammation and vascular complications (Akash et al., 2018; (Urschel & Cicha, 2015)). A report also depicted increased TNF- α levels in patients with diabetes (C. Liu et al., 2016).

In contrast to the pro-inflammatory effects exerted by TNF- α , MCSF leads to the polarization of macrophages to an anti-inflammatory M2 phenotype (Vogel et al., 2014). These M2 macrophages synthesize TGF- β that promotes tissue remodeling after myocardial infarction (Frangogiannis, 2017). MIP-1 α is also elevated in the supernatant of HUVECs cultured under diabetes-like conditions. This chemotactic cytokine is involved in the recruitment of leukocytes in response to vascular injury, further escalating inflammation (Bhavsar et al., 2015). SDF-1 α is a crucial chemokine that regulates various biological processes. It is involved in the pathogenesis of several diseases, including cancer, autoimmune and cardiovascular diseases (Mousavi, 2020). It is also known to

upregulate the expression of IL-1 α , IL-1 β , TNF- α , and TGF- β (Mousavi, 2020). It also upregulates the expression of several transcription factors inducing epithelial to mesenchymal transition (Onoue et al., 2006). SDF-1 α levels are also significantly abundant in patients with T2D as compared to healthy controls (Loader et al., 2008).

Beta cell dysfunction, adipose tissue remodeling, and endothelial dysfunction are integral components of the manifestation and progression of diabetes. These processes instigate a plethora of signaling cascades that release pro-inflammatory cytokines and chemokine into the blood. Our data demonstrate a similar phenomenon in the CC-genotype HUVECs upon exposure to the diabetes-like culture conditions.

6.2.4. Influence of a diabetes-like microenvironment on CD40 downstream signaling

Since CD40 lacks an intracellular kinase domain, the recruitment of additional adaptor molecules is required to initiate further downstream signaling. Such adapter molecules are the TNF receptor-associated factors (TRAFs). TRAF2 and TRAF6-mediated CD40 downstream signaling has been shown to promote endothelial dysfunction (Lutgens et al., 2010; Sultan et al., 2020).

High glucose did not seem to have an additional effect on *TRAF2* mRNA levels in HUVECs exposed to a pro-inflammatory microenvironment. However, hyperglycemia significantly elevated *TRAF6* transcript levels when combined with the pro-inflammatory mediators. Thus, hyperglycemia favours TRAF6-mediated CD40 downstream signaling during pro-inflammatory conditions. This observation supports previous findings confirming a role for TRAF6-induced NF- κ B signaling in modulating endothelial dysfunction under hyperglycemia (R. Liu et al., 2018). Furthermore, inhibition of TRAF6 has been shown to downregulate the expression of VACM-1 and ICAM-1. This inhibition also attenuated the progression of atherosclerosis (R. Liu et al., 2018). Finally, it restored endothelial dysfunction by mitigating inflammation and oxidative stress in the type 2 diabetic db/db mouse model (Steven et al., 2018).

These findings demonstrate that the cell culture model established in this study holds the potential to imitate the *in vivo* processes promoting atherosclerosis and diabetes to a certain extent. The current data confirm the observations made by other groups that suggest the involvement of TRAF6 in mediating atherosclerotic events during diabetes.

6.2.5. The diabetes-like microenvironment promotes EndMT

Endothelial cells maintain their phenotype under normal physiological conditions for years or a life span (Goncharov et al., 2017). However, recent studies demonstrated that endothelial cells possess remarkable phenotype plasticity and can undergo endothelial-to-mesenchymal transition upon exposure to various stress factors (Piera-Velazquez & Jimenez, 2019). EndMT is a complex biological process during which endothelial cells lose their lineage-specific markers and progressively acquire the expression of markers specific to the mesenchymal lineage (Dejana et al., 2017). As observed in the present study, this development is accompanied by morphological changes where these polygonal cells transform into elongated spindle-shaped cells and demonstrate the loss of cell-cell junctions and polarity (Dejana et al., 2017).

The expression of mesenchymal markers α -SMA and SM22- α was upregulated in the HUVECs cultured under diabetes-like conditions. In contrast, the endothelial marker NOS3 was significantly downregulated under the same conditions. To adapt to such a microenvironment, the cells undergo EndMT by modifying their extracellular matrix composition to a great extent (Zhao et al., 2021). Therefore, mRNA levels of prominent extracellular matrix markers generally modulated under EndMT conditions like *COL1a1*, *COL3a1*, and *FNI* were examined. While no significant changes in the expression of the collagen genes were observed, *FNI* transcript levels were significantly increased in the hyperglycemic group. Hyperglycemia further boosted the mRNA levels of *FNI* in HUVECs treated with pro-inflammatory mediators.

Matrix metalloproteinases also play a crucial role in maintaining extracellular matrix homeostasis by causing proteolytic cleavage of various extracellular matrix proteins (Laronha & Caldeira, 2020). The expression of MMP-2 and MMP-9 is known to be enhanced during EndMT (Cho et al., 2018). However, there was no difference in MMP-9 release in the diabetic HUVECs, but it was enhanced in the HUVECs subjected to the pro-inflammatory mediators. MMP-2 protein abundance was significantly decreased in the conditioned medium of the diabetic HUVECs. However, MMP-2 and MMP-9 can also cleave collagens (Laronha & Caldeira, 2020). Therefore, changes in the dynamics of collagen and fibronectin homeostasis may indirectly affect the expression of these MMPs. It would be interesting to measure the MMP activity under diabetic conditions in our cell culture model to better understand their role in our experimental settings.

After confirming the initiation of EndMT under these experimental conditions, the possible mechanisms associated therewith were investigated. TGF- β signaling is involved in the progression of diabetes (X. Ma et al., 2020; H.-L. Wang et al., 2022) and is also a mediator of EndMT (J. Ma et al., 2020; Pardali et al., 2017). While the secretion of TGF- β 1 was not altered in the diabetes-like microenvironment, the abundance of TGF- β 2 was significantly higher under these conditions. Other studies also report the involvement of TGF- β 2 in driving EndMT in endothelial cells of microvascular and macrovascular origins (Doerr et al., 2016; Maleszewska et al., 2013; Sabbineni et al., 2018). TGF- β signaling induces the expression of many other molecular components to exert its varied biological effects. In the case of EndMT, it is known to regulate the expression of transcription factors such as Snail1, Snail2, Twist, and Zeb family members (Piera-Velazquez & Jimenez, 2019). In this study, *ZEB2* mRNA levels were significantly augmented under the diabetes-like microenvironment. Increased expression of *ZEB2* during inflammation is reported in the literature and modulates EndMT under diabetes (Adjuto-Saccone et al., 2021; de Jesus et al., 2021; Kumar et al., 2016; Xian et al., 2020). An acquisition of mesenchymal markers with reduced NOS3 expression, ECM remodeling, and increased expression of EndMT mediators indicate the initiation of the EndMT program in our diabetes-like cell culture model. However, EndMT is a very complex phenomenon wherein endothelial cells undergo a spectrum of intermediate steps (Welch-Reardon et al., 2015). At such intermediate stages, the cells retain the expression of a few lineage markers and also express specific mesenchymal lineage markers (Piera-Velazquez & Jimenez, 2019). The HUVECs in our experimental setting express mesenchymal markers while retaining the expression of endothelial markers such as CD31 and VE-cadherin. These findings suggest that the HUVECs, when exposed to a long-term diabetes-like microenvironment, acquire a partial EndMT phenotype. Also, any increase in the expression of late EndMT markers such as collagen1 α 1 and collagen3 α 1 (Maleszewska et al., 2013) could not be verified.

6.2.6. Potential role of NFAT5 in the pathogenesis of diabetes

6.2.6.1. NFAT5 mediates progression of diabetes and contributes to the associated vascular complications

NFAT5 is a transcription factor belonging to the Rel/nuclear factor- (NF-) κ B family (Aramburu et al., 2006). Its DNA binding domain shares sequence homology with both the Rel family as well as other members of the NFAT family (Aramburu et al., 2006).

Under transient and short-term hypertonic stress conditions, NFAT5 is rapidly phosphorylated and translocates to the nucleus (Cheung & Ko, 2013). It then drives the transcription of its target genes to restore the osmolarity to normal (Cheung & Ko, 2013). Hence, NFAT5 mediates protective mechanisms under normal physiological conditions. However, the physiological role of NFAT5 is altered under prolonged periods of hyperosmolarity, such as under hyperglycemia.

In addition to the progression of diabetes, NFAT5 also contributes to the development of diabetes-associated vascular complications. Hyperglycemia downregulates the PI3K/AKT signaling, reducing NOS3 expression (Madonna et al., 2020). Initiation of these events is mediated by the nuclear translocation and transcriptional activity of NFAT5 (Madonna et al., 2020). NFAT5 is activated by biomechanical stretch generated at arterial bifurcations and promotes migration and remodeling of vascular smooth muscle cells, leading to arterial stiffening (Scherer et al., 2014). Moreover, NFAT5 causes the activation of NLRP3 inflammasome under hyperosmolarity (P. Ma et al., 2019). NLRP3 further upregulates IL-1 β expression, contributing to the progression of atherosclerosis (P. Ma et al., 2019).

6.2.6.2. Impact of NFAT5 on NF- κ B-induced downstream signaling

NFAT5 can indirectly activate NF- κ B by increasing the expression of TNF- α (Esensten et al., 2005). Another study reported the ability of NFAT5 to enhance NF- κ B expression under hyperosmolarity (Roth et al., 2010). Moreover, hyperosmolarity in kidney cells leads to the binding of p65/p50 dimers to the κ B domain of NFAT5 (Roth et al., 2010). The resulting p65/p50 NFAT5 complex further drives the expression of NF- κ B target genes. In addition, the promoter regions of genes such as E-selectin, MCP-1, CD40, SM22, and ZEB2 consist of several adjacent NF- κ B and NFAT5 binding sites (Example of the E-selectin promoter region in supplementary figure S4). The proximity of their binding sites in the promoter regions of these genes suggests a plausible NF- κ B/NFAT5 co-activity in the regulation of endothelial dysfunction and EndMT.

6.2.6.3. NFAT5 expression and abundance in the diabetes-like cell culture model

NFAT5 mRNA levels were significantly elevated in HUVECs exposed to high glucose concentrations in combination with cytokines compared to the treatment with cytokines alone. These results suggest a possible positive effect of hyperosmolarity on NFAT5

expression under pro-inflammatory conditions. Since NFAT5 can only exert its transcriptional activity after translocating to the nucleus, its nuclear and cytoplasmic abundance was further examined. Pro-inflammatory conditions generated by TNF- α and sCD40L double stimulation caused modest but significant increase in NFAT5 abundance in the nucleus compared to the control. In addition to these pro-inflammatory mediators, hyperglycemia further increased the abundance of NFAT5 in the nucleus. Moreover, a minimal but significant increase in NFAT5 protein was observed in the cytoplasm of HUVECs treated with cytokines only in the presence of high glucose concentrations. Due to the lack of an appropriate osmotic control, it is difficult to contemplate whether this effect was due to the pro-osmotic effect of the hyperglycemic conditions.

To understand the relevance of increased NFAT5 transcription and nuclear translocation, NFAT5 binding sites were blocked competitively by applying NFAT5 neutralizing decoy ODNs to the HUVECs. Decoy ODNs are short double-stranded DNA molecules with a sequence similar to the consensus binding site of the target transcription factor to the cis-regulatory promoter sequence of its target genes (Hecker & Wagner, 2017).

Pre-incubation of HUVECs with the NFAT5-neutralising decoy ODN significantly downregulated the expression of SM22 α , which was otherwise enhanced upon exposure to the diabetes-like microenvironment. As discussed earlier, there are neighbouring NF- κ B/NFAT5 binding sites in the promoter region of SM22 α . Competitive inhibition of these binding sites located in the promoter region by the decoy ODN seems plausible to explain the reduced SM22 α protein levels. As in the case of SM22 α , NFAT5 could also possibly regulate the expression of other EndMT markers containing NFAT5 binding sites in their promoter regions.

6.3. Limitations

Some further limitations of this study need to be considered. The allele frequencies with regard to the T-1C SNP of the *CD40* gene within the diabetic cohorts were compared to those of umbilical cords. Since it is difficult to find many age-matched individuals free of potentially confounding health conditions, DNA samples from the umbilical cords were considered an appropriate control. Furthermore, the patient cohorts were not stratified by additional risk factors such as obesity or CHD. As diabetes is a metabolic syndrome often accompanied by further health problems, stratifying the patient population by these common risk factors seemed unrealistic. The existence of strong

linkage disequilibrium between the T-1C SNP and another intronic T945G SNP of the *CD40* gene (rs 4810485) has been reported (Raychaudhuri et al., 2008). Hence, the possible confounding effect of this particular SNP and/or others strongly linked to the T-1C SNP of the *CD40* gene on our observations cannot be completely ruled out. However, to our knowledge, an association of the T945G SNP with diabetes has not yet been reported.

This study also provides insights into the differential gene expression between the sCD40L-stimulated CC and TT-genotype HUVECs. However, these findings are restricted to the mRNA level and must be validated at the protein level. Nevertheless, our data is in line with the findings made by Sultan et al. (Sultan et al., 2020), documenting similar differential protein expression amongst these two genotypes.

6.4. Summary and future perspectives

CD40 downstream signaling plays a crucial role in the pathogenesis of diabetes. It promotes apoptosis of the pancreatic β -cells and insulin secretion and signaling impairment. Systemic inflammation further stems from the CD40 signaling mediated events in the adipocytes, immune cells, endothelial cells, and vascular smooth muscle cells. This systemic inflammation leads to the progression of vascular and other diabetes-associated complications. The T-1C SNP of the *CD40* gene affects CD40 protein abundance and functions as a risk factor for immune-modulated diseases, including CHD.

This study provides novel insights into the association of the T-1C SNP in the *CD40* gene in the Caucasian population with T2D. As observed in the case of CHD, the C allele of this SNP confers a significantly enhanced risk of developing T2D. Plasma levels of the pro-inflammatory sCD40L were augmented in the diabetic cohort and depicted a positive correlation with the sCD40 plasma levels in patients homozygous for the C allele. Soluble CD40 acts as a decoy receptor that neutralizes the activity of CD40L to compensate for enhanced inflammation mediated by the downstream targets of CD40 signaling. The highest sCD40 levels were documented in the plasma of CC-genotype patients suffering from T2D patients than those with other genotypes, which denotes the increased extent of CD40 signaling occurring in these patients.

Upon stimulation with sCD40L, CC-genotype HUVECs demonstrated a higher transcriptional regulation than TT-genotype cells. Furthermore, sCD40L stimulation in the CC-genotype HUVECs activated pathways that promote inflammation, insulin

resistance, and EndMT. Contrarily, stimulation of the TT-genotype cells with sCD40L upregulated the expression of the gene products that resolve inflammation. The mediators of EndMT were also downregulated in these cells.

Further exposure of these pro-inflammatory CC-genotype HUVECs to a diabetes-like microenvironment boosted the expression of chemokines, cytokines, and adhesion molecules involved in the progression of systemic inflammation. Finally, the diabetes-like microenvironment shifted these cells towards an intermediate EndMT state.

Under these experimental conditions, an increased expression and nuclear translocation of the osmoadaptive transcription factor NFAT5 was also documented in the HUVECs. Neutralizing NFAT5 with a corresponding decoy ODN significantly reduced the expression of the otherwise upregulated mesenchymal marker SM22 α in these cells. Thus, this study confirms a role of NFAT5 in mediating EndMT in a diabetes-like microenvironment.

Though this study provides sufficient evidence to depict an association of the T-1C SNP of the *CD40* gene with T2D, increasing the number of patient and control samples shall add more power to this observation. Similarly, analysis of additional T1D patient samples shall provide a deeper insight into the association of this SNP with T1D, which currently is unclear due to low n-numbers. Furthermore, differential gene expression between sCD40L-stimulated CC vs. TT-genotype cells in this study was examined at the transcript level. Additional experiments to analyze these gene products' protein levels are essential to confirm these initial findings.

This study investigated the impact of a diabetes-like microenvironment on endothelial function and properties using only the CC-genotype HUVECs. Further experiments testing the effects of such a microenvironment on TT-genotype HUVECs shall provide insights into the impact of this SNP in modulating differential endothelial responses under pathological conditions.

In addition to its biological effects, glucose can also exert pro-osmotic effects, which might play a role in the activation of NFAT5. Additional experiments using an appropriate osmotic control shall be valuable in this context. While this study confirms the activation of NFAT5 under diabetes-like conditions, the exact mechanism of the complex interaction with other activated transcription factors remains to be elucidated.

Similarly, the downstream signaling initiated by NFAT5 and that promoting EndMT under the current model need to be further investigated.

Last but not least, confirmation of the role of NFAT5 in driving EndMT *in vivo* sounds promising. For this purpose, a T2D db/db and NFAT5 double knockout mice model can be generated to compare the markers and properties of the endothelial cells of these mice to those of the control. Histological staining of the endothelial cells for mesenchymal markers and NFAT5 in human tissues obtained from patients with diabetes during biopsies and kidney transplants might help to confirm the current findings.

7. REFERENCES

7.1. Websites

<https://www.mn-net.com/media/pdf/a0/12/3b/Instruction-NucleoSpin-TriPrep.pdf>,

accessed on 02.08.2022

https://www.who.int/health-topics/diabetes#tab=tab_1, accessed on 26.06.2022

<https://www.who.int/europe/news-room/fact-sheets/item/diabetes>, accessed on 26.06.2022

<https://www.geneandcell.com/blogs/molecular-biology-methods/human-tnf-alpha-stability-testing>, accessed on 08.09.2022

<https://www.who.int/news-room/fact-sheets/detail/diabetes>, accessed on 26.06.2022).

7.2. Publications

Adeyemo, A., & Rotimi, C. (2010). Genetic variants associated with complex human diseases show wide variation across multiple populations. *Public Health Genomics*, 13(2), 72–79. <https://doi.org/10.1159/000218711>

Adjuto-Saccone, M., Soubeyran, P., Garcia, J., Audebert, S., Camoin, L., Rubis, M., Roques, J., Binétruy, B., Iovanna, J. L., & Tournaire, R. (2021). TNF- α induces endothelial–mesenchymal transition promoting stromal development of pancreatic adenocarcinoma. *Cell Death & Disease*, 12(7), 649. <https://doi.org/10.1038/s41419-021-03920-4>

Agouni, A., Tual-Chalot, S., Chalopin, M., Duluc, L., Mody, N., Martinez, M. C., Andriantsitohaina, R., & Delibegović, M. (2014). Hepatic protein tyrosine phosphatase 1B (PTP1B) deficiency protects against obesity-induced endothelial dysfunction. *Biochemical Pharmacology*, 92(4), 607–617. <https://doi.org/10.1016/j.bcp.2014.10.008>

Ahlqvist, E., Prasad, R. B., & Groop, L. (2020). Subtypes of Type 2 Diabetes Determined From Clinical Parameters. *Diabetes*, 69(10), 2086–2093. <https://doi.org/10.2337/dbi20-0001>

Akash, M. S. H., Rehman, K., & Liaqat, A. (2018). Tumor Necrosis Factor-Alpha: Role in Development of Insulin Resistance and Pathogenesis of Type 2 Diabetes Mellitus. *Journal of Cellular Biochemistry*, 119(1), 105–110. <https://doi.org/10.1002/jcb.26174>

- Al-Dahr, M. H. S. (2016). Inflammatory biomarkers and endothelial dysfunction among obese type 2 diabetic patients: A correlational study. *Electronic Journal of General Medicine*, 13(3). <https://doi.org/10.29333/ejgm/81901>
- Aloui, C., Prigent, A., Sut, C., Tariket, S., Hamzeh-Cognasse, H., Pozzetto, B., Richard, Y., Cognasse, F., Laradi, S., & Garraud, O. (2014). The Signaling Role of CD40 Ligand in Platelet Biology and in Platelet Component Transfusion. *International Journal of Molecular Sciences*, 15(12), 22342–22364. <https://doi.org/10.3390/ijms151222342>
- Altshuler, D., Daly, M. J., & Lander, E. S. (2008). Genetic mapping in human disease. *Science* (New York, N.Y.), 322(5903), 881–888. <https://doi.org/10.1126/science.1156409>
- Apostolakis, S., Vogiatzi, K., Amanatidou, V., & Spandidos, D. A. (2009). Interleukin 8 and cardiovascular disease. *Cardiovascular Research*, 84(3), 353–360. <https://doi.org/10.1093/cvr/cvp241>
- Aramburu, J., Drews-Elger, K., Estrada-Gelonch, A., Minguillón, J., Morancho, B., Santiago, V., & López-Rodríguez, C. (2006). Regulation of the hypertonic stress response and other cellular functions by the Rel-like transcription factor NFAT5. *Biochemical Pharmacology*, 72(11), 1597–1604. <https://doi.org/10.1016/j.bcp.2006.07.002>
- Assar, M. E., Angulo, J., & Rodríguez-Mañas, L. (2016). Diabetes and ageing-induced vascular inflammation. *The Journal of Physiology*, 594(8), 2125–2146. <https://doi.org/10.1113/JP270841>
- Bachsais, M., Salti, S., Zaoui, K., Hassan, G. S., Aoudjit, F., & Mourad, W. (2020). CD154 inhibits death of T cells via a Cis interaction with the $\alpha 5\beta 1$ integrin. *PloS One*, 15(8), e0235753. <https://doi.org/10.1371/journal.pone.0235753>
- Bagnati, M., Ogunkolade, B. W., Marshall, C., Tucci, C., Hanna, K., Jones, T. A., Bugliani, M., Nedjai, B., Caton, P. W., Kieswich, J., Yaqoob, M. M., Ball, G. R., Marchetti, P., Hitman, G. A., & Turner, M. D. (2016). Glucolipototoxicity initiates pancreatic β -cell death through TNFR5/CD40-mediated STAT1 and NF- κ B activation. *Cell Death & Disease*, 7(8), e2329. <https://doi.org/10.1038/cddis.2016.203>
- Bakker, W., Eringa, E. C., Sipkema, P., & van Hinsbergh, V. W. M. (2009). Endothelial dysfunction and diabetes: Roles of hyperglycemia, impaired insulin signaling and

obesity. *Cell and Tissue Research*, 335(1), 165–189. <https://doi.org/10.1007/s00441-008-0685-6>

Ballak, D. B., Stienstra, R., Tack, C. J., Dinarello, C. A., & van Diepen, J. A. (2015). IL-1 family members in the pathogenesis and treatment of metabolic disease: Focus on adipose tissue inflammation and insulin resistance. *Cytokine*, 75(2), 280–290. <https://doi.org/10.1016/j.cyto.2015.05.005>

Barlic, J., McDermott, D. H., Merrell, M. N., Gonzales, J., Via, L. E., & Murphy, P. M. (2004). Interleukin (IL)-15 and IL-2 Reciprocally Regulate Expression of the Chemokine Receptor CX3CR1 through Selective NFAT1- and NFAT2-dependent Mechanisms. *Journal of Biological Chemistry*, 279(47), 48520–48534. <https://doi.org/10.1074/jbc.M406978200>

Bhatti, G. K., Bhadada, S. K., Vijayvergiya, R., Mastana, S. S., & Bhatti, J. S. (2016). Metabolic syndrome and risk of major coronary events among the urban diabetic patients: North Indian Diabetes and Cardiovascular Disease Study-NIDCVD-2. *Journal of Diabetes and Its Complications*, 30(1), 72–78. <https://doi.org/10.1016/j.jdiacomp.2015.07.008>

Bhavsar, I., Miller, C. S., & Al-Sabbagh, M. (2015). Macrophage Inflammatory Protein-1 Alpha (MIP-1 alpha)/CCL3: As a Biomarker. In V. R. Preedy & V. B. Patel (Eds.), *General Methods in Biomarker Research and their Applications* (pp. 223–249). Springer Netherlands. https://doi.org/10.1007/978-94-007-7696-8_27

Bosmans, L. A., Bosch, L., Kusters, P. J. H., Lutgens, E., & Seijkens, T. T. P. (2021). The CD40-CD40L Dyad as Immunotherapeutic Target in Cardiovascular Disease. *Journal of Cardiovascular Translational Research*, 14(1), 13–22. <https://doi.org/10.1007/s12265-020-09994-3>

Bowker, N., Shah, R. L., Sharp, S. J., Luan, J., Stewart, I. D., Wheeler, E., Ferreira, M. A. R., Baras, A., Wareham, N. J., Langenberg, C., & Lotta, L. A. (2020). Meta-analysis investigating the role of interleukin-6 mediated inflammation in type 2 diabetes. *EBioMedicine*, 61, 103062. <https://doi.org/10.1016/j.ebiom.2020.103062>

Brocker, C., Thompson, D. C., & Vasiliou, V. (2012). The role of hyperosmotic stress in inflammation and disease. *BioMolecular Concepts*, 3(4), 345–364. <https://doi.org/10.1515/bmc-2012-0001>

- Buse, M. G. (2006). Hexosamines, insulin resistance, and the complications of diabetes: Current status. *American Journal of Physiology-Endocrinology and Metabolism*, 290(1), E1–E8. <https://doi.org/10.1152/ajpendo.00329.2005>
- Cen, L., Xing, F., Xu, L., & Cao, Y. (2020). Potential Role of Gene Regulator NFAT5 in the Pathogenesis of Diabetes Mellitus. *Journal of Diabetes Research*, 2020, 1–13. <https://doi.org/10.1155/2020/6927429>
- Chakrabarti, S., Varghese, S., Vitseva, O., Tanriverdi, K., & Freedman, J. E. (2005). CD40 Ligand Influences Platelet Release of Reactive Oxygen Intermediates. *Arteriosclerosis, Thrombosis, and Vascular Biology*, 25(11), 2428–2434. <https://doi.org/10.1161/01.ATV.0000184765.59207.f3>
- Chatzigeorgiou, A., Lyberi, M., Chatzilymperis, G., Nezos, A., & Kamper, E. (2009). CD40/CD40L signaling and its implication in health and disease. *BioFactors*, 35(6), 474–483. <https://doi.org/10.1002/biof.62>
- Chen, X., Guo, X., Ge, Q., Zhao, Y., Mu, H., & Zhang, J. (2019). ER Stress Activates the NLRP3 Inflammasome: A Novel Mechanism of Atherosclerosis. *Oxidative Medicine and Cellular Longevity*, 2019, 1–18. <https://doi.org/10.1155/2019/3462530>
- Chen, Y., Huang, L., Qi, X., & Chen, C. (2019). Insulin Receptor Trafficking: Consequences for Insulin Sensitivity and Diabetes. *International Journal of Molecular Sciences*, 20(20), Article 20. <https://doi.org/10.3390/ijms20205007>
- Cheung, C. Y., & Ko, B. C. (2013). NFAT5 in cellular adaptation to hypertonic stress—Regulations and functional significance. *Journal of Molecular Signaling*, 8(1), 5. <https://doi.org/10.1186/1750-2187-8-5>
- Cho, J. G., Lee, A., Chang, W., Lee, M.-S., & Kim, J. (2018). Endothelial to Mesenchymal Transition Represents a Key Link in the Interaction between Inflammation and Endothelial Dysfunction. *Frontiers in Immunology*, 9, 294. <https://doi.org/10.3389/fimmu.2018.00294>
- Chung, S. S. M., Ho, E. C. M., Lam, K. S. L., & Chung, S. K. (2003). Contribution of Polyol Pathway to Diabetes-Induced Oxidative Stress. *Journal of the American Society of Nephrology*, 14(suppl 3), S233–S236. <https://doi.org/10.1097/01.ASN.0000077408.15865.06>

Cimini, F. A., Barchetta, I., Porzia, A., Mainiero, F., Costantino, C., Bertocchini, L., Ceccarelli, V., Morini, S., Baroni, M. G., Lenzi, A., & Cavallo, M. G. (2017). Circulating IL-8 levels are increased in patients with type 2 diabetes and associated with worse inflammatory and cardiometabolic profile. *Acta Diabetologica*, 54(10), 961–967. <https://doi.org/10.1007/s00592-017-1039-1>

Clyne, A. M. (2021). Endothelial response to glucose: Dysfunction, metabolism, and transport. *Biochemical Society Transactions*, 49(1), 313–325. <https://doi.org/10.1042/BST20200611>

Contin, C., Pitard, V., Delmas, Y., Pelletier, N., Defrance, T., Moreau, J.-F., Merville, P., & Déchanet-Merville, J. (2003). Potential role of soluble CD40 in the humoral immune response impairment of uraemic patients. *Immunology*, 110(1), 131–140. <https://doi.org/10.1046/j.1365-2567.2003.01716.x>

Contin, C., Pitard, V., Itai, T., Nagata, S., Moreau, J.-F., & Déchanet-Merville, J. (2003). Membrane-anchored CD40 is processed by the tumor necrosis factor-alpha-converting enzyme. Implications for CD40 signaling. *The Journal of Biological Chemistry*, 278(35), 32801–32809. <https://doi.org/10.1074/jbc.M209993200>

Cornelius, D. C., Baik, C. H., Travis, O. K., White, D. L., Young, C. M., Austin Pierce, W., Shields, C. A., Poudel, B., & Williams, J. M. (2019). NLRP 3 inflammasome activation in platelets in response to sepsis. *Physiological Reports*, 7(9), e14073. <https://doi.org/10.14814/phy2.14073>

Cyr, A. R., Huckaby, L. V., Shiva, S. S., & Zuckerbraun, B. S. (2020). Nitric Oxide and Endothelial Dysfunction. *Critical Care Clinics*, 36(2), 307–321. <https://doi.org/10.1016/j.ccc.2019.12.009>

Dai, J., Fang, P., Saredy, J., Xi, H., Ramon, C., Yang, W., Choi, E. T., Ji, Y., Mao, W., Yang, X., & Wang, H. (2017). Metabolism-associated danger signal-induced immune response and reverse immune checkpoint-activated CD40⁺ monocyte differentiation. *Journal of Hematology & Oncology*, 10(1), 141. <https://doi.org/10.1186/s13045-017-0504-1>

Dal Canto, E., Ceriello, A., Rydén, L., Ferrini, M., Hansen, T. B., Schnell, O., Standl, E., & Beulens, J. W. (2019). Diabetes as a cardiovascular risk factor: An overview of global

trends of macro and micro vascular complications. *European Journal of Preventive Cardiology*, 26(2_suppl), 25–32. <https://doi.org/10.1177/2047487319878371>

Daub, S., Lutgens, E., Münzel, T., & Daiber, A. (2020). CD40/CD40L and Related Signaling Pathways in Cardiovascular Health and Disease-The Pros and Cons for Cardioprotection. *International Journal of Molecular Sciences*, 21(22), E8533. <https://doi.org/10.3390/ijms21228533>

de Jesus, D. S., Mak, T. C. S., Wang, Y.-F., von Ohlen, Y., Bai, Y., Kane, E., Chabosseau, P., Chahrour, C. M., Distaso, W., Salem, V., Tomas, A., Stoffel, M., Rutter, G. A., & Latreille, M. (2021). Dysregulation of the Pdx1/Ovol2/Zeb2 axis in dedifferentiated β -cells triggers the induction of genes associated with epithelial–mesenchymal transition in diabetes. *Molecular Metabolism*, 53, 101248. <https://doi.org/10.1016/j.molmet.2021.101248>

De Nigris, V., Pujadas, G., La Sala, L., Testa, R., Genovese, S., & Ceriello, A. (2015). Short-term high glucose exposure impairs insulin signaling in endothelial cells. *Cardiovascular Diabetology*, 14(1), 114. <https://doi.org/10.1186/s12933-015-0278-0>

Dejana, E., Hirschi, K. K., & Simons, M. (2017). The molecular basis of endothelial cell plasticity. *Nature Communications*, 8(1), 14361. <https://doi.org/10.1038/ncomms14361>

Derosa, G., & Maffioli, P. (2016). A review about biomarkers for the investigation of vascular function and impairment in diabetes mellitus. *Vascular Health and Risk Management*, 12, 415–419. <https://doi.org/10.2147/VHRM.S64460>

Dimitrakopoulos, F.-I. D., Antonacopoulou, A. G., Kottorou, A. E., Kalofonou, M., Panagopoulos, N., Dougenis, D., Makatsoris, T., Tzelepi, V., Koutras, A., & Kalofonos, H. P. (2021). Genetic Variations of CD40 and LT β R Genes Are Associated With Increased Susceptibility and Clinical Outcome of Non-Small-Cell Carcinoma Patients. *Frontiers in Oncology*, 11, 721577. <https://doi.org/10.3389/fonc.2021.721577>

Dinarello, C. A. (2018). Overview of the IL-1 family in innate inflammation and acquired immunity. *Immunological Reviews*, 281(1), 8–27. <https://doi.org/10.1111/imr.12621>

Doerr, M., Morrison, J., Bergeron, L., Coomber, B. L., & Vilorio-Petit, A. (2016). Differential effect of hypoxia on early endothelial–mesenchymal transition response to transforming growth beta isoforms 1 and 2. *Microvascular Research*, 108, 48–63. <https://doi.org/10.1016/j.mvr.2016.08.001>

- Dogné, S., Flamion, B., & Caron, N. (2018). Endothelial Glycocalyx as a Shield Against Diabetic Vascular Complications: Involvement of Hyaluronan and Hyaluronidases. *Arteriosclerosis, Thrombosis, and Vascular Biology*, 38(7), 1427–1439. <https://doi.org/10.1161/ATVBAHA.118.310839>
- Domingueti, C. P., Dusse, L. M. S., Carvalho, M. das G., de Sousa, L. P., Gomes, K. B., & Fernandes, A. P. (2016). Diabetes mellitus: The linkage between oxidative stress, inflammation, hypercoagulability and vascular complications. *Journal of Diabetes and Its Complications*, 30(4), 738–745. <https://doi.org/10.1016/j.jdiacomp.2015.12.018>
- Donath, M. Y., & Shoelson, S. E. (2011). Type 2 diabetes as an inflammatory disease. *Nature Reviews. Immunology*, 11(2), 98–107. <https://doi.org/10.1038/nri2925>
- Du, W., Ren, L., Hamblin, M. H., & Fan, Y. (2021). Endothelial Cell Glucose Metabolism and Angiogenesis. *Biomedicines*, 9(2), Article 2. <https://doi.org/10.3390/biomedicines9020147>
- Eelen, G., de Zeeuw, P., Treps, L., Harjes, U., Wong, B. W., & Carmeliet, P. (2018). Endothelial Cell Metabolism. *Physiological Reviews*, 98(1), 3–58. <https://doi.org/10.1152/physrev.00001.2017>
- Egaña-Gorroño, L., López-Díez, R., Yepuri, G., Ramirez, L. S., Reverdatto, S., Gugger, P. F., Shekhtman, A., Ramasamy, R., & Schmidt, A. M. (2020). Receptor for Advanced Glycation End Products (RAGE) and Mechanisms and Therapeutic Opportunities in Diabetes and Cardiovascular Disease: Insights From Human Subjects and Animal Models. *Frontiers in Cardiovascular Medicine*, 7. <https://www.frontiersin.org/articles/10.3389/fcvm.2020.00037>
- Einarson, T. R., Acs, A., Ludwig, C., & Panton, U. H. (2018). Prevalence of cardiovascular disease in type 2 diabetes: A systematic literature review of scientific evidence from across the world in 2007–2017. *Cardiovascular Diabetology*, 17(1), 83. <https://doi.org/10.1186/s12933-018-0728-6>
- El Haouari, M., & Rosado, J. A. (2008). Platelet signalling abnormalities in patients with type 2 diabetes mellitus: A review. *Blood Cells, Molecules, and Diseases*, 41(1), 119–123. <https://doi.org/10.1016/j.bcmed.2008.02.010>

- Elmetwali, T., Salman, A., Wei, W., Hussain, S. A., Young, L. S., & Palmer, D. H. (2020). CD40L membrane retention enhances the immunostimulatory effects of CD40 ligation. *Scientific Reports*, 10(1), 342. <https://doi.org/10.1038/s41598-019-57293-y>
- Engel, D., Seijkens, T., Poggi, M., Sanati, M., Thevissen, L., Beckers, L., Wijnands, E., Lievens, D., & Lutgens, E. (2009). The immunobiology of CD154–CD40–TRAF interactions in atherosclerosis. *Seminars in Immunology*, 21(5), 308–312. <https://doi.org/10.1016/j.smim.2009.06.004>
- Erez, O., Romero, R., Hoppensteadt, D., Fareed, J., Chaiworapongsa, T., Kusanovic, J. P., Mazaki-Tovi, S., Gotsch, F., Than, N. G., Vaisbuch, E., Kim, C. J., Espinoza, J., Mittal, P., Hamill, N., Nhan-Chang, C.-L., Mazor, M., & Hassan, S. (2008). Premature labor: A state of platelet activation? *Journal of Perinatal Medicine*, 36(5). <https://doi.org/10.1515/JPM.2008.082>
- Eringa, E. C., Serne, E. H., Meijer, R. I., Schalkwijk, C. G., Houben, A. J. H. M., Stehouwer, C. D. A., Smulders, Y. M., & van Hinsbergh, V. W. M. (2013). Endothelial dysfunction in (pre)diabetes: Characteristics, causative mechanisms and pathogenic role in type 2 diabetes. *Reviews in Endocrine and Metabolic Disorders*, 14(1), 39–48. <https://doi.org/10.1007/s11154-013-9239-7>
- Esensten, J. H., Tsytsykova, A. V., Lopez-Rodriguez, C., Ligeiro, F. A., Rao, A., & Goldfeld, A. E. (2005). NFAT5 binds to the TNF promoter distinctly from NFATp, c, 3 and 4, and activates TNF transcription during hypertonic stress alone. *Nucleic Acids Research*, 33(12), 3845–3854. <https://doi.org/10.1093/nar/gki701>
- Eshel, D., Toporik, A., Efrati, T., Nakav, S., Chen, A., & Douvdevani, A. (2008). Characterization of natural human antagonistic soluble CD40 isoforms produced through alternative splicing. *Molecular Immunology*, 46(2), 250–257. <https://doi.org/10.1016/j.molimm.2008.08.280>
- Esposito, P., Rampino, T., Gregorini, M., Gabanti, E., Bianzina, S., & Dal Canton, A. (2012). Mechanisms underlying sCD40 production in hemodialysis patients. *Cellular Immunology*, 278(1–2), 10–15. <https://doi.org/10.1016/j.cellimm.2012.06.007>
- Figueredo, C. M., Martins, A. P., Lira-Junior, R., Menegat, J. B., Carvalho, A. T., Fischer, R. G., & Gustafsson, A. (2017). Activity of inflammatory bowel disease influences the

expression of cytokines in gingival tissue. *Cytokine*, 95, 1–6.
<https://doi.org/10.1016/j.cyto.2017.01.016>

Figuroa-Romero, C., Sadidi, M., & Feldman, E. L. (2008). Mechanisms of Disease: The Oxidative Stress Theory of Diabetic Neuropathy. *Reviews in Endocrine & Metabolic Disorders*, 9(4), 301–314. <https://doi.org/10.1007/s11154-008-9104-2>

Forbes, J. M., & Cooper, M. E. (2013). Mechanisms of Diabetic Complications. *Physiological Reviews*, 93(1), 137–188. <https://doi.org/10.1152/physrev.00045.2011>

Frangogiannis, N. G. (2017). The role of transforming growth factor (TGF)- β in the infarcted myocardium. *Journal of Thoracic Disease*, 9(S1), S52–S63. <https://doi.org/10.21037/jtd.2016.11.19>

Gero, D., & Gero, D. (2017). Hyperglycemia-Induced Endothelial Dysfunction. In *Endothelial Dysfunction—Old Concepts and New Challenges*. IntechOpen. <https://doi.org/10.5772/intechopen.71433>

Ghareeb, D., Fawzy, M., & Maaty, A. I. (2020). Association of CD40 rs1883832 Polymorphism with Susceptibility of Diabetic Nephropathy and Neuropathy in Egyptian Population. *The Egyptian Journal of Immunology*, 27(1), 87–96.

Giacco, F., Brownlee, M., & Schmidt, A. M. (2010). Oxidative Stress and Diabetic Complications. *Circulation Research*, 107(9), 1058–1070. <https://doi.org/10.1161/CIRCRESAHA.110.223545>

Glogner, S., Rosengren, A., Olsson, M., Gudbjörnsdottir, S., Svensson, A.-M., & Lind, M. (2014). The association between BMI and hospitalization for heart failure in 83 021 persons with Type 2 diabetes: A population-based study from the Swedish National Diabetes Registry. *Diabetic Medicine*, 31(5), 586–594. <https://doi.org/10.1111/dme.12340>

Glovaci, D., Fan, W., & Wong, N. D. (2019). Epidemiology of Diabetes Mellitus and Cardiovascular Disease. *Current Cardiology Reports*, 21(4), 21. <https://doi.org/10.1007/s11886-019-1107-y>

Goncharov, N. V., Nadeev, A. D., Jenkins, R. O., & Avdonin, P. V. (2017). Markers and Biomarkers of Endothelium: When Something Is Rotten in the State. *Oxidative Medicine and Cellular Longevity*, 2017, 9759735. <https://doi.org/10.1155/2017/9759735>

- Gonzalez, L. L., Garrie, K., & Turner, M. D. (2018). Type 2 diabetes – An autoinflammatory disease driven by metabolic stress. *Biochimica et Biophysica Acta (BBA) - Molecular Basis of Disease*, 1864(11), 3805–3823. <https://doi.org/10.1016/j.bbadis.2018.08.034>
- Gonzalez, Y., Herrera, M. T., Soldevila, G., Garcia-Garcia, L., Fabián, G., Pérez-Armendariz, E. M., Bobadilla, K., Guzmán-Beltrán, S., Sada, E., & Torres, M. (2012). High glucose concentrations induce TNF- α production through the down-regulation of CD33 in primary human monocytes. *BMC Immunology*, 13(1), 19. <https://doi.org/10.1186/1471-2172-13-19>
- Grandl, G., & Wolfrum, C. (2018). Hemostasis, endothelial stress, inflammation, and the metabolic syndrome. *Seminars in Immunopathology*, 40(2), 215–224. <https://doi.org/10.1007/s00281-017-0666-5>
- Gurzov, E. N., Stanley, W. J., Pappas, E. G., Thomas, H. E., & Gough, D. J. (2016). The JAK/STAT pathway in obesity and diabetes. *The FEBS Journal*, 283(16), 3002–3015. <https://doi.org/10.1111/febs.13709>
- Haczeyni, F., Bell-Anderson, K. S., & Farrell, G. C. (2018). Causes and mechanisms of adipocyte enlargement and adipose expansion: Hypertrophy and hyperplasia in adipose. *Obesity Reviews*, 19(3), 406–420. <https://doi.org/10.1111/obr.12646>
- Halim, M., & Halim, A. (2019). The effects of inflammation, aging and oxidative stress on the pathogenesis of diabetes mellitus (type 2 diabetes). *Diabetes & Metabolic Syndrome: Clinical Research & Reviews*, 13(2), 1165–1172. <https://doi.org/10.1016/j.dsx.2019.01.040>
- Hameed, I., Masoodi, S. R., Mir, S. A., Nabi, M., Ghazanfar, K., & Ganai, B. A. (2015). Type 2 diabetes mellitus: From a metabolic disorder to an inflammatory condition. *World Journal of Diabetes*, 6(4), 598. <https://doi.org/10.4239/wjd.v6.i4.598>
- Han, E.-J., Kim, H. Y., Lee, N., Kim, N.-H., Yoo, S.-A., Kwon, H. M., Jue, D.-M., Park, Y.-J., Cho, C.-S., De, T. Q., Jeong, D. Y., Lim, H.-J., Park, W. K., Lee, G. H., Cho, H., & Kim, W.-U. (2017). Suppression of NFAT5-mediated Inflammation and Chronic Arthritis by Novel κ B-binding Inhibitors. *EBioMedicine*, 18, 261–273. <https://doi.org/10.1016/j.ebiom.2017.03.039>

- Hariharan, S., & Dharmaraj, S. (2020). Selenium and selenoproteins: It's role in regulation of inflammation. *Inflammopharmacology*, 28(3), 667–695. <https://doi.org/10.1007/s10787-020-00690-x>
- Hassan, G. S., Salti, S., & Mourad, W. (2022). Novel Functions of Integrins as Receptors of CD154: Their Role in Inflammation and Apoptosis. *Cells*, 11(11), Article 11. <https://doi.org/10.3390/cells11111747>
- Hayden, M. S., & Ghosh, S. (2014). Regulation of NF- κ B by TNF family cytokines. *Seminars in Immunology*, 26(3), 253–266. <https://doi.org/10.1016/j.smim.2014.05.004>
- Hecker, M., & Wagner, A. H. (2017). Transcription factor decoy technology: A therapeutic update. *Biochemical Pharmacology*, 144, 29–34. <https://doi.org/10.1016/j.bcp.2017.06.122>
- Hegazy, G. A., Awan, Z., Hashem, E., Al-Ama, N., & Abunaji, A. B. (2020). Levels of soluble cell adhesion molecules in type 2 diabetes mellitus patients with macrovascular complications. *The Journal of International Medical Research*, 48(4), 300060519893858. <https://doi.org/10.1177/0300060519893858>
- Henn, V., Steinbach, S., Büchner, K., Presek, P., & Kroczeck, R. A. (2001). The inflammatory action of CD40 ligand (CD154) expressed on activated human platelets is temporally limited by coexpressed CD40. *Blood*, 98(4), 1047–1054. <https://doi.org/10.1182/blood.v98.4.1047>
- Herren, B. (2002). ADAM-Mediated Shedding and Adhesion: A Vascular Perspective. *Physiology*, 17(2), 73–76. <https://doi.org/10.1152/nips.01373.2001>
- Hirano, T. (2018). Pathophysiology of Diabetic Dyslipidemia. *Journal of Atherosclerosis and Thrombosis*, 25(9), 771–782. <https://doi.org/10.5551/jat.RV17023>
- Hudish, L. I., Reusch, J. E. B., & Sussel, L. (2019). β Cell dysfunction during progression of metabolic syndrome to type 2 diabetes. *Journal of Clinical Investigation*, 129(10), 4001–4008. <https://doi.org/10.1172/JCI129188>
- Ighodaro, O. M. (2018). Molecular pathways associated with oxidative stress in diabetes mellitus. *Biomedicine & Pharmacotherapy*, 108, 656–662. <https://doi.org/10.1016/j.biopha.2018.09.058>

- Jacobson, E. M., Concepcion, E., Oashi, T., & Tomer, Y. (2005). A Graves' disease-associated Kozak sequence single-nucleotide polymorphism enhances the efficiency of CD40 gene translation: A case for translational pathophysiology. *Endocrinology*, 146(6), 2684–2691. <https://doi.org/10.1210/en.2004-1617>
- Jansen, M. F., Hollander, M. R., van Royen, N., Horrevoets, A. J., & Lutgens, E. (2016). CD40 in coronary artery disease: A matter of macrophages? *Basic Research in Cardiology*, 111(4), 38. <https://doi.org/10.1007/s00395-016-0554-5>
- Jinchuan, Y., Zonggui, W., Jinming, C., Li, L., & Xiantao, K. (2004). Upregulation of CD40—CD40 ligand system in patients with diabetes mellitus. *Clinica Chimica Acta; International Journal of Clinical Chemistry*, 339(1–2), 85–90. <https://doi.org/10.1016/j.cccn.2003.09.007>
- Junttila, I. S. (2018). Tuning the Cytokine Responses: An Update on Interleukin (IL)-4 and IL-13 Receptor Complexes. *Frontiers in Immunology*, 9. <https://www.frontiersin.org/articles/10.3389/fimmu.2018.00888>
- Kammoun, H. L., Kraakman, M. J., & Febbraio, M. A. (2014). Adipose tissue inflammation in glucose metabolism. *Reviews in Endocrine & Metabolic Disorders*, 15(1), 31–44. <https://doi.org/10.1007/s11154-013-9274-4>
- Katsonis, P., Koire, A., Wilson, S. J., Hsu, T.-K., Lua, R. C., Wilkins, A. D., & Lichtarge, O. (2014). Single nucleotide variations: Biological impact and theoretical interpretation: Predictors of SNV Impact. *Protein Science*, 23(12), 1650–1666. <https://doi.org/10.1002/pro.2552>
- Kaur, R., Kaur, M., & Singh, J. (2018). Endothelial dysfunction and platelet hyperactivity in type 2 diabetes mellitus: Molecular insights and therapeutic strategies. *Cardiovascular Diabetology*, 17(1), 121. <https://doi.org/10.1186/s12933-018-0763-3>
- Kim, J., Montagnani, M., Chandrasekran, S., & Quon, M. J. (2012). Role of Lipotoxicity in Endothelial Dysfunction. *Heart Failure Clinics*, 8(4), 589–607. <https://doi.org/10.1016/j.hfc.2012.06.012>
- Kolka, C. M., & Bergman, R. N. (2012). The Barrier Within: Endothelial Transport of Hormones. *Physiology*, 27(4), 237–247. <https://doi.org/10.1152/physiol.00012.2012>

- Kovacic, J. C., Dimmeler, S., Harvey, R. P., Finkel, T., Aikawa, E., Krenning, G., & Baker, A. H. (2019). Endothelial to Mesenchymal Transition in Cardiovascular Disease: JACC State-of-the-Art Review. *Journal of the American College of Cardiology*, 73(2), 190–209. <https://doi.org/10.1016/j.jacc.2018.09.089>
- Kreiner, F. F., Kraaijenhof, J. M., von Herrath, M., Hovingh, G. K. K., & von Scholten, B. J. (2022). Interleukin 6 in diabetes, chronic kidney disease, and cardiovascular disease: Mechanisms and therapeutic perspectives. *Expert Review of Clinical Immunology*, 18(4), 377–389. <https://doi.org/10.1080/1744666X.2022.2045952>
- Kumar, P. A., Welsh, G. I., Raghu, G., Menon, R. K., Saleem, M. A., & Reddy, G. B. (2016). Carboxymethyl lysine induces EMT in podocytes through transcription factor ZEB2: Implications for podocyte depletion and proteinuria in diabetes mellitus. *Archives of Biochemistry and Biophysics*, 590, 10–19. <https://doi.org/10.1016/j.abb.2015.11.003>
- La Sala, L., Prattichizzo, F., & Ceriello, A. (2019). The link between diabetes and atherosclerosis. *European Journal of Preventive Cardiology*, 26(2_suppl), 15–24. <https://doi.org/10.1177/2047487319878373>
- Lamine, L. B., Turki, A., Al-Khateeb, G., Sellami, N., Amor, H. B., Sarray, S., Jailani, M., Ghorbel, M., Mahjoub, T., & Almawi, W. Y. (2020). Elevation in Circulating Soluble CD40 Ligand Concentrations in Type 2 Diabetic Retinopathy and Association with its Severity. *Experimental and Clinical Endocrinology & Diabetes: Official Journal, German Society of Endocrinology [and] German Diabetes Association*, 128(5), 319–324. <https://doi.org/10.1055/a-0647-6860>
- Lamouille, S., & Derynck, R. (2007). Cell size and invasion in TGF-beta-induced epithelial to mesenchymal transition is regulated by activation of the mTOR pathway. *The Journal of Cell Biology*, 178(3), 437–451. <https://doi.org/10.1083/jcb.200611146>
- Laronha, H., & Caldeira, J. (2020). Structure and Function of Human Matrix Metalloproteinases. *Cells*, 9(5), 1076. <https://doi.org/10.3390/cells9051076>
- Lee, Y. H., Bae, S.-C., Choi, S. J., Ji, J. D., & Song, G. G. (2015). Associations between the functional CD40 rs4810485 G/T polymorphism and susceptibility to rheumatoid arthritis and systemic lupus erythematosus: A meta-analysis. *Lupus*, 24(11), 1177–1183. <https://doi.org/10.1177/0961203315583543>

- Lemmer, I. L., Willemsen, N., Hilal, N., & Bartelt, A. (2021). A guide to understanding endoplasmic reticulum stress in metabolic disorders. *Molecular Metabolism*, 47, 101169. <https://doi.org/10.1016/j.molmet.2021.101169>
- Leonetti, S., Tricò, D., Nesti, L., Baldi, S., Kozakova, M., Goncalves, I., Nilsson, J., Shore, A., Khan, F., & Natali, A. (2022). Soluble CD40 receptor is a biomarker of the burden of carotid artery atherosclerosis in subjects at high cardiovascular risk. *Atherosclerosis*, 343, 1–9. <https://doi.org/10.1016/j.atherosclerosis.2022.01.003>
- Li, W., Cao, T., Luo, C., Cai, J., Zhou, X., Xiao, X., & Liu, S. (2020). Crosstalk between ER stress, NLRP3 inflammasome, and inflammation. *Applied Microbiology and Biotechnology*, 104(14), 6129–6140. <https://doi.org/10.1007/s00253-020-10614-y>
- Lin, J., Kakkar, V., & Lu, X. (2014). Impact of MCP -1 in Atherosclerosis. *Current Pharmaceutical Design*, 20(28), 4580–4588. <https://doi.org/10.2174/1381612820666140522115801>
- Liu, C., Feng, X., Li, Q., Wang, Y., Li, Q., & Hua, M. (2016). Adiponectin, TNF- α and inflammatory cytokines and risk of type 2 diabetes: A systematic review and meta-analysis. *Cytokine*, 86, 100–109. <https://doi.org/10.1016/j.cyto.2016.06.028>
- Liu, R., Shen, H., Wang, T., Ma, J., Yuan, M., Huang, J., Wei, M., & Liu, F. (2018). TRAF6 mediates high glucose-induced endothelial dysfunction. *Experimental Cell Research*, 370(2), 490–497. <https://doi.org/10.1016/j.yexcr.2018.07.014>
- Loader, B., Stokic, D., Riedl, M., Hickmann, S., Katzinger, M., Willinger, U., Luger, A., Thurner, S., & Wick, N. (2008). Combined analysis of audiologic performance and the plasma biomarker stromal cell-derived factor 1a in type 2 diabetic patients. *Otology & Neurotology: Official Publication of the American Otological Society, American Neurotology Society [and] European Academy of Otology and Neurotology*, 29(6), 739–744. <https://doi.org/10.1097/MAO.0b013e318172cf89>
- Lontchi-Yimagou, E., Sobngwi, E., Matsha, T. E., & Kengne, A. P. (2013). Diabetes Mellitus and Inflammation. *Current Diabetes Reports*, 13(3), 435–444. <https://doi.org/10.1007/s11892-013-0375-y>
- Lordan, R., Tsoupras, A., & Zabetakis, I. (2021). Platelet activation and prothrombotic mediators at the nexus of inflammation and atherosclerosis: Potential role of antiplatelet agents. *Blood Reviews*, 45, 100694. <https://doi.org/10.1016/j.blre.2020.100694>

- Low Wang, C. C., Hess, C. N., Hiatt, W. R., & Goldfine, A. B. (2016). Clinical Update: Cardiovascular Disease in Diabetes Mellitus: Atherosclerotic Cardiovascular Disease and Heart Failure in Type 2 Diabetes Mellitus – Mechanisms, Management, and Clinical Considerations. *Circulation*, 133(24), 2459–2502. <https://doi.org/10.1161/CIRCULATIONAHA.116.022194>
- Ludewig, B., Henn, V., Schröder, J. M., Graf, D., & Kroczeck, R. A. (1996). Induction, regulation, and function of soluble TRAP (CD40 ligand) during interaction of primary CD4⁺ CD45RA⁺ T cells with dendritic cells. *European Journal of Immunology*, 26(12), 3137–3143. <https://doi.org/10.1002/eji.1830261246>
- Lutgens, E., Lievens, D., Beckers, L., Wijnands, E., Soehnlein, O., Zernecke, A., Seijkens, T., Engel, D., Cleutjens, J., Keller, A. M., Naik, S. H., Boon, L., Oufella, H. A., Mallat, Z., Ahonen, C. L., Noelle, R. J., de Winther, M. P., Daemen, M. J., Biessen, E. A., & Weber, C. (2010). Deficient CD40-TRAF6 signaling in leukocytes prevents atherosclerosis by skewing the immune response toward an antiinflammatory profile. *Journal of Experimental Medicine*, 207(2), 391–404. <https://doi.org/10.1084/jem.20091293>
- Ma, J., Sanchez-Duffhues, G., Goumans, M.-J., & ten Dijke, P. (2020). TGF- β -Induced Endothelial to Mesenchymal Transition in Disease and Tissue Engineering. *Frontiers in Cell and Developmental Biology*, 8, 260. <https://doi.org/10.3389/fcell.2020.00260>
- Ma, P., Zha, S., Shen, X., Zhao, Y., Li, L., Yang, L., Lei, M., & Liu, W. (2019). NFAT5 mediates hypertonic stress-induced atherosclerosis via activating NLRP3 inflammasome in endothelium. *Cell Communication and Signaling*, 17(1), 102. <https://doi.org/10.1186/s12964-019-0406-7>
- Ma, X., Cui, Z., Du, Z., & Lin, H. (2020). Transforming growth factor- β signaling, a potential mechanism associated with diabetes mellitus and pancreatic cancer? *Journal of Cellular Physiology*, 235(9), 5882–5892. <https://doi.org/10.1002/jcp.29605>
- Maamoun, H., Benameur, T., Pintus, G., Munusamy, S., & Agouni, A. (2019). Crosstalk Between Oxidative Stress and Endoplasmic Reticulum (ER) Stress in Endothelial Dysfunction and Aberrant Angiogenesis Associated With Diabetes: A Focus on the Protective Roles of Heme Oxygenase (HO)-1. *Frontiers in Physiology*, 10, 70. <https://doi.org/10.3389/fphys.2019.00070>

- Madonna, R., Pieragostino, D., Rossi, C., Confalone, P., Cicalini, I., Minnucci, I., Zucchelli, M., Del Boccio, P., & De Caterina, R. (2020). Simulated hyperglycemia impairs insulin signaling in endothelial cells through a hyperosmolar mechanism. *Vascular Pharmacology*, 130, 106678. <https://doi.org/10.1016/j.vph.2020.106678>
- Maleszewska, M., Moonen, J.-R. A. J., Huijkman, N., van de Sluis, B., Krenning, G., & Harmsen, M. C. (2013). IL-1 β and TGF β 2 synergistically induce endothelial to mesenchymal transition in an NF κ B-dependent manner. *Immunobiology*, 218(4), 443–454. <https://doi.org/10.1016/j.imbio.2012.05.026>
- Martínez-Reyes, I., & Chandel, N. S. (2020). Mitochondrial TCA cycle metabolites control physiology and disease. *Nature Communications*, 11(1), Article 1. <https://doi.org/10.1038/s41467-019-13668-3>
- Medina-Leyte, D. J., Zepeda-García, O., Domínguez-Pérez, M., González-Garrido, A., Villarreal-Molina, T., & Jacobo-Albavera, L. (2021). Endothelial Dysfunction, Inflammation and Coronary Artery Disease: Potential Biomarkers and Promising Therapeutical Approaches. *International Journal of Molecular Sciences*, 22(8), Article 8. <https://doi.org/10.3390/ijms22083850>
- Meigs, J. B., Hu, F. B., Rifai, N., & Manson, J. E. (2004). Biomarkers of endothelial dysfunction and risk of type 2 diabetes mellitus. *JAMA*, 291(16), 1978–1986. <https://doi.org/10.1001/jama.291.16.1978>
- Meltzer, S., Torgunrud, A., Abrahamsson, H., Solbakken, A. M., Flatmark, K., Dueland, S., Bakke, K. M., Bousquet, P. A., Negård, A., Johansen, C., Lyckander, L. G., Larsen, F. O., Schou, J. V., Redalen, K. R., & Ree, A. H. (2021). The circulating soluble form of the CD40 costimulatory immune checkpoint receptor and liver metastasis risk in rectal cancer. *British Journal of Cancer*, 125(2), 240–246. <https://doi.org/10.1038/s41416-021-01377-y>
- Michel, N. A., Zirlik, A., & Wolf, D. (2017). CD40L and Its Receptors in Atherothrombosis-An Update. *Frontiers in Cardiovascular Medicine*, 4, 40. <https://doi.org/10.3389/fcvm.2017.00040>
- Møller, L. L. V., Klip, A., & Sylow, L. (2019). Rho GTPases—Emerging Regulators of Glucose Homeostasis and Metabolic Health. *Cells*, 8(5), Article 5. <https://doi.org/10.3390/cells8050434>

- Moosad et al. 2015. (n.d.). Article Detail. International Journal of Advanced Research. Retrieved July 25, 2022, from <https://www.journalijar.com/article/>
- Mousavi, A. (2020). CXCL12/CXCR4 signal transduction in diseases and its molecular approaches in targeted-therapy. *Immunology Letters*, 217, 91–115. <https://doi.org/10.1016/j.imlet.2019.11.007>
- Muris, D. M. J., Houben, A. J. H. M., Schram, M. T., & Stehouwer, C. D. A. (2012). Microvascular Dysfunction Is Associated With a Higher Incidence of Type 2 Diabetes Mellitus: A Systematic Review and Meta-Analysis. *Arteriosclerosis, Thrombosis, and Vascular Biology*, 32(12), 3082–3094. <https://doi.org/10.1161/ATVBAHA.112.300291>
- Nair, A., Chakraborty, S., Banerji, L. A., Srivastava, A., Navare, C., & Saha, B. (2020). Ras isoforms: Signaling specificities in CD40 pathway. *Cell Communication and Signaling*, 18(1), 3. <https://doi.org/10.1186/s12964-019-0497-1>
- NATIONAL DIABETES SURVEILLANCE REPORT 2019 Diabetes in Germany. (n.d.). https://diabsurv.rki.de/SharedDocs/downloads/DE/DiabSurv/diabetes-report_2019_eng.pdf?__blob=publicationFile&v=12
- Neuhofer, W. (2010). Role of NFAT5 in Inflammatory Disorders Associated with Osmotic Stress. *Current Genomics*, 11(8), 584–590. <https://doi.org/10.2174/138920210793360961>
- Oakes, S. A., & Papa, F. R. (2015). The Role of Endoplasmic Reticulum Stress in Human Pathology. *Annual Review of Pathology: Mechanisms of Disease*, 10(1), 173–194. <https://doi.org/10.1146/annurev-pathol-012513-104649>
- Oguntibeju, O. O. (2019). Type 2 diabetes mellitus, oxidative stress and inflammation: Examining the links. *International Journal of Physiology, Pathophysiology and Pharmacology*, 11(3), 45–63.
- Onoue, T., Uchida, D., Begum, N. M., Tomizuka, Y., Yoshida, H., & Sato, M. (2006). Epithelial-mesenchymal transition induced by the stromal cell-derived factor-1/CXCR4 system in oral squamous cell carcinoma cells. *International Journal of Oncology*, 29(5), 1133–1138.

- Ouchi, N., Parker, J. L., Lugus, J. J., & Walsh, K. (2011). Adipokines in inflammation and metabolic disease. *Nature Reviews Immunology*, 11(2), 85–97. <https://doi.org/10.1038/nri2921>
- Paneni, F., Beckman, J. A., Creager, M. A., & Cosentino, F. (2013). Diabetes and vascular disease: Pathophysiology, clinical consequences, and medical therapy: part I. *European Heart Journal*, 34(31), 2436–2443. <https://doi.org/10.1093/eurheartj/eh149>
- Pardali, E., Sanchez-Duffhues, G., Gomez-Puerto, M., & ten Dijke, P. (2017). TGF- β -Induced Endothelial-Mesenchymal Transition in Fibrotic Diseases. *International Journal of Molecular Sciences*, 18(10), 2157. <https://doi.org/10.3390/ijms18102157>
- Patel, S., Srivastava, S., Singh, M. R., & Singh, D. (2019). Mechanistic insight into diabetic wounds: Pathogenesis, molecular targets and treatment strategies to pace wound healing. *Biomedicine & Pharmacotherapy*, 112, 108615. <https://doi.org/10.1016/j.biopha.2019.108615>
- Peng, H., Li, Y., Wang, C., Zhang, J., Chen, Y., Chen, W., Cao, J., Wang, Y., Hu, Z., & Lou, T. (2016). ROCK1 Induces Endothelial-to-Mesenchymal Transition in Glomeruli to Aggravate Albuminuria in Diabetic Nephropathy. *Scientific Reports*, 6(1), 20304. <https://doi.org/10.1038/srep20304>
- Pereira-da-Silva, T., Napoleao, P., Pinheiro, T., Selas, M., Silva, F., Ferreira, R. C., & Carmo, M. M. (2020). Inflammation is associated with the presence and severity of chronic coronary syndrome through soluble CD40 ligand. *American Journal of Cardiovascular Disease*, 10(4), 329–339.
- Petrie, J. R., Guzik, T. J., & Touyz, R. M. (2018). Diabetes, Hypertension, and Cardiovascular Disease: Clinical Insights and Vascular Mechanisms. *Canadian Journal of Cardiology*, 34(5), 575–584. <https://doi.org/10.1016/j.cjca.2017.12.005>
- Pfeiler, S., Winkels, H., Kelm, M., & Gerdes, N. (2019). IL-1 family cytokines in cardiovascular disease. *Cytokine*, 122, 154215. <https://doi.org/10.1016/j.cyto.2017.11.009>
- Piera-Velazquez, S., & Jimenez, S. A. (2019). Endothelial to Mesenchymal Transition: Role in Physiology and in the Pathogenesis of Human Diseases. *Physiological Reviews*, 99(2), 1281–1324. <https://doi.org/10.1152/physrev.00021.2018>

- Poggi, M., Jager, J., Paulmyer-Lacroix, O., Peiretti, F., Gremeaux, T., Verdier, M., Grino, M., Stepanian, A., Msika, S., Burcelin, R., de Prost, D., Tanti, J. F., & Alessi, M. C. (2009). The inflammatory receptor CD40 is expressed on human adipocytes: Contribution to crosstalk between lymphocytes and adipocytes. *Diabetologia*, *52*(6), 1152–1163. <https://doi.org/10.1007/s00125-009-1267-1>
- Polet, F., & Feron, O. (2013). Endothelial cell metabolism and tumour angiogenesis: Glucose and glutamine as essential fuels and lactate as the driving force. *Journal of Internal Medicine*, *273*(2), 156–165. <https://doi.org/10.1111/joim.12016>
- Popa, M., Tahir, S., Elrod, J., Kim, S. H., Leuschner, F., Kessler, T., Bugert, P., Pohl, U., Wagner, A. H., & Hecker, M. (2018). Role of CD40 and ADAMTS13 in von Willebrand factor-mediated endothelial cell–platelet–monocyte interaction. *Proceedings of the National Academy of Sciences*, *115*(24). <https://doi.org/10.1073/pnas.1801366115>
- Potenza, M. A., Addabbo, F., & Montagnani, M. (2009). Vascular actions of insulin with implications for endothelial dysfunction. *American Journal of Physiology. Endocrinology and Metabolism*, *297*(3), E568-577. <https://doi.org/10.1152/ajpendo.00297.2009>
- Pradhan, A. D., Manson, J. E., Rifai, N., Buring, J. E., & Ridker, P. M. (2001). C-reactive protein, interleukin 6, and risk of developing type 2 diabetes mellitus. *JAMA*, *286*(3), 327–334. <https://doi.org/10.1001/jama.286.3.327>
- Qiao, Y., Chen, Y., Pan, Y., Tian, F., Xu, Y., Zhang, X., & Zhao, H. (2017). The change of serum tumor necrosis factor alpha in patients with type 1 diabetes mellitus: A systematic review and meta-analysis. *PLOS ONE*, *12*(4), e0176157. <https://doi.org/10.1371/journal.pone.0176157>
- Qin, J., Xing, J., Liu, R., Chen, B., Chen, Y., & Zhuang, X. (2017). Association between CD40 rs1883832 and immune-related diseases susceptibility: A meta-analysis. *Oncotarget*, *8*(60), 102235–102243. <https://doi.org/10.18632/oncotarget.18704>
- Ramasamy, R., Yan, S. F., & Schmidt, A. M. (2011). Receptor for AGE (RAGE): Signaling mechanisms in the pathogenesis of diabetes and its complications: RAGE, signal transduction, and diabetes. *Annals of the New York Academy of Sciences*, *1243*(1), 88–102. <https://doi.org/10.1111/j.1749-6632.2011.06320.x>

- Raychaudhuri, S., Remmers, E. F., Lee, A. T., Hackett, R., Guiducci, C., Burt, N. P., Gianniny, L., Korman, B. D., Padyukov, L., Kurreeman, F. A. S., Chang, M., Catanese, J. J., Ding, B., Wong, S., van der Helm-van Mil, A. H. M., Neale, B. M., Coblyn, J., Cui, J., Tak, P. P., ... Plenge, R. M. (2008). Common variants at CD40 and other loci confer risk of rheumatoid arthritis. *Nature Genetics*, 40(10), 1216–1223. <https://doi.org/10.1038/ng.233>
- Rehman, K., & Akash, M. S. H. (2016). Mechanisms of inflammatory responses and development of insulin resistance: How are they interlinked? *Journal of Biomedical Science*, 23(1), 87. <https://doi.org/10.1186/s12929-016-0303-y>
- Robert, F., & Pelletier, J. (2018). Exploring the Impact of Single-Nucleotide Polymorphisms on Translation. *Frontiers in Genetics*, 9, 507. <https://doi.org/10.3389/fgene.2018.00507>
- Roth, I., Leroy, V., Kwon, H. M., Martin, P.-Y., Féraillé, E., & Hasler, U. (2010). Osmoprotective transcription factor NFAT5/TonEBP modulates nuclear factor-kappaB activity. *Molecular Biology of the Cell*, 21(19), 3459–3474. <https://doi.org/10.1091/mbc.E10-02-0133>
- Sabbineni, H., Verma, A., & Somanath, P. R. (2018). Isoform-specific effects of transforming growth factor β on endothelial-to-mesenchymal transition. *Journal of Cellular Physiology*, 233(11), 8418–8428. <https://doi.org/10.1002/jcp.26801>
- Salti, S., Al-Zoobi, L., Darif, Y., Hassan, G. S., & Mourad, W. (2021). CD154 Resistant to Cleavage from Intracellular Milieu and Cell Surface Induces More Potent CD40-Mediated Responses. *The Journal of Immunology*, 206(8), 1793–1805. <https://doi.org/10.4049/jimmunol.2001340>
- Sandoval, R., Lazcano, P., Ferrari, F., Pinto-Pardo, N., González-Billault, C., & Utreras, E. (2018). TNF- α Increases Production of Reactive Oxygen Species through Cdk5 Activation in Nociceptive Neurons. *Frontiers in Physiology*, 9. <https://www.frontiersin.org/articles/10.3389/fphys.2018.00065>
- Santilli, F., Simeone, P., Liani, R., & Davì, G. (2015). Platelets and diabetes mellitus. *Prostaglandins & Other Lipid Mediators*, 120, 28–39. <https://doi.org/10.1016/j.prostaglandins.2015.05.002>

- Schalkwijk, C. G., & Stehouwer, C. D. A. (2005). Vascular complications in diabetes mellitus: The role of endothelial dysfunction. *Clinical Science (London, England: 1979)*, 109(2), 143–159. <https://doi.org/10.1042/CS20050025>
- Scherer, C., Pfisterer, L., Wagner, A. H., Hödebeck, M., Cattaruzza, M., Hecker, M., & Korff, T. (2014). Arterial Wall Stress Controls NFAT5 Activity in Vascular Smooth Muscle Cells. *Journal of the American Heart Association*, 3(2), e000626. <https://doi.org/10.1161/JAHA.113.000626>
- Schindelin, J., Arganda-Carreras, I., Frise, E., Kaynig, V., Longair, M., Pietzsch, T., Preibisch, S., Rueden, C., Saalfeld, S., Schmid, B., Tinevez, J.-Y., White, D. J., Hartenstein, V., Eliceiri, K., Tomancak, P., & Cardona, A. (2012). Fiji: An open-source platform for biological-image analysis. *Nature Methods*, 9(7), 676–682. <https://doi.org/10.1038/nmeth.2019>
- Schwabe, R. F., Engelmann, H., Hess, S., & Fricke, H. (1999). Soluble CD40 in the serum of healthy donors, patients with chronic renal failure, haemodialysis and chronic ambulatory peritoneal dialysis (CAPD) patients. *Clinical and Experimental Immunology*, 117(1), 153–158. <https://doi.org/10.1046/j.1365-2249.1999.00935.x>
- Seijkens, T., Kusters, P., Chatzigeorgiou, A., Chavakis, T., & Lutgens, E. (2014). Immune Cell Crosstalk in Obesity: A Key Role for Costimulation? *Diabetes*, 63(12), 3982–3991. <https://doi.org/10.2337/db14-0272>
- Seijkens, T., Kusters, P., Engel, D., & Lutgens, E. (2013). CD40–CD40L: Linking pancreatic, adipose tissue and vascular inflammation in type 2 diabetes and its complications. *Diabetes and Vascular Disease Research*, 10(2), 115–122. <https://doi.org/10.1177/1479164112455817>
- Sena, C. M., Carrilho, F., Seica, R. M., Sena, C. M., Carrilho, F., & Seica, R. M. (2018). Endothelial Dysfunction in Type 2 Diabetes: Targeting Inflammation. In *Endothelial Dysfunction—Old Concepts and New Challenges*. IntechOpen. <https://doi.org/10.5772/intechopen.76994>
- Sena, C. M., Pereira, A. M., & Seica, R. (2013). Endothelial dysfunction—A major mediator of diabetic vascular disease. *Biochimica et Biophysica Acta (BBA) - Molecular Basis of Disease*, 1832(12), 2216–2231. <https://doi.org/10.1016/j.bbadis.2013.08.006>

Shah, R., Hinkle, C. C., Ferguson, J. F., Mehta, N. N., Li, M., Qu, L., Lu, Y., Putt, M. E., Ahima, R. S., & Reilly, M. P. (2011). Fractalkine Is a Novel Human Adipochemokine Associated With Type 2 Diabetes. *Diabetes*, 60(5), 1512–1518. <https://doi.org/10.2337/db10-0956>

Shami, A., Edsfeldt, A., Bengtsson, E., Nilsson, J., Shore, A. C., Natali, A., Khan, F., Lutgens, E., & Gonçalves, I. (2021). Soluble CD40 Levels in Plasma Are Associated with Cardiovascular Disease and in Carotid Plaques with a Vulnerable Phenotype. *Journal of Stroke*, 23(3), 367–376. <https://doi.org/10.5853/jos.2021.00178>

Shastri, B. S. (2002). SNP alleles in human disease and evolution. *Journal of Human Genetics*, 47(11), 561–566. <https://doi.org/10.1007/s100380200086>

Shi, Y., & Vanhoutte, P. M. (2017). Macro- and microvascular endothelial dysfunction in diabetes: 糖尿病诱导的内皮细胞功能损伤. *Journal of Diabetes*, 9(5), 434–449. <https://doi.org/10.1111/1753-0407.12521>

Singh, A., Kukreti, R., Saso, L., & Kukreti, S. (2022). Mechanistic Insight into Oxidative Stress-Triggered Signaling Pathways and Type 2 Diabetes. *Molecules*, 27(3), 950. <https://doi.org/10.3390/molecules27030950>

Singh, S., Anshita, D., & Ravichandiran, V. (2021). MCP-1: Function, regulation, and involvement in disease. *International Immunopharmacology*, 101(Pt B), 107598. <https://doi.org/10.1016/j.intimp.2021.107598>

Smith, M. H., Ploegh, H. L., & Weissman, J. S. (2011). Road to Ruin: Targeting Proteins for Degradation in the Endoplasmic Reticulum. *Science*, 334(6059), 1086–1090. <https://doi.org/10.1126/science.1209235>

Steven, S., Dib, M., Hausding, M., Kashani, F., Oelze, M., Kröller-Schön, S., Hanf, A., Daub, S., Roohani, S., Gramlich, Y., Lutgens, E., Schulz, E., Becker, C., Lackner, K. J., Kleinert, H., Knosalla, C., Niesler, B., Wild, P. S., Münzel, T., & Daiber, A. (2018). CD40L controls obesity-associated vascular inflammation, oxidative stress, and endothelial dysfunction in high fat diet-treated and db/db mice. *Cardiovascular Research*, 114(2), 312–323. <https://doi.org/10.1093/cvr/cvx197>

- Strassheim, D., Gerasimovskaya, E., Irwin, D., Dempsey, E. C., Stenmark, K., & Karoor, V. (2019). RhoGTPase in Vascular Disease. *Cells*, 8(6), Article 6. <https://doi.org/10.3390/cells8060551>
- Sultan, C. S., Weitnauer, M., Turinsky, M., Kessler, T., Brune, M., Gleissner, C. A., Leuschner, F., Wagner, A. H., & Hecker, M. (2020). Functional association of a CD40 gene single-nucleotide polymorphism with the pathogenesis of coronary heart disease. *Cardiovascular Research*, 116(6), 1214–1225. <https://doi.org/10.1093/cvr/cvz206>
- Tamba, S. M., Ewane, M. E., Bonny, A., Muisi, C. N., Nana, E., Ellon, A., Mvogo, C. E., & Mandengue, S. H. (2013). Micro and macrovascular complications of diabetes mellitus in cameroon: Risk factors and effect of diabetic check-up - a monocentric observational study. *Pan African Medical Journal*, 15. <https://doi.org/10.11604/pamj.2013.15.141.2104>
- Tang, T., Cheng, X., Truong, B., Sun, L., Yang, X., & Wang, H. (2021). Molecular basis and therapeutic implications of CD40/CD40L immune checkpoint. *Pharmacology & Therapeutics*, 219, 107709. <https://doi.org/10.1016/j.pharmthera.2020.107709>
- Testa, R., Bonfigli, A. R., Prattichizzo, F., La Sala, L., De Nigris, V., & Ceriello, A. (2017). The “Metabolic Memory” Theory and the Early Treatment of Hyperglycemia in Prevention of Diabetic Complications. *Nutrients*, 9(5), 437. <https://doi.org/10.3390/nu9050437>
- Theodorou, K., & Boon, R. A. (2018). Endothelial Cell Metabolism in Atherosclerosis. *Frontiers in Cell and Developmental Biology*, 6. <https://www.frontiersin.org/articles/10.3389/fcell.2018.00082>
- Tian, D., Zeng, X., Wang, W., Wang, Z., Zhang, Y., & Wang, Y. (2019). Protective effect of rapamycin on endothelial-to-mesenchymal transition in HUVECs through the Notch signaling pathway. *Vascular Pharmacology*, 113, 20–26. <https://doi.org/10.1016/j.vph.2018.10.004>
- Tousoulis, D., Androulakis, E., Papageorgiou, N., Briasoulis, A., Siasos, G., Antoniadis, C., & Stefanadis, C. (2010). From atherosclerosis to acute coronary syndromes: The role of soluble CD40 ligand. *Trends in Cardiovascular Medicine*, 20(5), 153–164. <https://doi.org/10.1016/j.tcm.2010.12.004>

van Greevenbroek, M. M. J., Schalkwijk, C. G., & Stehouwer, C. D. A. (2013). Obesity-associated low-grade inflammation in type 2 diabetes mellitus: Causes and consequences. *The Netherlands Journal of Medicine*, 71(4), 174–187.

Velnar, T., & Gradisnik, L. (2018). Tissue Augmentation in Wound Healing: The Role of Endothelial and Epithelial Cells. *Medical Archives*, 72(6), 444. <https://doi.org/10.5455/medarh.2018.72.444-448>

Villalba, N., Baby, S., & Yuan, S. Y. (2021). The Endothelial Glycocalyx as a Double-Edged Sword in Microvascular Homeostasis and Pathogenesis. *Frontiers in Cell and Developmental Biology*, 9, 711003. <https://doi.org/10.3389/fcell.2021.711003>

Vogel, D. Y. S., Glim, J. E., Stavenuiter, A. W. D., Breur, M., Heijnen, P., Amor, S., Dijkstra, C. D., & Beelen, R. H. J. (2014). Human macrophage polarization in vitro: Maturation and activation methods compared. *Immunobiology*, 219(9), 695–703. <https://doi.org/10.1016/j.imbio.2014.05.002>

Wagner, A. H., Conzelmann, M., Fitzner, F., Giese, T., Gülow, K., Falk, C. S., Krämer, O. H., Dietrich, S., Hecker, M., & Luft, T. (2015). JAK1/STAT3 activation directly inhibits IL-12 production in dendritic cells by preventing CDK9/P-TEFb recruitment to the p35 promoter. *Biochemical Pharmacology*, 96(1), 52–64. <https://doi.org/10.1016/j.bcp.2015.04.019>

Wagner, A. H., Hildebrandt, A., Baumgarten, S., Jungmann, A., Müller, O. J., Sharov, V. S., Schöneich, C., & Hecker, M. (2011). Tyrosine nitration limits stretch-induced CD40 expression and disconnects CD40 signaling in human endothelial cells. *Blood*, 118(13), 3734–3742. <https://doi.org/10.1182/blood-2010-11-320259>

Walter, P., & Ron, D. (2011). The Unfolded Protein Response: From Stress Pathway to Homeostatic Regulation. *Science*, 334(6059), 1081–1086. <https://doi.org/10.1126/science.1209038>

Wang, C., Guan, Y., & Yang, J. (2010). Cytokines in the Progression of Pancreatic β -Cell Dysfunction. *International Journal of Endocrinology*, 2010, 515136. <https://doi.org/10.1155/2010/515136>

Wang, D. G., Fan, J. B., Siao, C. J., Berno, A., Young, P., Sapolsky, R., Ghandour, G., Perkins, N., Winchester, E., Spencer, J., Kruglyak, L., Stein, L., Hsie, L., Topaloglou, T., Hubbell, E., Robinson, E., Mittmann, M., Morris, M. S., Shen, N., ... Lander, E. S.

- (1998). Large-scale identification, mapping, and genotyping of single-nucleotide polymorphisms in the human genome. *Science (New York, N.Y.)*, 280(5366), 1077–1082. <https://doi.org/10.1126/science.280.5366.1077>
- Wang, H.-L., Wang, L., Zhao, C.-Y., & Lan, H.-Y. (2022). Role of TGF-Beta Signaling in Beta Cell Proliferation and Function in Diabetes. *Biomolecules*, 12(3), 373. <https://doi.org/10.3390/biom12030373>
- Way, K. J., Katai, N., & King, G. L. (2001). Protein kinase C and the development of diabetic vascular complications. *Diabetic Medicine*, 18(12), 945–959. <https://doi.org/10.1046/j.0742-3071.2001.00638.x>
- Welch-Reardon, K. M., Wu, N., & Hughes, C. C. W. (2015). A Role for Partial Endothelial–Mesenchymal Transitions in Angiogenesis? *Arteriosclerosis, Thrombosis, and Vascular Biology*, 35(2), 303–308. <https://doi.org/10.1161/ATVBAHA.114.303220>
- Wentworth, J. M., Fourlanos, S., & Colman, P. G. (2012). Body mass index correlates with ischemic heart disease and albuminuria in long-standing type 2 diabetes. *Diabetes Research and Clinical Practice*, 97(1), 57–62. <https://doi.org/10.1016/j.diabres.2012.02.012>
- Wu, H., & Ballantyne, C. M. (2020). Metabolic Inflammation and Insulin Resistance in Obesity. *Circulation Research*, 126(11), 1549–1564. <https://doi.org/10.1161/CIRCRESAHA.119.315896>
- Xian, S., Chen, A., Wu, X., Lu, C., Wu, Y., Huang, F., & Zeng, Z. (2020). Activation of activin/Smad2 and 3 signaling pathway and the potential involvement of endothelial-mesenchymal transition in the valvular damage due to rheumatic heart disease. *Molecular Medicine Reports*, 23(1), 1–1. <https://doi.org/10.3892/mmr.2020.11648>
- Xie, J. X., Alderson, H., Ritchie, J., Kalra, P. A., Xie, Y., Ren, K., Nguyen, H., Chen, T., Brewster, P., Gupta, R., Dworkin, L. D., Malhotra, D., Cooper, C. J., Tian, J., & Haller, S. T. (2017). Circulating CD40 and sCD40L Predict Changes in Renal Function in Subjects with Chronic Kidney Disease. *Scientific Reports*, 7(1), 7942. <https://doi.org/10.1038/s41598-017-08426-8>

- Yang, J., Hamade, M., Wu, Q., Wang, Q., Axtell, R., Giri, S., & Mao-Draayer, Y. (2022). Current and Future Biomarkers in Multiple Sclerosis. *International Journal of Molecular Sciences*, 23(11), 5877. <https://doi.org/10.3390/ijms23115877>
- Yau, J. W., Teoh, H., & Verma, S. (2015). Endothelial cell control of thrombosis. *BMC Cardiovascular Disorders*, 15(1), 130. <https://doi.org/10.1186/s12872-015-0124-z>
- Yazdani, S., Jaldin-Fincati, J. R., Pereira, R. V. S., & Klip, A. (2019). Endothelial cell barriers: Transport of molecules between blood and tissues. *Traffic*, 20(6), 390–403. <https://doi.org/10.1111/tra.12645>
- Yngen, D. M. (2005). Platelet Hyperactivity in Diabetes Mellitus. *European Cardiology Review*, 1(1), 1. <https://doi.org/10.15420/ECR.2005.1o>
- Yun, J.-H., Park, S. W., Kim, K.-J., Bae, J.-S., Lee, E. H., Paek, S. H., Kim, S. U., Ye, S., Kim, J.-H., & Cho, C.-H. (2017). Endothelial STAT3 Activation Increases Vascular Leakage Through Downregulating Tight Junction Proteins: Implications for Diabetic Retinopathy: ROLE OF ENDOTHELIAL STAT3 IN VASCULAR LEAKAGE. *Journal of Cellular Physiology*, 232(5), 1123–1134. <https://doi.org/10.1002/jcp.25575>
- Yung, J. H. M., & Giacca, A. (2020). Role of c-Jun N-terminal Kinase (JNK) in Obesity and Type 2 Diabetes. *Cells*, 9(3), 706. <https://doi.org/10.3390/cells9030706>
- Zhang, S., Breidenbach, J. D., Russell, B. H., George, J., & Haller, S. T. (2020). CD40/CD40L Signaling as a Promising Therapeutic Target for the Treatment of Renal Disease. *Journal of Clinical Medicine*, 9(11), Article 11. <https://doi.org/10.3390/jcm9113653>
- Zhao, P., Yao, Q., Zhang, P.-J., The, E., Zhai, Y., Ao, L., Jarrett, M. J., Dinarello, C. A., Fullerton, D. A., & Meng, X. (2021). Single-cell RNA-seq reveals a critical role of novel pro-inflammatory EndMT in mediating adverse remodeling in coronary artery-on-a-chip. *Science Advances*, 7(34), eabg1694. <https://doi.org/10.1126/sciadv.abg1694>
- Zikherman, J., & Au-Yeung, B. (2015). “The role of T cell receptor signaling thresholds in guiding T cell fate decisions.” *Current Opinion in Immunology*, 33, 43–48. <https://doi.org/10.1016/j.coi.2015.01.012>

8. SUPPLEMENTARY DATA

8.1. Supplementary figures

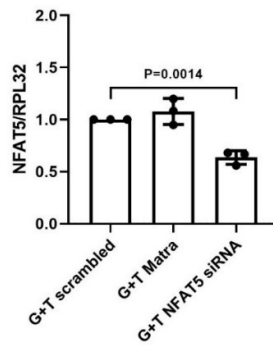


Figure S1: Impact of siRNA-based silencing of NFAT5 on NFAT5 mRNA levels in HUVECs treated with TNF- α and high glucose. The scatter plot represents NFAT5 mRNA levels after 32 hr of NFAT5 siRNA transfection under glucose/TNF- α co-incubation. Data are represented as means \pm SD; n=3.

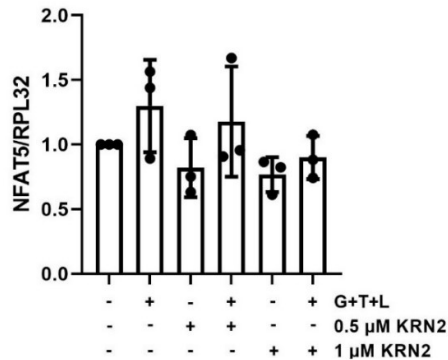


Figure S3: Impact of KRN2 inhibitor on NFAT5 mRNA expression of HUVECs exposed to pro-inflammatory mediators with high glucose. The scatter plot denotes NFAT5 mRNA levels in HUVECs subjected to sCD40L/TNF- α co-stimulation with high glucose upon exposure to varying concentrations of KRN2 inhibitor. The control group was treated with 0.01% DMSO. Data are represented as means \pm SD; n=3.

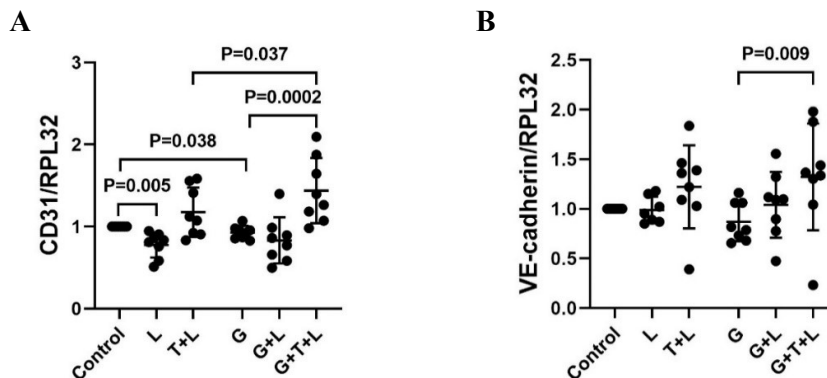


Figure S2: Impact of pro-inflammatory mediators with/out glucose on the mRNA expression of endothelial markers in HUVECs. (A) CD31, and (B) VE-cadherin mRNA levels in HUVECs exposed to sCD40L/TNF- α co-stimulation with/out glucose. Data are represented as means \pm SD; n=7-8.

```

453)                               +nnBGGGNTTCCnnn (V$CREL.01 (0.932))
457)                               +nRNYTTCYRRGAANNnnn (V$STAT6.01 (0.950))
463)                               +nnnTGAAAAATTNYnnnnn (V$NFAT5.02 (0.891)) NFAT5
421) AGAGTTTCTGACATCATTGTAATTTTAAGCATCGTGGATATCCCGGCAAACTTTTGGG
453)                               -nnnGGRRANTCCnnn (V$NFκPAB.0 (0.934)) NF-κB
456)                               -nnnNNTTCYRGAARNYn (V$STAT6.01 (0.971))

486)                               +nnBGGGNTTCCnnn (V$CREL.01 (0.998))
527)                               +nRNYTTCYRRGAANNnnn (V$STAT6.01 (0.906))
481) TGCCATTGGGGATTTCCTCTTTACTGGATGTGGACAATATCCCTATTATTACACAGGAA
485)                               -nnnnnTNTTCCWYnnnn (V$NFAT.01 (0.965))
526)                               -nnnNNTTCYRGAARNYn (V$STAT6.01 (0.937))

541) GCAATCCCTCCTATAAAAAGGGCCTCAGCCGAAGTAGTGTTCAGCTGTTCTTGGCTGACTT
601) CACATCAAAACTCCTATACTGACCTGAGACAGAGGCAGCAGTGATACCCACCTGAGAGAT
661) CCTGTGTTTGAACAACCTGCTTCCCAAAACGGTAAGTGCAGAACGCTTTATAAGGGCAGCC
674)                               -nnnnnTCCCRKAAnnnn (V$STAT.01 (0.925))

721) TCGGGCCATGAAACACAGATATGCAAAAGGCCTTCTAATAAAAACCATCTGTACAAGC
781) TCTTATTGTATTGTAGCTAAAACCTGTCTTTTCTCTTTGACCTAAATAATGAAAGTCTTA
803)                               -nnnnNRSTTTCRCTTTCnnnnnnn (V$IRF2.01 (0.859))

841) AAATTTGTTTATTATTGATTAAACTCTGAAATAAAGATTATTGCACCTAGTGTCTTTG
901) CCCAAAATCTTAGGATGCTGCCTTAAACATCATGGTAGAATAATGTAAGTACTAGCTACCCAC

```

Figure S4: Human E-selectin promoter sequence. The promoter region of E-selectin and other genes promoting atherosclerosis and EndMT depict several closely located NFAT5/NF-κB binding sites. Analysis of the binding sites was performed using Genomatix MatInspector software.

8.2. Supplementary tables

Table S1: Pathway analysis for the upregulated gene products in sCD40L stimulated CC-genotype HUVECs.

Pathway name	Entities found	Entities total	P-Value	Reactions found	Reactions total
Neutrophil degranulation	24	480	<0.0001	10	10
Platelet degranulation	12	141	0.0002	7	11
Response to elevated platelet cytosolic Ca ²⁺	12	148	0.0023	8	14
Aryl hydrocarbon receptor signaling	2	8	0.0093	5	5
Striated Muscle Contraction	4	40	0.0138	4	4
Post-translational protein phosphorylation	6	109	0.0144	1	1
Insulin receptor recycling	3	28	0.0187	5	6
Interleukin receptor SHC signaling	3	29	0.0203	6	6
Laminin interactions	3	31	0.0219	13	15
Advanced glycosylation endproduct receptor signaling	3	16	0.0219	3	4
Smooth Muscle Contraction	6	49	0.0278	6	11
ERKs are inactivated	2	15	0.0300	2	2
RhoV GTPase cycle	3	39	0.0335	1	2
NOTCH4 Activation and Transmission of Signal to the Nucleus	2	12	0.0337	4	5

Table S2: Pathway analysis for the downregulated gene products in sCD40L stimulated CC-genotype HUVECs.

Pathway name	Entities found	Entities total	P-Value	Reactions found	Reactions total
Peptide chain elongation	30	97	<0.0001	5	5
Eukaryotic Translation Termination	31	106	<0.0001	5	5
Formation of a pool of free 40S subunits	30	106	0.0001	2	2

SRP-dependent co-translational protein targeting membrane	31	119	0.0001	5	5
Selenocysteine synthesis	29	112	0.0003	2	7
Nonsense Mediated Decay (NMD) independent of the Exon Junction Complex (EJC)	30	101	0.0004	1	1
L13a-mediated translational silencing of Ceruloplasmin expression	30	120	0.0006	3	3
Viral mRNA Translation	29	114	0.0040	2	2
Eukaryotic Translation Elongation	31	102	0.0087	7	9
CDC42 GTPase cycle	30	159	0.0169	4	6
RHOA GTPase cycle	29	154	0.0190	5	6
GTP hydrolysis and joining of the 60S ribosomal subunit	30	120	0.0297	3	3
Insertion of tail-anchored proteins into the endoplasmic reticulum membrane	7	25	0.0377	7	7
Signaling by MAP2K mutants	3	6	0.0391	1	1
ERKs are inactivated	5	15	0.0400	2	2
Defective B3GALT6 causes EDSP2 and SEMDJL1	6	21	0.0481	1	1
Defective B4GALT7 causes EDS, progeroid type	6	21	0.0481	1	1

Table S3: Pathway analysis for the upregulated gene products in sCD40L stimulated TT-genotype HUVECs.

Pathway name	Entities found	Entities total	P-Value	Reactions found	Reactions total
Laminin interactions	3	31	0.0003	5	15
Rho GTPases activate KTN1	2	12	0.0011	2	2
IL-4 and IL-13 signaling	6	211	0.0031	5	47
Rho GTPase Effectors	10	326	0.0036	18	113
Rho GTPases Activate WASPs and WAVES	3	41	0.0053	7	10
RAC1 GTPase cycle	4	191	0.0071	3	6
Signaling by Rho GTPases	12	709	0.0073	37	203
Rho GTPases Activate Formins	4	149	0.0079	7	27
Signaling by Rho GTPases, Miro GTPases, and RHOBTB3	12	725	0.0084	37	212
Molecules associated with elastic fibres	2	38	0.0111	2	10
FCGR3A-mediated phagocytosis	4	157	0.0120	11	27
Parasite infection	4	157	0.0120	11	27
Leishmania phagocytosis	4	157	0.0120	11	27
Interleukin-6 signaling	3	17	0.0139	17	20
ECM proteoglycans	3	79	0.0147	4	23
Syndecan interactions	3	29	0.0186	4	15
Rho GTPase cycle	6	460	0.0231	19	91
RhoA GTPase cycle	3	154	0.0234	3	6
CDC42 GTPase cycle	3	159	0.0254	3	6
Elastic fibre formation	2	46	0.0260	3	17

Table S4: Pathway analysis for the downregulated gene products in sCD40L stimulated TT-genotype HUVECs.

Pathway name	Entities found	Entities total	P-Value	Reactions found	Reactions total
Defective SERPING1 causes hereditary angioedema	1	3	0.0100	3	3
Defective SLC40A1 causes hemochromatosis 4 (HFE4) (duodenum)	1	4	0.0134	1	1
HHAT G278V doesn't palmitoylate Hh-Np	1	4	0.0167	1	1
Defective LFNG causes SCDO3	1	6	0.0200	1	1
IRS activation	1	7	0.0233	1	3
Signaling by RNF43 mutants	1	8	0.0266	1	1
Signaling by Retinoic Acid	2	73	0.0300	2	21

RORA activates gene expression	2	26	0.0343	2	4
Degradation of the extracellular matrix	3	148	0.0419	14	105
TP53 regulates transcription of additional cell cycle genes whose exact role in the p53 pathway remain uncertain	2	28	0.0458	3	14
Pre-NOTCH Transcription and Translation	3	89	0.0470	12	28
TGF-beta receptor signaling in EMT (epithelial to mesenchymal transition)	0	19	0.1021	1	6

9. ACKNOWLEDGEMENTS

I am incredibly grateful to Prof. Markus Hecker for providing me with an opportunity to work under his supervision. He has contributed significantly to sharpening my scientific knowledge and research skills. I shall also like to thank him for his consideration and support during the challenging phases of my Ph.D. and personal life.

I express my deepest gratitude to my group leader and mentor, apl. Prof. Dr. Andreas Wagner. His unconditional belief in my abilities and research ideas always motivates me greatly. He always guided me through the problems, be it academic or otherwise. I am sincerely thankful for his teachings, kindness, and patience. This endeavour would not have been possible without him.

I am grateful to my thesis advisory committee members: Prof. Marc Freichel and Prof. Jörg Heineke, for providing valuable insights into developing my research project. I also thank my examination committee members: Prof. Marc Freichel, Prof. Ilse Hofmann, and PD Dr. Karin Müller-Decker for their time and effort in evaluating my thesis and defence.

I also take this opportunity to express my gratitude to the faculties of my graduate schools, DIAMICOM and HBIGS. These graduate programs have helped me to acquire the skillsets and knowledge necessary to achieve my research goals and to embark on my future endeavours. I wish to especially thank Prof. Hans-Peter Hammes for taking a keen interest in my project developments. His views and perspectives inspired me to view a research idea from different angles.

A big thanks to all our scientific collaborations, whose contributions were crucial for completing my thesis. I express my highest gratitude to Dr. Stefan Kopf for providing us with control and diabetic patient samples. I am also thankful to Dr. Eugen Rempel and Olga Ermakova for offering their help with the RNASeq data analysis. I thank Dr. Holger Lorenz for sharing his expertise in fluorescence microscopy image analysis. Finally, I thank Dr. Guido Krenning and his student Jolien Fledderus for contributing to the EndMT-related part of my thesis.

The professors, post-docs, technicians, and my colleagues from the institute contributed to my progress in several ways. I express my sincere gratitude to all of them. A special thanks to Prof. Thomas Korff for his scientific lectures on highly relevant topics and for providing his expertise on NFAT5 in my research project. I am also thankful to our post-

doc Dr. Hebatullan Laban for sharing her knowledge and advice during several stages of my PhD. I would also like to acknowledge Dr. Jaafar Al-Hasani for helping me learn and improve my microscopy and analytical skills. I am very grateful to Franziska Mohr for introducing me to the laboratory techniques and providing her feedback during troubleshooting. I would like to thank her for her valuable help and support during the final experiments of my thesis. I am thankful to Cathrin Ott for her efforts in isolating and providing me with the HUVECs for the cell culture experiments. A special thanks to Janina and Emili for sharing a wonderful time with me

I express my utmost gratitude to Ms. Barbara Richards and Ms. Michaela Neidig. They were always very kind and patient towards my several inquiries and found ways to solve my problems. The administrative part of my Ph.D. journey was smoothly managed because of their help and support.

I am grateful to my friends Abhijeet, Namita, Saurabh, and Shruti for their immense support during the crucial phases of my thesis. They had always shown tremendous faith in me and never failed to motivate me when things seemed unmanageable. I thank you all for being there with me and boosting my morale to the highest.

Last but not least, I would like to thank my backbone, my family. My sisters Sheetal and Madhuri motivate me by reminding me that they are always proud of me. Their unconditional belief in me pushes me to achieve more. I can never express enough gratitude to my parents for their love, support, and blessings. They never let me lose hope and give up during difficult times. I dedicate my thesis to my parents, who are the reason behind all my success.